

THE ROLE OF ALCOHOL IN MICELLAR SOLUBILIZATION
AND SURFACTANT SORPTION IN AQUIFER MEDIA

By

MEIFANG ZHOU

A DISSERTATION PRESENTED TO THE GRADUATE SCHOOL
OF THE UNIVERSITY OF FLORIDA IN PARTIAL FULFILLMENT
OF THE REQUIREMENTS FOR THE DEGREE OF
DOCTOR OF PHILOSOPHY

UNIVERSITY OF FLORIDA

1998

ACKNOWLEDGMENTS

I would like to thank my committee members, Dr. P.S.C. Rao, Dr. M.D. Annable, Dr. B.L. McNeal and Dr. P.A. Chadik, for their guidance and helpful comments. I especially thank Dr. Rao for providing some financial support.

I want to express my deep appreciation to my outstanding advisor, Dr. R. Dean Rhue, for both his monetary and emotional support. This work would be impossible without his encouragement and guidance.

I would like to thank Dr. W.G. Harris for his help with X-ray diffraction, GTA analysis, and data interpretation. Thanks also to William Reve for his help in lab method development and other technical capacities with this research. He also helped in editing the first draft of this dissertation. Thanks as well to Marcy Rhue for her help with alcohol partitioning sample analysis, and to Dongping Dai for her help and friendship.

Finally, my very special thanks go to my parents and my wife, Yiqun Ding, for their love and encouragement through

these years, and to my daughter, Alice, who provided joy and love.

TABLE OF CONTENTS

ACKNOWLEDGMENTS	ii
LIST OF TABLES	vi
LIST OF FIGURES	viii
ABSTRACT	xiii
CHAPTER	
1 INTRODUCTION	1
Alcohol: Cosurfactant or Cosolvent?	3
Solubilization	5
Mobilization	7
Surfactant Adsorption	9
Surfactant Precipitation	14
Dissertation Scope	15
2 PSEUDOPHASE MODEL AND COSURFACTANT PARTITIONING	17
Introduction	17
Materials and Methods	23
Calculation of Alcohol Partitioning	24
Results and Discussion	27
Alcohol Partitioning in Water/Dodecane Systems	27
Alcohol Partitioning in Water/dodecane/SDS Systems	32
Conclusions	39
3 TWO-REGION MODEL OF ALCOHOL IN NAPL SOLUBILIZATION	40
Introduction	40
Materials and Methods	43
Results and Discussion	47
Conclusions	61

4	SORPTION OF SDS AND PENTANOL ON SOILS	62
	Introduction	62
	Theory	67
	Materials and Methods	75
	Results and Discussion	76
	Soil Properties	76
	Kinetics of SDS Sorption	77
	Precipitation in Hill Soils	82
	Adsorption on Dover Soil	89
	Conclusions	99
5	DYNAMIC SURFACTANT ADSORPTION AT INTERFACES	101
	Introduction	101
	Theory	103
	Materials and Methods	106
	Results and Discussion	111
	Conclusions	131
6	SOLUBILIZATION OF PCE IN SURFACTANT/ALCOHOL SOLUTIONS	133
	Introduction	133
	Materials and Methods	139
	Surfactant and Cosurfactant	139
	PCE Solubilization Screen Study	139
	Partitioning Tracers in Batch Experiments . .	140
	Column Studies	141
	Results and Discussion	144
	PCE Solubilization Screen	144
	Partitioning Tracers in Batch	151
	Basic Properties of Brij 97 Solution	153
	Column Studies	153
	Conclusions	171
7	SUMMARY AND CONCLUSIONS	175
	ABBREVIATIONS	180
	LIST OF REFERENCES	186
	BIOGRAPHICAL SKETCH	200

LIST OF TABLES

<u>Table</u>	<u>page</u>
2-1. Partition coefficients for pentanol between water and dodecane at different isopropanol concentrations	30
2-2. Partition coefficients for isopropanol between water and dodecane at different pentanol concentrations	31
2-3. Alcohol partitioning and dodecane solubilization data for Winsor Type I microemulsions	33
4-1. List of constants	71
4-2. Chemical and physical properties of the soils . .	78
5-1. The surface tension of water, IFT between PCE and Water, and the measured and calculated diameter of burette tips	108
5-2. Correction factors for the drop weight method .	110
5-3. Equilibrium adsorption (Γ) of Brij 97 at the interfaces as calculated the from Gibbs equation	113
5-4. Apparent diffusion coefficient for Brij 97 at the water/air interface	127
5-5. Apparent diffusion coefficient for Brij 97 at the water/PCE interface	128
5-6. The effect of IPA on the apparent diffusion coefficient of Brij 97 at the water/PCE interface for different surfactant concentrations	130

6-1.	Phase behavior and visually estimated PCE solubilization in alcohol-free surfactant solutions. All surfactant solutions were 3% concentrations	145
6-2.	PCE Solubilization and partition coefficient for IPA between water and PCE in 12 nonionic surfactant solutions	149
6-3.	The partition coefficients of alcohol tracers between PCE and water	154
6-4.	Some basic properties of Brij 97 solutions . . .	155
6-5.	Experimental conditions and physical properties of each PCE contaminated column	156
6-6.	Recovery of PCE from columns and estimation of the surfactant solution pore volumes required for full recovery of PCE	157

LIST OF FIGURES

<u>Figure</u>	<u>page</u>
1-1. Schematic of a typical surfactant adsorption isotherm	11
2-1. Schematic diagram of the pseudophase model for partitioning of alcohol between oil and aqueous phases and between aqueous and interfacial phases	21
2-2. The pentanol partitioning coefficient between oil and aqueous phases ($^{\circ}K_p$) as a function of the total pentanol concentration in the oil phase (C_A^o). . .	28
2-3. The mole fraction-based partitioning coefficient of pentanol and IPA between aqueous and micelle interfacial phases as a function of the mole fraction of pentanol in the interface.. . . .	34
2-4. The total pentanol concentration in the oil phase as a function of the mole fraction of pentanol in the interface.. . . .	36
2-5. Dodecane solubilization in the Type I microemulsion with 3% SDS as a function of the mole fraction of pentanol in the interface.	37
2-6. Dodecane solubilization in the Type I microemulsion with 4.5% SDS/50 mM CaCl_2 as a function of the mole fraction of pentanol in the interface	38
3-1. Two-region model of alcohol partitioning in oil solubilization before interfacial pentanol saturation	44

3-2.	Two-region model of alcohol partitioning in oil solubilization after interfacial pentanol saturation	45
3-3.	The calibration curve for viscosity measurements .	48
3-4.	Gasoline solubilization contours for the SDS/pentanol/50 mM KCl system	49
3-5.	Gasoline solubilization contours for the SDS/pentanol/10mM CaCl ₂ system	50
3-6.	The effect of pentanol on dodecane solubilization by 3% SDS/water	51
3-7.	The effect of pentanol on PCE solubilization at three SDS concentrations	52
3-8.	The effect of pentanol and IPA on PCE solubilization by 1% SDS/100mM NaCl	53
3-9.	Conductivity of 3% SDS solution as a function of pentanol concentration	55
3-10.	Viscosity of SDS solutions as a function of pentanol concentration	60
4-1.	Anionic surfactant sorption by calcareous soils .	69
4-2.	Anionic surfactant/cosurfactant adsorption isotherm	74
4-3.	Kinetics of SDS sorption on Hill soil 1	79
4-4.	Kinetics of SDS sorption on Hill soil 2	80
4-5.	Kinetics of SDS sorption on the Dover soil	81
4-6.	The relationship between divalent cation concentrations in solution and SDS sorption for Hill soil 1 (uncontaminated soil)	83

4-7.	The relationship between divalent cation concentrations in solution and SDS sorption for Hill soil 2 (treated contaminated soil)	84
4-8.	SDS sorption and divalent cation concentrations as a function of pentanol concentration in solution for Hill soil 1 (uncontaminated soil)	87
4-9.	SDS sorption and divalent cation concentrations as a function of pentanol concentration in solution for Hill soil 2 (treated contaminated soil)	88
4-10.	Log adsorbed SDS on Dover soil as a function of log equilibrium SDS concentration in solution	90
4-11.	Divalent cation concentrations and adsorbed SDS as a function of log equilibrium SDS concentration in solution for the Dover soil	91
4-12.	The effect of pentanol on SDS adsorption at Region I of the adsorption isotherm	93
4-13.	The effect of pentanol on SDS adsorption at Region II of the adsorption isotherm	94
4-14.	The effect of pentanol on SDS adsorption at Region III of the adsorption isotherm	95
4-15.	The effect of pentanol on SDS adsorption at Region IV of the adsorption isotherm	96
5-1.	Surface and interfacial tension measurement apparatus	109
5-2.	Plot of surface tension of Brij 97 solution versus log concentration	112
5-3.	Plot of interfacial tension between Brij 97 solution and PCE versus log surfactant concentration	114

5-4.	Relationship between the surface tension of Brij 97 solution and $t^{-1/2}$ at surfactant concentrations below the CMC	116
5-5.	Relationship between the surface tension of Brij 97 solution and $t^{-1/2}$ at surfactant concentrations above the CMC	117
5-6.	Relationship between the interfacial tension of Brij 97 solution ($C=2.45 \times 10^{-4}M$) and $t^{-1/2}$	118
5-7.	Relationship between the interfacial tension of Brij 97 solution ($C=5.08 \times 10^{-4}M$) and $t^{-1/2}$	119
5-8.	Relationship between the interfacial tension of Brij 97 solution ($C=8.47 \times 10^{-4}M$) and $t^{-1/2}$	120
5-9.	Relationship between the interfacial tension of Brij 97 solution ($C=1.53 \times 10^{-3}M$) and $t^{-1/2}$	121
5-10.	Relationship between the interfacial tension of Brij 97 solution ($C=8.47 \times 10^{-3}M$) and $t^{-1/2}$	122
5-11.	Relationship between the interfacial tension of Brij 97 solution ($C=8.47 \times 10^{-2}M$) and $t^{-1/2}$	123
5-12.	Relationship between the interfacial tension of Brij 97 solution ($C=2.12 \times 10^{-1}M$) and $t^{-1/2}$	124
5-13.	Relationship between the interfacial tension of Brij 97 solution ($C=4.24 \times 10^{-1}M$) and $t^{-1/2}$	125
6-1.	Relationship between the surfactant HLB and PCE solubilization.	148
6-2.	PCE solubilization in 3.5% SDS with and without IPA as a function of the pentanol concentration in solutions.	152
6-3.	The exponential decrease of PCE solubilization in the BTC tail.	159

6-4.	PCE and IPA concentrations in effluent from a glass column flushed with 3% Brij 97/3% IPA with upward flow mode.	160
6-5.	PCE and IPA concentrations in effluent from a glass column flushed with 3% Brij 97/3% IPA with downward flow mode.	161
6-6.	Pentanol, IPA and solubilized PCE concentrations in effluent from a glass column flushed with 3.5% SDS/3.5% pentanol/3.5% IPA at downward flow mode.	162
6-7.	Solubilized, mobilized PCE volumes from a glass bead column flushed with 3.5% SDS/3.5% pentanol/3.5% IPA solution	163
6-8.	Pentanol, IPA and solubilized dodecane concentrations in effluent from a glass bead column flushed with 4.5% SDS/5% pentanol/2% IPA/50 mM CaCl ₂ solution	168
6-9.	Solubilized and mobilized dodecane volumes from a glass bead column flushed with 4.5% SDS/5% pentanol/2% IPA/50 mM CaCl ₂ solution	169
6-10.	Normalized pentanol, IPA and solubilized dodecane concentrations in effluent of front BTC from a glass bead column flushed with 4.5% SDS/5% pentanol/2% IPA/50 mM CaCl ₂ solution	170
6-11.	Normalized IPA, pentanol, SDS and solubilized PCE concentrations in effluent of front BTC from a glass bead column flushed with 3.5% SDS/3.5% pentanol/3.5% IPA solution	172

Abstract of Dissertation Presented to the Graduate School
of the University of Florida in Partial Fulfillment of the
Requirements for the Degree of Doctor of Philosophy

THE ROLE OF ALCOHOL IN MICELLAR SOLUBILIZATION AND
SURFACTANT SORPTION IN AQUIFER MEDIA

By

Meifang Zhou

May 1998

Chairperson: Dr. R. Dean Rhue
Major Department: Soil and Water Science

The effectiveness of microemulsions in aquifer remediation depends on both the surfactant's interactions with the nonaqueous phase liquid (NAPL) and with the aquifer media. Knowledge of the effects of alcohols, which are an indispensable ingredient to microemulsions, on these interactions is essential for the optimum microemulsion formulation.

The partitioning behavior of alcohols in Winsor Type I microemulsions was investigated using the pseudophase model coupled with the alcohol self-association model. A linear

relationship was found between interfacial cosurfactant concentration and NAPL solubilization. A two-region partitioning model for alcohol in the micelle was proposed. Alcohol prefers to partition into the micelle interface, acting as a cosurfactant before interfacial alcohol saturation, and it prefers to partition into the micelle inner core, acting as a polar oil after interfacial alcohol saturation.

Based on the alcohol partitioning behavior, NAPL solubilization and phase behavior, I found that medium-chain alcohol is a good cosurfactant for solubilizing light nonaqueous phase liquid (LNAPL), while branched short-chain alcohol is a good interfacial modifier for solubilizing dense nonaqueous phase liquid (DNAPL).

Relatively high perchlorethylene (PCE) solubilization and high interfacial tension (IFT) were simultaneously achieved by using a nonionic surfactant/cosurfactant system. Experimental data suggest that remediation of aquifers, contaminated with DNAPL, can be achieved via in-situ solubilization, without mobilization.

Precipitation is the primary mechanism for anionic surfactant loss in calcareous soils, while adsorption is the

predominant loss mechanism in soils with high iron oxide content. Cosurfactant decreases anionic surfactant precipitation and adsorption through comicellization.

CHAPTER 1 INTRODUCTION

Organic solvents (e.g., chlorinated hydrocarbons) and other petroleum-based products (e.g., gasoline and jet fuel) entering the subsurface as a nonaqueous phase liquid (NAPL) have become a major environmental concern. As NAPL is transported through the subsurface, a portion of the NAPL will be retained within the soil pores. Because of their low solubility in water, this residual NAPL phase represents a long-term source of aquifer contamination and creates a large dissolved plume. It is now widely acknowledged that pump-and-treat remediation technologies are an ineffective and costly means of aquifer remediation since they only effectively manage the dissolved plume (NRC, 1993, 1997). Innovative technologies are necessary to address the source-zone remediation (NRC, 1997). Surfactant-enhanced subsurface remediation has been identified as a promising technology for expediting NAPL source-zone treatment (EPA, 1992). This approach is based on the ability of surfactants to (a)

increase the aqueous solubility of NAPLs via micellar solubilization, and (b) mobilize the entrapped NAPL phase by lowering the interfacial tension between the NAPL and the aqueous phase (West and Harwell, 1992).

The formation of microemulsions with surfactant, oil and water is the main key for NAPL solubilization and mobilization. A microemulsion is a thermodynamically stable, transparent dispersion of liquid droplets ($<0.1 \mu\text{m}$) suspended within a second immiscible liquid, and stabilized by an interfacial film of surface-active molecules (Rosen, 1989). Alcohols are normally also considered an indispensable ingredient of microemulsions (Bowcott and Schulman, 1955). Most commercial surfactants are not balanced with respect to their affinity for oil and water. Water-soluble surfactants tend to be too hydrophilic to form a high efficiency microemulsion with a nonpolar hydrocarbon. Addition of medium chain-alcohols, such as pentanol can increase the hydrophobicity of the surfactant system. Furthermore, alcohols, especially the branched-chain alcohols, can promote the formation of microemulsions by preventing the formation of liquid crystalline or gel structures (Abe et al., 1986).

The efficiency of surfactant-enhanced aquifer remediation depends on the interactions between not only the surfactant and NAPL, but also the surfactant and the aquifer media. The mechanisms of surfactant and media interactions are characterized mainly by surfactant loss via precipitation and adsorption. Surfactant adsorption or precipitation decreases the success of surfactant-enhanced remediation because the concentration of the active ingredient is reduced.

Alcohol: Cosurfactant or Cosolvent ?

Alcohol-free microemulsions in most systems cannot be made except at high temperatures (Abe et al., 1986). The importance of alcohol in microemulsion phase behavior is widely accepted (Bowcott and Schulman, 1955; Abe et al., 1986; John and Rakshit, 1995). whether the alcohol acts as a cosurfactant or a cosolvent is unresolved (Kahlweit et al., 1991; Strey and Jonstromer, 1992; Graciaa et al., 1993).

The effect of alcohol on the phase behavior of water-oil-surfactant mixtures has been explained by considering alcohols as cosurfactants that act mainly on the properties of the interface. Mitchell and Ninham (1981) proposed that alcohol molecules enter the monolayer and thereby change its natural

curvature. De Gennes and Taupin (1982) suggested that one major effect of alcohol is the increase in flexibility of the interfacial layer. Graciaa and coworkers (1993) viewed the medium-chain alcohol as a cosurfactant because of its correlation with the optimum formulation of microemulsions and production of additional lipophilicity at the interface.

Strey and coworkers (Kahlweit et al., 1991; Strey and Jonstromer, 1992), on the other hand, suggested that medium-chain alcohols should be considered cosolvents that distribute themselves between the aqueous and oil phases, and the interface. These alcohols effectively decrease the hydrophilicity of the surfactant as well as the hydrophobicity of the oil. The relatively high alcohol:surfactant molecular ratio in the interface is due to the intermediate polarity of the interfaces, rather than to any true surface action of the alcohols.

The "dilution" effect is caused by short-chain alcohols entering the interfacial area of surfactant molecules and pulling them apart. This may result in an overall reduction in the intensity of molecular properties, such as interfacial order, tension lowering, and solubilization. In this case it may be said that the alcohol behaves like a very poor

surfactant. This "dilution" effect of alcohols on surfactant molecules inhibits the formation of liquid crystals and gels.

Solubilization

The use of surfactants to increase NAPL solubility is essentially a modification of the pump-and-treat approach. Surfactant solutions are injected, pumped through the NAPL source-zone, and surfactant solution with solubilized NAPL is then recovered at extraction wells.

Enhanced NAPL solubilization with surfactants is a micellar phenomenon. If the solubility of a very low water-soluble oil is plotted against the concentration of the surfactant solution that is solubilizing it, solubilization is very slight until a critical concentration of surfactant is reached. Solubilization will increase almost linearly past this surfactant concentration (Edwards et al., 1991; Jafvert et al., 1994). This critical concentration is equal to the critical micelle concentration (CMC) of the surfactant in the presence of a solubilizate. The amount of oil that is solubilized depends on the surfactant structure, ionic strength, temperature, solubilizate structure, cloud point of surfactant, HLB of surfactant, and the presence of organic

additives such as alcohols (Mackay, 1987; Rosen, 1989). The locus of solubilization varies with the nature of the material solubilized and reflects the type of interaction occurring between surfactant and NAPL. Based upon ultraviolet spectral studies, Mukerjee (1979) proposed a two-state model of solubilization involving a distribution between a dissolved state in the micelle core and an adsorbed state in the interface. Although a distribution favoring the adsorbed state is expected of solubilizates with high polarity, increased concentration of the solubilize appears to produce a redistribution favoring the dissolved state (Mukerjee, 1979).

For the solubilization of low water-soluble hydrocarbons by nonionic surfactant solutions, the rate of solubilization is directly proportional to the surfactant concentration above the CMC (Carroll, 1981). The mechanism suggested involves diffusion of the micelles to the hydrocarbon/water interface.

The solubilization of NAPL is inversely related to the interfacial tension (IFT), which can be described by the Chun-Huh equation (Chun, 1979)

$$\gamma = C/S^2 \quad (1-1)$$

where γ is the interfacial tension (dynes/cm), S the solubilization ratio (volume of oil or water solubilized per volume of neat surfactant, ml/ml) and C is a constant. This equation shows that high NAPL solubilization in surfactant systems must produce low IFTs. However, low IFTs may enhance mobilization of NAPL as discussed below.

Mobilization

The use of surfactants to enhance NAPL mobility by reduction of IFT is an extension of enhanced oil recovery technology (Pope and Wade, 1996). Because the capillary forces in oil reservoirs are generally large compared to viscous forces, the IFT must be reduced enough to mobilize all of the residual oil. The ratio between viscous and capillary forces is called the capillary number, N_c , and is defined as

$$N_c = \frac{|k \nabla \phi_w|}{\gamma} \quad (1-2)$$

where $\phi = P + \rho_w g z$, where P is hydrostatic pressure potential, ρ_w density of water, g the gravity, z elevation, k the intrinsic permeability of the porous medium, and γ the IFT. Buoyancy forces can also be expected to strongly affect the

mobilization of DNAPL (Pennell et al. 1996). The Bond number, N_B , represents the ratio of buoyancy forces to capillary forces, and is defined as:

$$N_B = \frac{gk(\rho_w - \rho_o)}{\gamma} \quad (1-3)$$

where ρ_o is the density of the oil. A total trapping number, N_T , which relates viscous and buoyancy forces to the capillary forces acting to retain the NAPL, is calculated as the sum of the Capillary and Bond numbers. For horizontal flow, N_T can be expressed as (Pennell et al., 1996):

$$N_T = \sqrt{N_C^2 + N_B^2} \quad (1-4)$$

For vertical upward flow, N_T can be expressed as

$$N_T = |N_C + N_B| \quad (1-5)$$

and for vertical downward flow, N_T can be expressed as

$$N_T = |N_C - N_B| \quad (1-6)$$

The critical value of N_T required to initiate PCE mobilization falls within the range of 2×10^{-5} to 5×10^{-5} , which corresponds to an IFT range of 4.3-1.7 dyn/cm (for 20-30 mesh Ottawa sand), while an N_T on the order of 0.001 is required to completely displace PCE (Pennell et al., 1996).

Mobilization can rapidly remove the residual NAPL with a small volume of surfactant solution. However, there is a greater risk of vertical mobilization if DANPL is present, and there is an increased potential for leaving a significant amount of NAPL behind due to structural trapping or imperfect flow paths (Fountain, 1997).

Surfactant Adsorption

Studies involving anionic surfactant adsorption have been mostly focused on positively charged sorbents such as alumina (Blokhus, 1990; Blokhus and Sjoblom, 1991; Sjoblom et al., 1990; Ruths et al., 1991; Fu et al., 1996; Forland et al., 1996) and rutile (Bohmer and Koopal, 1992; Koopal et al., 1995). anionic surfactant adsorption on soils is seldom studied, because it has always been assumed that soils are negatively charged, and that anionic surfactant adsorption on soils was less important than precipitation. Nonionic surfactant adsorption on soils, on the other hand, has been investigated by several authors (Abdul and Gibson, 1991; Brownawell et al., 1991; Palmer et al., 1992; Pennell et al., 1993; Edwards et al., 1994; Adeel and Luthy, 1995; Ching and Jafvert, 1997). Because of poor detergency and high cost

(Martel et al., 1993), cationic surfactant have been excluded for remediation and sorption study. High adsorption capacity of cationic surfactants on negatively charged soils can be expected, which also eliminates the cationic surfactants from use in aquifer remediation.

Figure 1-1 is a schematic of a typical surfactant adsorption isotherm. Such isotherms are common for ionic surfactants adsorbing from aqueous solutions onto surfaces with a charge opposite to that of the surfactant. Similar isotherms are also sometimes observed for nonionic surfactants, but they do not adsorb strongly enough to show all the details of the ionic surfactant isotherm (O'Haver and Harwell, 1995).

Isotherms like those in Figure 1-1 are commonly divided into four regions (Somasundaran and Fuerstenau, 1966; Scamehorn et al., 1982; Harwell et al., 1985; Koopal et al., 1995). Region 1 is an area of low adsorption density and is sometimes referred to as the Henry's law region in which linear isotherm approximation may be adequate. In this region the surfactants are adsorbed as monomers and do not interact with each other. There should be no aggregates of adsorbed surfactants found here.

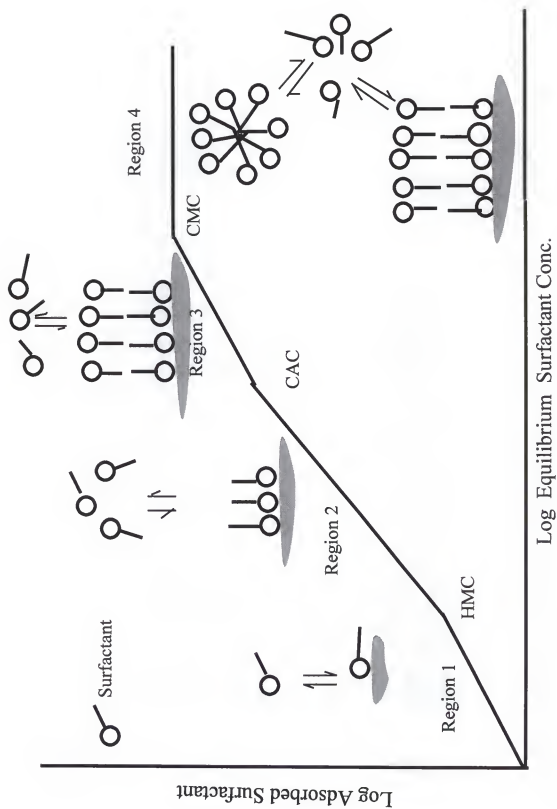


Figure 1-1. Schematic of a typical surfactant adsorption isotherm.

Region 2 is indicated by a sharp increase in the isotherm slope that occurs at the transition between Region 1 and Region 2. which has been attributed to the formation of micelle-like aggregates of adsorbed surfactants. The transition has been given designations analogous to the hemimicelle concentration (HMC) or critical admicelle concentration (CAC) (Somasundaran and Fuerstenau, 1966; Harwell et al., 1985). The differences in the terminology emphasize differing views of the morphology of the aggregates at the transition (monolayered or bilayered). They also emphasize the consensus that the aggregation phenomenon, which occurs at the solid/liquid interface, is analogous to micelle formation.

The Region 2/Region 3 transition is marked by a decrease in the slope of the isotherm, and there is little agreement about the reason for this change in slope. The most common explanation is that the aggregates forming in Region 2 are monolayers adsorbing surfactant head down on an oppositely charged surface, and that the change in slope coincides with the cancellation of the charge on the solid surface by the charge on the adsorbed aggregates so that subsequent surfactants are adsorbing onto a like-charged surface (Somasundaran and Fuerstenau, 1966). Sometimes it is proposed

that a second layer of aggregates does not begin to form until Region 3 (Chandar et al., 1987). Still other workers have attributed the change in slope to a heterogeneous distribution of energies on the surface (Harwell et al., 1985).

Region 4 is called the plateau adsorption region. In most systems the Region 3/Region 4 transition occurs near the CMC of the surfactant. When the surfactant is monoisomeric (or nearly so, as in the case of some commercial polyethoxylated alcohols or phenols), no additional surfactant adsorption occurs above the CMC. This phenomenon is easily understood in terms of the pseudophase separation model of micelle formation (Shinoda, 1978). Micelles that form at the CMC have the same chemical potential as the monomers at the CMC. As the concentration of surfactant increases, the increase of surfactant chemical potential is negligible. In general, the better a surfactant is at forming micelles, the more pronounced will be the Region 3/Region 4 transition, the closer that transition will be to the CMC, and the less the adsorption will increase above the CMC.

The adsorption isotherm in Figure 1-1 represents the ideal condition. Smooth transitions may exist at the

boundaries between isotherm regions when sorbents are heterogeneous.

Surfactant Precipitation

Precipitation has been reported as the primary mechanism anionic surfactant loss by soils (Jafvert and Heath, 1991; West and Harwell, 1992). The precipitation behavior of ionic surfactants is dramatically different from that of simple inorganic salts, because of surfactant's ability to form micelles.

The precipitation of ionic surfactants in solution due to the presence of divalent cations has been extensively studied (Somasundaran et al. 1984; Kallay et al., 1985, 1986; Matheson et al., 1985a, 1985b; Noik et al., 1987; Fan et al., 1988; Stellner and Scamehorn, 1989a, 1989b). When the surfactant concentration is below the CMC, surfactant precipitation, like that of an inorganic salt, is controlled by the solubility product of the divalent cationic surfactant. When the surfactant concentration is above the CMC, the complexation of divalent cations with the micelle will decrease the activity of divalent cations and precipitation.

Surfactant precipitation studies in porous media have been less extensive than studies in solutions. Jafvert and Heath (1991) adapted the solution theory to surfactant precipitation on soils and sediments. Schweich and coauthors (Schweich and Sardin, 1985; Krebs et al., 1987) included in their calculation the sources of the divalent cations, cation exchange, and solubilization of trace calcite. They excluded, however, the surfactant concentration above the CMC.

Dissertation Scope

The main goal of this research is to try to understand the effect of cosurfactants on the interactions between surfactant and NAPL (e.g. solubilization and mobilization) and between surfactant and porous media (e.g. adsorption and precipitation). Cosurfactant partitioning behavior in the Type I microemulsion system (oil in water microemulsion in equilibrium with an excess oil phase) was investigated using the pseudophase model coupled with the alcohol self-association model. The relationship between interfacial cosurfactant concentration and NAPL solubilization is discussed in Chapter 2. A two-region model is proposed in Chapter 3 for describing cosurfactant partitioning in the

micelle. This model is based on the effects of cosurfactant on NAPL solubilization and the electrical conductivity of the surfactant solution. The interaction between surfactant and porous media is studied in Chapter 4, including (a) the effect of soil properties and surfactant concentration on surfactant precipitation and adsorption; (b) the use of alcohol as a cosurfactant to decrease surfactant precipitation; and (c) the effect of cosurfactant on surfactant adsorption in different isotherm regions. The role of cosurfactants on the rate of adsorption of surfactant at the interface is investigated in Chapter 5. Surfactant/cosurfactant systems with relatively high DNAPL solubilization and IFTs are evaluated using batch and column studies in Chapter 6. Cosurfactant selection based on properties of the NAPL and the surfactant is also addressed in Chapter 6. A summary of these findings, and suggestions for further work are presented in Chapter 7.

CHAPTER 2 PSEUDOPHASE MODEL AND COSURFACTANT PARTITIONING

Introduction

When a surfactant is used to remediate a NAPL contaminated aquifer, cosurfactants such as medium chain-length alcohols and/or branched short-chain alcohols, are usually combined with a water-soluble surfactant to form a microemulsion system (Desnoyers et al., 1983; Martel et al., 1993; Martel and Gelinas, 1996). Alcohols play an important role as cosurfactants in the solubilization and phase behavior of microemulsions. Most commercially available surfactants are not balanced with respect to their affinity toward aqueous and oil phases (Strey and Jonstromer, 1992; John and Rakshit, 1995). Water-soluble surfactants are normally too hydrophilic relative to LNAPL and may have low LNAPL solubilization capacity. Addition of medium chain-length alcohols, such as pentanol, can make the interfacial phase more hydrophobic. Alcohols, especially the branched-chain alcohols, can also

prevent the formation of rigid structures such as gels and liquid crystals (Abe et al., 1986).

There has been considerable debate as to whether the alcohol in the microemulsion system acts as a cosurfactant or a cosolvent (Kahlweit et al., 1991; Strey and Jonstromer, 1992; Graciaa et al., 1993). It has been reported that oil solubilization is linearly related to the surfactant micelle concentration (Edwards et al., 1991; Jafvert et al., 1994), and is also log-linearly related to the cosolvent concentration (Yalkowsky, 1987). It would be interesting to know whether the oil solubilization is linearly related to the alcohol concentration in the interfacial phase, or log-linearly related to the alcohol concentration in the system when the surfactant concentration is kept constant. A log-linear relationship would imply a cosolvent role for alcohol in solubilization. The study of the relationship between oil solubilization and alcohol concentration can help us to understand the function of alcohol in oil solubilization.

The molar ratio of cosurfactant to surfactant at the interface is not only of fundamental importance to the NAPL solubilization process in microemulsion systems, but is also related to certain microemulsion properties such as

viscosity, conductivity and interfacial tension, which will be addressed in the next chapter. The Schulman-Bowcott plot (Bowcott and Schulman, 1955; Pithapurwala and Shah, 1984) is a popular method used to calculate the molar ratio of alcohol to surfactant in a microemulsion interface. Unfortunately, this plot can only be applied to water-in-oil (w/o) microemulsions using long-chain alcohols (C6 and more), whose concentration in the aqueous phase is negligible. Since the oil phase in w/o microemulsions acts as a sink for both surfactant and cosurfactant, o/w (oil-in-water) microemulsions are the preferred systems used for NAPL remediation. The ratio of alcohol to surfactant in an o/w microemulsion interface can be calculated if the alcohol partitioning coefficient between the aqueous phase and the interface is known. Alcohol partitioning coefficient at both low alcohol concentrations and concentrations at 'saturation' has been measured (Stilbs, 1982; Hoiland et al., 1984; Treiner et al., 1987; Muto et al., 1989; Gao et al., 1990). Partitioning coefficient data are limited for the intermediate to high alcohol concentrations commonly used in NAPL remediation. Alcohol partitioning coefficient is much lower at 'saturation' than at low alcohol concentrations, and the plot of partitioning coefficient vs

alcohol mole fraction in the interface is "S" shaped for hexanol and heptanol in aqueous solutions of SDS (Abuin and Lissi, 1983). However, data is sparse and therefore insufficient to determine the actual slope of the curve at medium to high alcohol concentrations.

Methods available to measure the alcohol partitioning coefficient between the aqueous phase and the interface (Stilbs, 1982; Shih and Williams, 1986; Gao et al. 1989) either require special instrumentation or can only measure the partitioning coefficient at low alcohol concentrations. Equilibrium partitioning, coupled with a "pseudophase" model, has been used to describe alcohol partitioning among oil, aqueous and interfacial phases in microemulsion systems (Lalanne et al., 1984; Biais et al., 1988; Bourrel and Schechter, 1988; Voca et al., 1988). Figure 2-1 is a schematic describing the concepts embodied in the pseudophase model. A Winsor Type I microemulsion system consists of a water-continuous microemulsion in equilibrium with excess oil. It is assumed that the oil phase will contain some alcohol but no water or surfactant. The microemulsion phase will contain water, surfactant, and alcohol, along with some oil. The pseudophase model assumes that the components in the

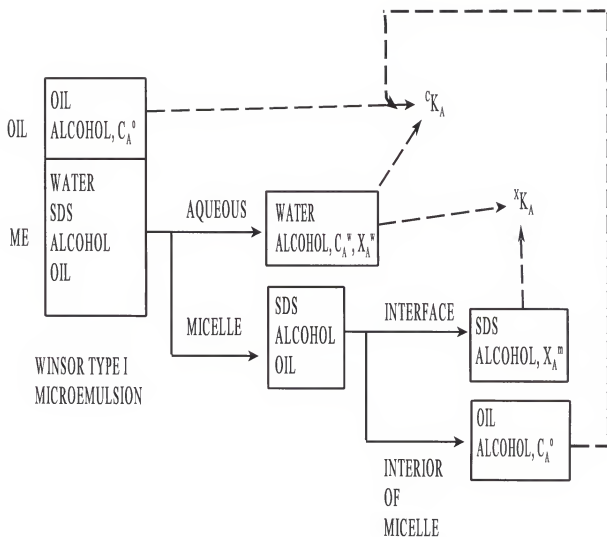


Figure 2-1. Schematic diagram of the pseudophase model for partitioning of alcohol between oil and aqueous phases and between aqueous and interfacial phases.

microemulsion phase can partition among 3 pseudophases: 1) an aqueous phase containing only water and alcohol; 2) an interfacial phase containing only surfactant and alcohol; and 3) the interior of the micelle containing only oil and alcohol. It is also assumed that the partitioning coefficient, cK_A , can be measured in water/oil systems (i.e., without surfactant) and used to describe partitioning between oil and aqueous phases in the presence of surfactant micelles. Thus, using the pseudophase model and the appropriate mass balances, the partitioning coefficient between aqueous and interfacial phases, xK_A , can be calculated. This model allows us to relate oil solubilization in the microemulsion phase to alcohol partitioning behavior.

Since alcohol in the oil phase tends to self-associate (Prigogine and Defay, 1965), alcohol self-association must also be included in this model when calculating xK_A . The partitioning behavior of several alcohols has been studied, but it is not clear whether isopropanol (IPA), a water-miscible alcohol used to control microemulsion viscosity, will self-associate in oil at low concentrations. Moreover, the mutual effects of pentanol and IPA on their partitioning behavior have not been well documented.

In the present investigation the partitioning coefficient of pentanol, at alcohol concentrations normally used in NAPL remediation studies, was determined. The mutual effects of pentanol and isopropanol on their partitioning among aqueous, interfacial, and oil phases were also investigated.

Materials and Methods

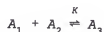
Alcohol partitioning between the oil and aqueous phases was conducted at oil to water ratios of 1:4 and 1:8. Two ml or 4 ml of 50mM CaCl_2 , or DI water containing 0, 0.5, 1, 1.5, or 2% isopropanol, and 0.5 ml of dodecane were added to a 5 ml vial with a Teflon lined cap. Pentanol was added to the vial resulting in concentrations ranging from 0 to 4%. Samples were equilibrated on a rotator for eight hours at 24°C. The sample vials then were allowed to settle for 24h to achieve complete phase separation. Pentanol and isopropanol in the oil and aqueous phases were determined by GC.

Alcohol partitioning in the Type I microemulsion was measured at 24°C using 10ml screw cap vials. Four ml or 7ml of 4.5% SDS / 2% isopropanol / 2% pentanol / 50mM CaCl_2 or 3% SDS and 1ml dodecane were added to each vial. Addition of pentanol was made to reach the desired pentanol concentration. Samples

were equilibrated on a rotator for eight hours and then equilibrated for 24h to 1 week to achieve complete phase separation. The pentanol and isopropanol concentrations in the oil, Type I microemulsion phase (aqueous phase plus interface phase), and dodecane in the type I microemulsion phase were analyzed by GC.

Calculation of Alcohol Partitioning

The interfacial region between oil and water containing only surfactant and alcohol can be treated as a separate phase. Alcohol partitioning among the aqueous phase, oil phase, and micelle interface has been described using equilibrium partitioning coupled with a pseudophase model (Lalanne et al., 1984; Biais et al., 1988; Voca et al., 1988). Alcohols such as pentanol tend to self-associate in the oil phase (Prigogine and Defay, 1965), such that monomers tend to form dimers, trimers, and so on. Self association can be described by the following equations:





where K is defined as

$$K = \frac{\phi_{i+1}^o}{\phi_1^o \phi_i^o} \quad 2-2$$

and ϕ_i^o is the volume fraction of the i th association unit in the oil phase. The total alcohol volume fraction, ϕ_A^o , is related to ϕ_i^o ,

$$\phi_A^o = \phi_1^o + \phi_2^o + \phi_3^o + \dots \phi_i^o + \dots \quad 2-3$$

Substituting equation (2-2) into (2-3) gives

$$\phi_A^o = \phi_1^o (1 + K\phi_1^o + K^2\phi_1^{o^2} + \dots K^i\phi_1^{o^i} + \dots) \quad 2-4$$

The expression in parentheses on the RHS of equation (2-4) sums to $1/(1-K\phi_1^o)$. Rearranging (2-4) with this substitution leads to

$$\phi_1^o = \frac{\phi_A^o}{\phi_A^o K + 1} \quad 2-5$$

Equation (2-5) can be rearranged to:

$$K = \frac{100\rho(C_A^o - C_1^o)}{C_A^o C_1^o} \quad 2-6$$

where C_A^o represents alcohol concentrations in the oil phase (g/dL) and ρ is the density of pure alcohol and is assumed to be the density of alcohol in the oil phase.

The alcohol in the aqueous phase is in equilibrium with alcohol monomers in the oil phase with a constant K' :

$$K' = \frac{C_1^o}{C_A^w} \quad 2-7$$

where C_A^w is the alcohol concentration (g/dL) in the aqueous phase.

The relation between total alcohol concentrations in the aqueous and oil phases is as follows:

$$C_{K_A} = \frac{C_A^o}{C_A^w} \quad 2-8$$

Substitution of equation (2-7) and (2-8) into (2-6) yields:

$$C_{K_A} = \frac{KK'}{100\rho} C_A^o + K' \quad 2-9$$

Thus, C_{K_A} is linearly related to the total alcohol concentration in the oil phase. The partitioning

coefficients, K and K' , can be calculated from the slope and intercept of a plot of cK_A vs C_A^o .

If we treat the interface as a bulk phase, the mole fraction-based partition coefficient of alcohol between the aqueous phase and micelle can be defined as:

$${}^xK_A = \frac{X_A^m}{X_A^w} \quad 2-10$$

where X_A^m is the mole fraction of alcohol in the interface and X_A^w is the mole fraction of alcohol in the aqueous phase. The xK_A can be calculated by measuring the alcohol concentration in the oil and microemulsion phases, and using the partitioning coefficients K , K' , and cK_A .

Results and Discussion

Alcohol Partitioning in Water/Dodecane Systems

Equation 2-9 predicts a linear relationship between cK_A and C_A^o . Figure 2-2 shows that this was true for the partitioning of pentanol between water and dodecane (with no surfactant present). According to equation 2-9, the intercept in Figure 2-2 is K' and the slope is $K K' / 100\rho$. Thus, slope

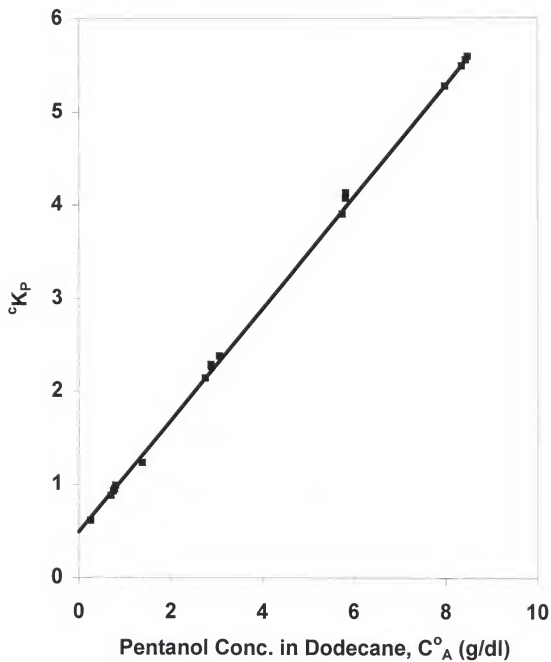


Figure 2-2. The pentanol partitioning coefficient between oil and aqueous phases (cK_p) as a function of the total pentanol concentration in the oil phase (C°_A).

and intercept data shown in Figure 2-2 can be used to calculate K and K' for the water/dodecane system.

Table 2-1 summarizes the pentanol partitioning data for water-dodecane systems. The subscript "A" on cK_A has been replaced with a "P" to indicate that pentanol is the alcohol being considered. Note that isopropanol had no effect on pentanol partitioning between aqueous and oil phases. This may result from the fact that isopropanol is very insoluble in dodecane. Using the overall slope and intercept data in Table 1 gave values for the self-association constant, K , and the partitioning coefficient for alcohol monomers, K' , of 99 and 0.49, respectively.

The partitioning coefficient of isopropanol between aqueous and oil phases, ${}^cK_{IPA}$, was 0.02 in the absence of pentanol regardless of isopropanol concentration (Table 2-2). This suggests that isopropanol does not self-associate in dodecane, a likely result of the high water solubility and low surface activity of isopropanol. The low concentration of isopropanol in the oil phase and the fact that isopropanol is a branched-chain molecule may decrease its ability to self-associate.

Table 2-1. Partition coefficients for pentanol between water and dodecane at different isopropanol concentrations.

Isopropanol conc. %	cK_p VS C_p^o	R^2	K	K'
0	$^cK_p = 0.60C_p^o + 0.48$	0.998	101	0.48
0.5	$^cK_p = 0.60C_p^o + 0.51$	0.999	95	0.51
1	$^cK_p = 0.61C_p^o + 0.46$	0.999	107	0.46
1.5	$^cK_p = 0.60C_p^o + 0.54$	0.999	90	0.54
2	$^cK_p = 0.61C_p^o + 0.50$	0.999	99	0.50
over all	$^cK_p = 0.60C_p^o + 0.49$	0.999	99	0.49

Table 2-2. Partition coefficients for isopropanol between water and dodecane at different pentanol concentrations.

Pentanol Conc.(%)	Isopropanol Conc.(%)	$^cK_{IPA}$	R^2
0	0.5-2	$^cK_{IPA} = 0.02$	-
0.5-4	0.5	$^cK_{IPA} = 0.024C_p^o + 0.018$	0.993
0.5-4	1	$^cK_{IPA} = 0.024C_p^o + 0.020$	0.999
0.5-4	1.5	$^cK_{IPA} = 0.024C_p^o + 0.021$	0.999
0.5-4	2	$^cK_{IPA} = 0.024C_p^o + 0.018$	0.999
over all		$^cK_{IPA} = 0.024C_p^o + 0.019$	0.997

When pentanol was present in the system, the partitioning of isopropanol between the aqueous and oil phases was linearly related to the pentanol concentration in the oil phase (Table 2-2). The effect of pentanol on isopropanol partitioning was constant for pentanol concentrations as high as 4% and isopropanol concentrations as high as 2%. These results suggest that isopropanol associates with pentanol in dodecane.

Alcohol Partitioning in Water/Dodecane/SDS System

Table 2-3 shows the alcohol partitioning data obtained in Winsor Type I microemulsion systems. Alcohol concentrations in the oil phase (dodecane) were measured; however, aqueous and interfacial alcohol concentrations were calculated from the pseudophase model in Figure 2-1 and using values for cK_A (Tables 2-1 and 2-2.)

Partitioning of alcohol between the aqueous and interfacial phases was nearly constant. xK_p averaged 229 with 50 mM CaCl_2 , and 222 without CaCl_2 present in the microemulsions; ${}^xK_{\text{IPA}}$, 8.7 (Figure 2-3). Increasing the pentanol concentration had no effect on IPA partitioning, and vice versa, indicating little or no competition between these two alcohols for the interfacial region.

Table 2-3. Alcohol partitioning and dodecane solubilization data for Winsor Type I microemulsions.

SDS	In Oil Phase		Aqueous		Interfacial		xK_A		Dodecane In ME g/dL
	Pentanol	IPA g/dL	Pentanol	IPA	Pentanol	IPA	Pentanol	IPA	
3.00	2.85	---	1.30	---	0.59	---	221	---	0.78
3.00	3.27	---	1.33	---	0.63	---	226	---	1.01
3.00	7.90	---	1.51	---	0.70	---	224	---	1.21
3.00	9.43	---	1.53	---	0.71	---	224	---	1.49
3.00	14.5	---	1.58	---	0.72	---	219	---	1.63
3.00	19.5	---	1.60	---	0.74	---	223	---	1.72
3.00	20.9	---	1.60	---	0.74	---	222	---	1.74
3.00	21.2	---	1.60	---	0.74	---	222	---	1.74
3.00	21.2	---	1.60	---	0.75	---	224	---	1.74
3.00	23.0	---	1.61	---	0.74	---	222	---	1.64
3.00	24.3	---	1.61	---	0.75	---	222	---	1.77
3.00	25.9	---	1.62	---	0.73	---	218	---	1.76
4.50	2.28	0.14	1.23	1.93	0.59	0.05	229	8.30	3.01
4.50	3.29	0.19	1.34	1.91	0.65	0.04	231	7.35	4.27
4.50	4.55	0.24	1.41	1.88	0.69	0.04	232	7.44	5.22
4.50	5.78	0.29	1.46	1.82	0.71	0.05	231	8.75	5.91
4.50	7.80	0.37	1.51	1.80	0.74	0.04	231	7.88	7.32
4.50	2.73	0.17	1.28	1.95	0.61	0.04	226	7.39	3.10
4.50	3.87	0.21	1.38	1.87	0.66	0.06	226	10.1	4.62
4.50	5.87	0.29	1.46	1.81	0.69	0.06	223	11.1	5.51
4.50	7.51	0.36	1.50	1.79	0.73	0.06	229	9.91	7.53

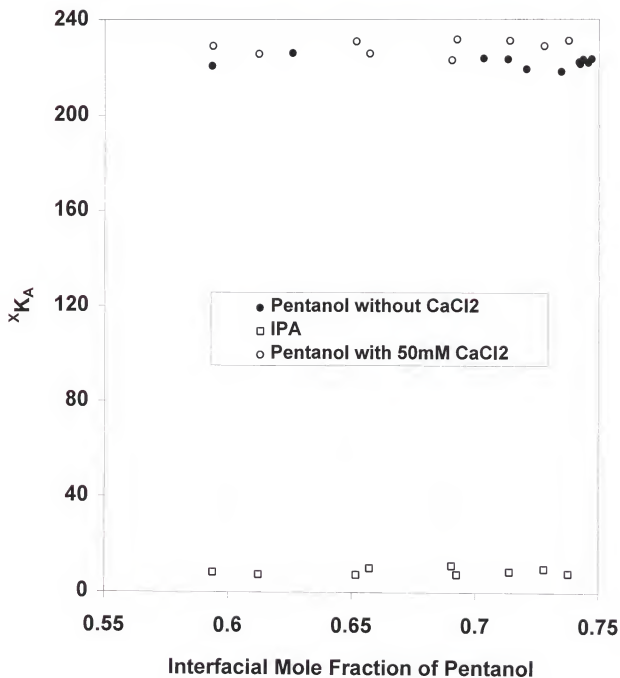


Figure 2-3. The mole fraction-based partitioning coefficient of pentanol and IPA between aqueous and micelle interfacial phases as a function of the mole fraction of pentanol in the interface. Open symbols (\circ, \square) with 50 mM CaCl_2 , and solid symbols (\bullet) without CaCl_2 .

At 3% SDS, the interface appears to "saturate" with pentanol at a mole ratio of 3:1 (pentanol/SDS). Additional pentanol partitions strongly into the oil phase, reaching concentrations in excess of 25 g/dL (Figure 2-4). At 4.5% SDS, more pentanol can go into the interface, but pentanol still showed a strong tendency to saturate the interface at a mole ratio of about 3:1 pentanol to SDS (Figure 2-4).

Oil solubilization increased linearly with the pentanol mole fraction in the interface, at least for mole fractions of 0.59 and above (Figures 2-5, and 2-6). Since pentanol concentrations in the oil phase increased by a factor of about 10 in this region, it could be argued that dodecane solubilization is controlled by the interfacial pentanol concentration and not by the total pentanol concentration in the system.

It has been reported that relatively lower amounts of alcohol can achieve phase transformations (i.e., from L1 to L1+D) at high surfactant concentrations as spherical micelles grow to become rod-like micelles. This has been investigated using surfactant solution conductivity, viscosity, speed of sound, small angle neutron scattering and dynamic light scattering (Forland et al., 1993). They found that micelles

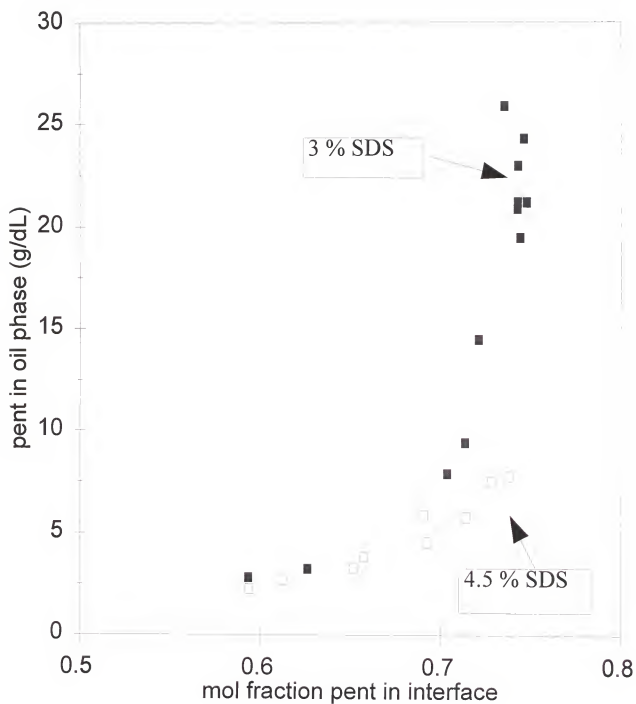


Figure 2-4. The total pentanol concentration in the oil phase as a function of the mole fraction of pentanol in the interface.

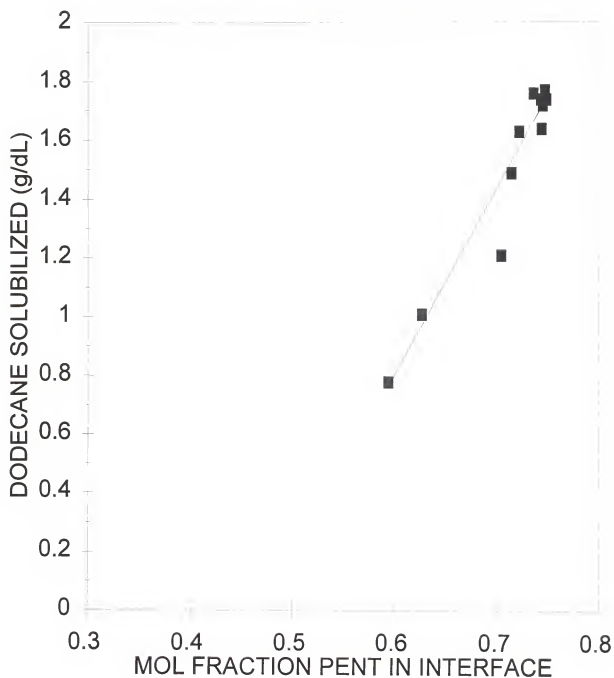


Figure 2-5. Dodecane solubilization in the Type I microemulsion with 3% SDS as a function of the mole fraction of pentanol in the interface.

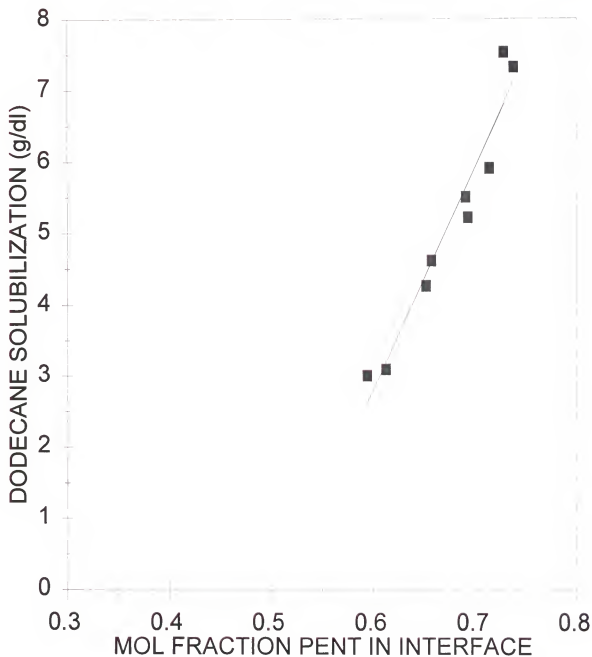


Figure 2-6. Dodecane solubilization in the Type I microemulsion with 4.5% SDS/50 mM CaCl_2 as a function of the mole fraction of pentanol in the interface.

may change from sphere to rod-like as the SDS concentration increases to above 5%. The effect of pentanol on oil solubilization is also quite different in these two micelle regions (see chapter 2). As alcohol partitioning behavior between the aqueous and interfacial phases in these two regions may not be the same, alcohol partitioning behavior at high SDS concentrations needs further study.

Conclusions

The pentanol partitioning coefficient between the aqueous and interfacial phases remained nearly constant as long as the mole fraction of pentanol was in the range 0.59 to 0.75. Pentanol may saturate the interfacial phase at a mole ratio of 1:3, SDS to pentanol. Dodecane solubilization increased linearly with the pentanol mole fraction in the interface. Therefore, the pentanol in this surfactant system is acting as a cosurfactant and not a cosolvent. Pentanol tends to self-associate in the oil phase, while IPA appears to co-associate with pentanol in the oil phase rather than to self-associate. Low concentrations of isopropanol appear to have no significant effect on pentanol partitioning among the aqueous, interfacial, and oil phases.

CHAPTER 3

TWO-REGION MODEL OF ALCOHOL IN NAPL SOLUBILIZATION

Introduction

When using a microemulsion to solubilize and/or mobilize NAPL for contaminated aquifer remediation, at least one alcohol is usually included in the microemulsion system (Desnoyers et al., 1983; Martel et al., 1993; Martel and Gelinas, 1996). An alcohol acting as a cosurfactant in the microemulsion interface can increase oil solubilization and decrease the interfacial tension. Martel and coworkers have reported that the average optimum ratio of surfactant and cosurfactant is near 1:1, but that variability of the optimum ratio becomes quite large when different surfactant/cosurfactant concentrations are used in the microemulsion systems. This may be because only the cosurfactant in the interface contributes to the increase of oil solubilization and decrease of IFTs. Thus, the amount of cosurfactant, or the molar ratio of surfactant to cosurfactant, in the interface is more important

to a microemulsion system than the total amount of cosurfactant in the system.

In the w/o microemulsion systems with long-chain alcohol cosurfactants (C6 or higher), the Schulman-Bowcott plot has been used to calculate the ratio of surfactant and alcohol at the interface (Bowcott and Schulman, 1955; Pithapurwala and Shah, 1984). In the w/o microemulsion, water solubilization reached its maximum at a 1:3 molecular ratio of interfacial potassium oleate to hexanol (Bowcott and Schulman, 1955; Shah, 1971), and the emulsion is most stable at a 1:3 SDS to cetyl alcohol molar ratio (Choi et al., 1985; Wang et al., 1996). Shah (1971) proposed that the hexagonal arrangement of a 1:3 molecular ratio provides the closest packing of molecules and results in the highest solubilization, and greatest stability, of the system.

Since the oil phase of w/o microemulsions acts as a sink for surfactant and cosurfactant, the o/w microemulsion is always used for NAPL remediation. Whether this 1:3 surfactant to cosurfactant molar interfacial ratio is also optimum for o/w microemulsions has not been reported. Equilibrium partitioning, coupled with a pseudophase phase model, provides us a tool to calculate the molecular ratio of surfactant to

cosurfactant at the interface (see chapter 1), and to examine the optimum surfactant to cosurfactant ratio for o/w microemulsions.

Interfacial tension is related to oil solubilization. Those micellar solutions which solubilize the largest quantities of oil will exhibit the lowest interfacial tension (Bourrel and Schechter, 1988). The reciprocal relationship between the solubilization parameter (S), expressed as volume of oil or water solubilized per unit volume of neat surfactant, and interfacial tension (γ) has been quantified by Chun Huh (1979). Using a thermodynamic approach, it has been predicted that

$$\gamma s^2 = \text{constant}$$

with γ in dynes/cm and s in ml/ml. It has been reported that the constant is approximately 0.35 with some variability (Graciaa et al., 1982, 1983a; Barakat et al., 1983) when a branched-chain alcohol is included in the system. However, a cosurfactant was not included in the equation and therefore any variability may be due to the alcohol partitioning into the interface (Huh, 1979). Since alcohol, especially a medium single-chain alcohol such as pentanol, acts as a surfactant at the interface, the interfacial pentanol should be taken as a

surfactant for better prediction of the interfacial tension.

In this work, the effect of the molecular ratio of SDS and pentanol at the micellar interface has been studied in the L1 (normal micelle) region. Salt and isopropanol effects on the solubilization of nonpolar oil (dodecane), polar oil (PCE), and a nonpolar and polar mixture (gasoline) have been studied as well. As a result of these studies a two-region model of pentanol partitioning in the micelle has been proposed. There are two regions in a micelle for pentanol partitioning (Figure 3-1; Figure 3-2). In region I, which is the micelle interface, pentanol acts as a cosurfactant. In region II, which is the micelle inner core, pentanol acts as a polar oil. When the molar fraction of interfacial pentanol is less than 0.75, pentanol prefers to partition into region I. When pentanol saturates the micelle interface, it prefers to partition into region II.

Materials and Methods

SDS was purchased from Fisher Scientific and used without further purification. Pentanol, isopropanol, NaCl, KCl and CaCl_2 were also obtained from Fisher Scientific, and had a

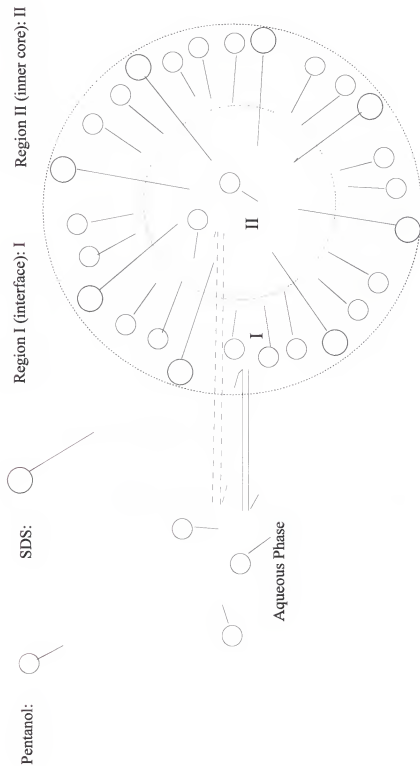


Figure 3-1. Two-region model of alcohol partitioning in oil solubilization before interfacial pentanol saturation.

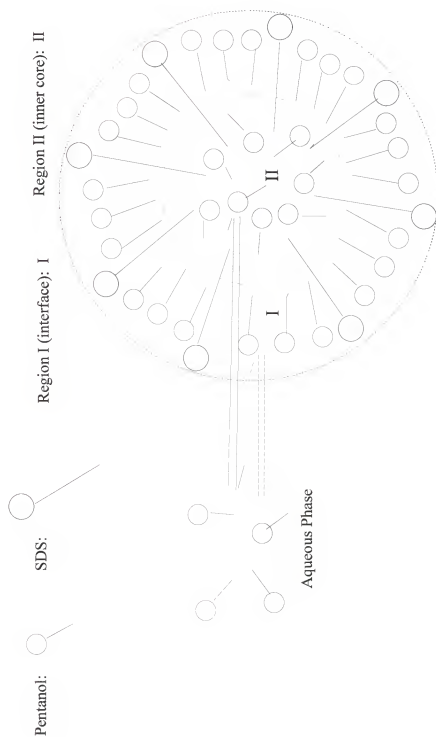


Figure 3-2. Two-region model of alcohol partitioning in oil solubilization after interfacial pentanol saturation.

purity of 99+%. Dodecane and PCE were purchased from Sigma Chemicals at 99+% purity.

Oil solubilization was determined using a titration method. The solubilization of dodecane, PCE, and gasoline in o/w microemulsions were determined for a designated SDS concentration with or without salt (NaCl , KCl or CaCl_2) as a function of the amount of pentanol. Four or 8ml of SDS and pentanol solution were transferred to a 5ml or 10ml vial. Oil was titrated into the solution, drop by drop, until the solution became hazy, turbid, or two-phased. After each addition of NAPL, the vials were reweighed and the amount of NAPL added calculated from the difference between initial and final weights.

The phase transform boundary of the precursor (the SDS/pentanol/water or brine mixture) was also determined by titration. Four ml of solution with different SDS concentrations were added to a 5 ml vial. Pentanol was titrated into the solution, drop by drop, until the solution become hazy, turbid, or two-phased.

Viscosity of the surfactant and cosurfactant solutions was measured using a capillary viscosity meter at 24 °C with deionized water, propanol, and butanol as standards. The

viscosity and density of the standards were taken from the CRC Handbook of Chemistry and Physics (1988). Sample viscosity is related to the time (t) required for a given volume of sample to flow through the capillary:

$$\eta/\rho = v_k = at + b/t$$

where η is the dynamic viscosity, ρ the density of the fluid, v_k the kinematic viscosity, and a and b instrument constants. The last term is related to the kinetic energy correction and is negligible for flow times over about two minutes. The plot of kinematic viscosity of the standards vs time is shown in Figure 3-3.

Conductivity of the surfactant solution was determined with a digital electrical conductivity meter (Model 1054, Amber Science Inc).

Results and Discussion

The solubilization of dodecane, PCE, and gasoline in an o/w microemulsion, with SDS concentrations less than 5%, increases until the molar ratio of SDS and pentanol at the interface approaches 1:3 (Figures 3-4, 3-5, 3-6, 3-7, and 3-8). As more pentanol is added to the system the dodecane solubilization first reaches a plateau and then decreases.

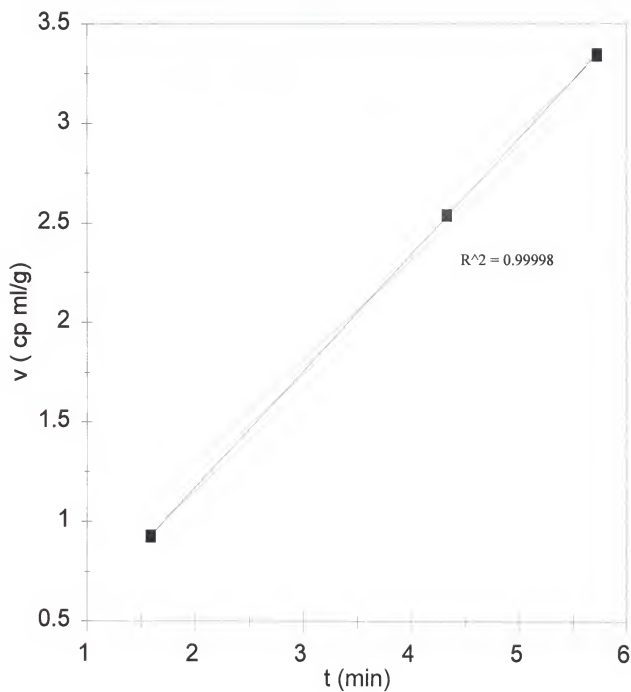


Figure 3-3. The calibration curve for viscosity measurements.

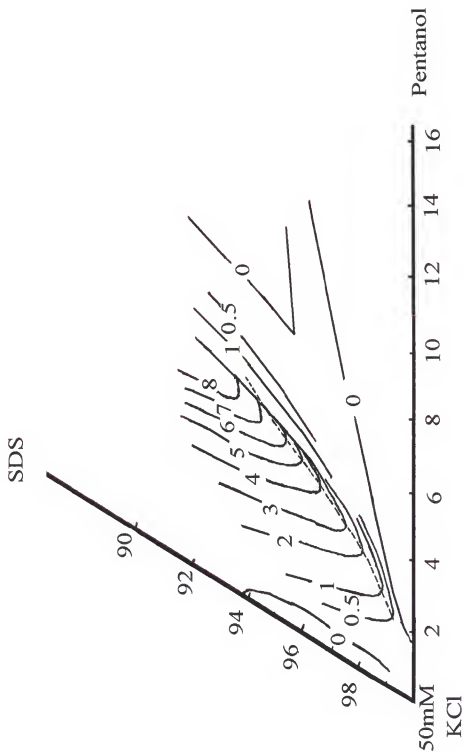


Figure 3-4. Gasoline solubilization contours for the SDS/pentanol/50mM KCl system. The dotted line represents the 1:3 SDS and pentanol molar ratio at the interface as determined by the pseudophase model.

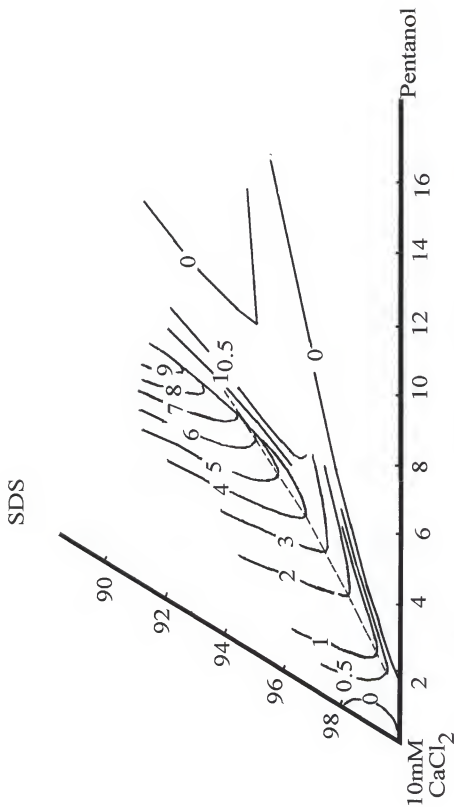


Figure 3-5. Gasoline solubilization contours for the SDS/pentanol/10mM CaCl₂ system. The dotted line represents the 1:3 SDS and pentanol molar ratio at the interface as determined by the pseudophase model.

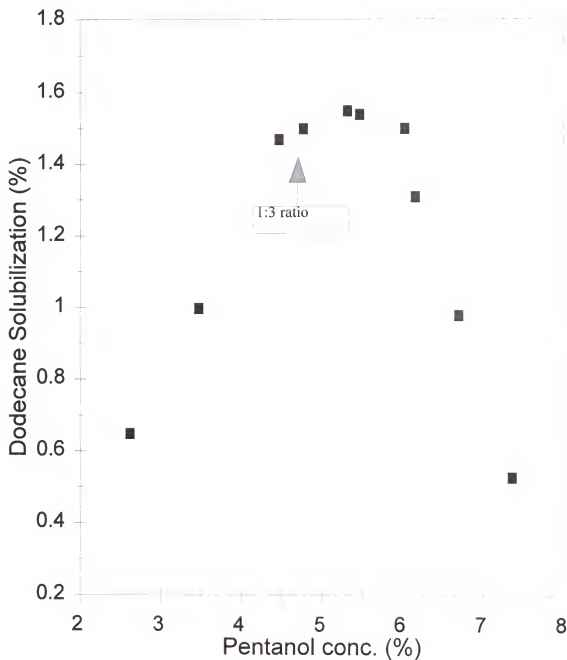


Figure 3-6. The effect of pentanol on dodecane solubilization by 3% SDS/water. The arrow indicates the pentanol concentration where the molar ratio of SDS and pentanol at the interface is 1:3 as determined by the pseudophase model.

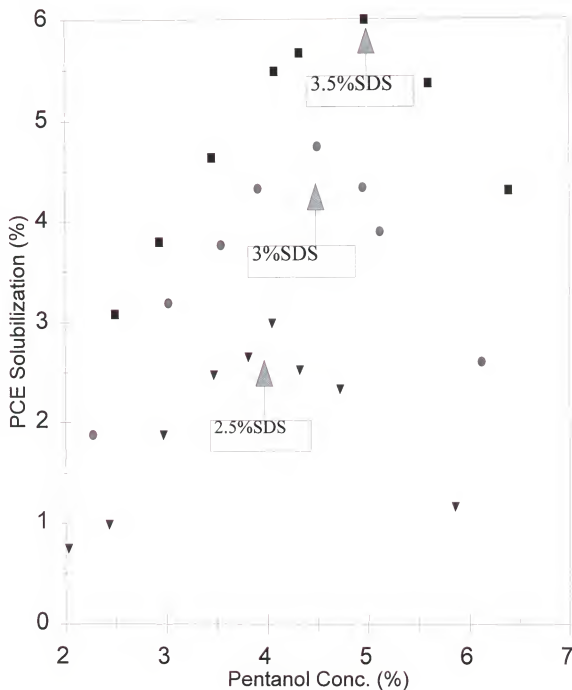


Figure 3-7. The effect of pentanol on PCE solubilization at three SDS concentrations: ▼ 2.5% SDS; ● 3% SDS; and ▲ 3.5 % SDS. The arrows indicate pentanol concentrations where the molar ratio of SDS and pentanol at the interface is 1:3 as determined by the pseudophase model.

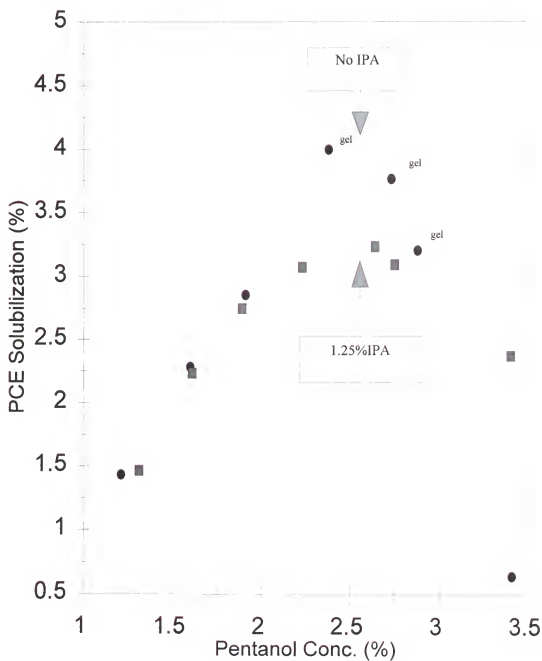


Figure 3-8. The effect of pentanol and IPA on PCE solubilization by 1% SDS/100mM NaCl. ■ 1.25% IPA. ● no IPA. The arrows indicate pentanol concentrations where the molar ratio of SDS and pentanol at the interface is 1:3 as determined by the pseudophase model.

PCE and gasoline solubilization have no such plateau. The results suggest that pentanol acts as a cosurfactant before reaching interfacial saturation. When the molar fraction of pentanol at the interface reaches 0.75, the interface is probably saturated with alcohol molecules. This is indicated by the highest pentanol molar fraction in the interface being almost 0.75 (chapter 2). Aoudia and coauthors (1991) also reported that butanol may saturate the sodium 4-dodecylbenzenesulfonate micelle interface at the same mole fraction. This was determined by measuring the degree of polarization as a function of the ratio of butanol. The electrical conductivity data (Figure 3-9), which will be discussed later, may also indirectly support this conclusion. Shah (1971) proposed that the interface is most stable and the interaction between interface and oil is strongest at a 1:3 molecular ratio, due to the close molecular packing of the hexagonal arrangement. After pentanol saturates the interface, it will partition preferentially into the micelle inner core and act as a polar oil. Therefore, the solubilization of polar oils, such as PCE and gasoline, can be expected to decrease as excess amounts of polar alcohol partitions into the inner core of the microemulsion. The plateau region in

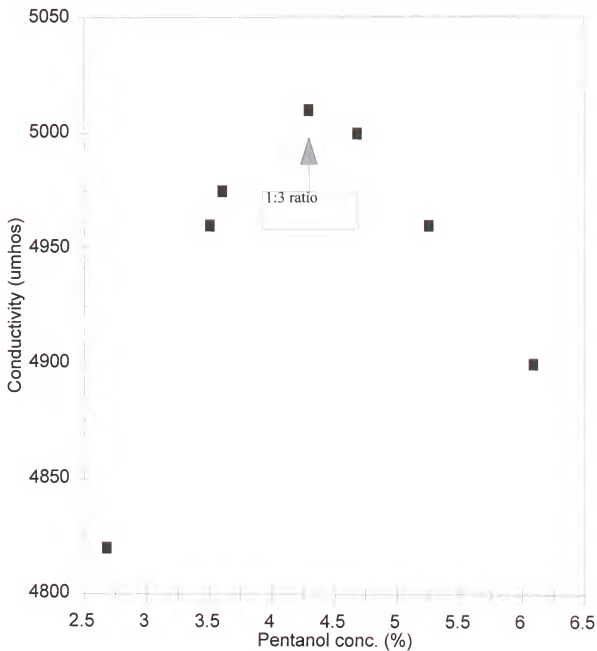


Figure 3-9. Conductivity of 3% SDS solution as a function of pentanol concentration. The arrow indicates pentanol concentration where the molar ratio of SDS and pentanol at the interface is 1:3 as determined by the pseudophase model.

nonpolar oil solubilization, which is a function of the amount of pentanol added to the microemulsion system, may be due to the nonpolar oil gradually becoming more polar as pentanol partitions into the oil phase. The solubilization of nonpolar oil after interfacial pentanol saturation may be due to both decreased hydrophobicity of the nonpolar oil and competition with pentanol for space in the micelle inner core.

Salt can decrease the repelling force between the negatively charged surfactant heads in the micelle interface by masking surfactant charge and causing closer packing of the interface. When the interfacial mole fraction of pentanol is less than 0.75, oil solubilization can be expected to increase after the addition of salt (Figure 3-8). Salt may decrease the solubilization of oil, when the interface palisade layer is alcohol saturated, by inducing the formation of a rigid phase. In contrast, isopropanol has almost no effect on oil solubilization at low pentanol interfacial molar fractions. Having very low surface activity, isopropanol slightly decreases oil solubilization near the pentanol interfacial saturation point. Beyond this point, solubilization decreases, but only at a low rate with IPA present. Small amounts of isopropanol in the interface have little effect on the

interface when pentanol interfacial concentrations are less than saturation. The branched short-chain in isopropanol tends to destabilize the interface as pentanol approaches interfacial saturation, and also reduces some of the salt effect on the interface. The opposite effect of isopropanol and salt on oil solubilization can be anticipated by the effect of salt and isopropanol on surfactant solution viscosity and gel formation. Salt increases the viscosity of surfactant solutions and induces gel formation as pentanol approaches interfacial saturation. The addition of isopropanol prevents both these conditions by destabilizing the interface.

When SDS concentration is less than 5%, the solubilization of polar and nonpolar oil reaches its maximum at a 1:3 molar interfacial SDS and pentanol ratio. This ratio of 1:3 is thought to be the result of hexagonal molecular packing at the interface. As more pentanol is added to the system it will penetrate into the inner micelle core, acting as a polar oil to maintain the lowest energy status. However, when SDS concentration is above 5% and the same partitioning coefficient is used to calculate the interfacial pentanol concentration, the maximum solubilization of gasoline is no longer at a 1:3 molar ratio. There is no guarantee that the

partitioning coefficient is the same for both these systems, and the 1:3 ratio may not be applicable to high surfactant concentrations due to the formation of different micelle structures at high SDS concentrations.

Electrical conductivity of the SDS solution increases as the interfacial SDS and pentanol ratio approaches 1:3, and then decreases as more pentanol is added to the system (Fig 3-9). The monomers and micelles of SDS each contribute to the conductivity of the surfactant solution. There are at least four factors that effect the conductivity of the surfactant solution. First, as alcohol is added to surfactant aqueous solution, alcohol will dilute the charge density of the micelle and increase counter ion dissociation from the interface (Manable et al., 1980; Attwood et al., 1995), which will increase the conductivity of the solution. Second, medium chain alcohols decrease the CMC, which is the monomer concentration in the solution (Hayase and Hayano, 1978; Muto et al., 1989; Attwood et al., 1995). Therefore, solution conductivity will decrease as the monomer concentration decreases. Third, the aggregate number of micelles, which is also related to the solution conductivity, increases as medium-chain alcohol concentration increases (Forland et al.,

1993). Finally, when the surfactant concentration is high or the alcohol chain length is long, it can be expected that the micelles will transform from spheres to rod-like shapes (Forland et al., 1993) with an accompanying conductivity decrease. The viscosity data (Figure 3-10), and the L1 (normal micelle)/ L1+L2 (normal micelle+reverse micelle) and L1 (normal micelle)/L1+D (normal micelle+lamellar) phase boundaries of the SDS/pentanol system (Clausse et al., 1987; Guerinand and Bellocq, 1988) suggest that the addition of pentanol will not change spherical micelles to rod-like form at low SDS concentrations (less than 5%). The size of the micelle will increase and finally break to form the L1+L2 two-phase systems as the pentanol concentration increases. The initial increase in the conductivity may be due to ionization of the surfactant as alcohol incorporates into the micelle to form a mixed micelle. The decrease in conductivity at about the 1:3 SDS and pentanol molar ratio appears to be due to pentanol penetrating the micellar inner core and acting as a polar oil, in conjunction with an increase in the micelle aggregate number and a decrease in the CMC. This is because pentanol being solubilized inside the micelle inner core may not effect counter-ion dissociation. The maximum conductivity

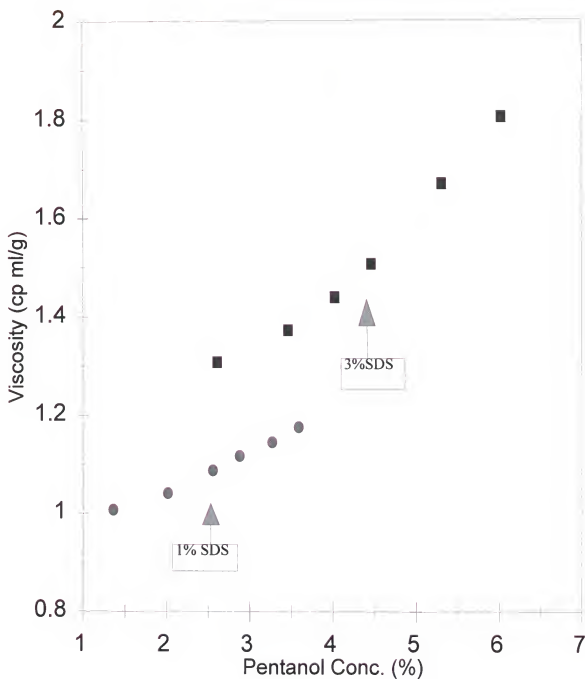


Figure 3-10. Viscosity of SDS solutions as a function of pentanol concentration. ■ represents 3% SDS. ● represents 1% SDS. The arrows indicate pentanol concentrations where the molar ratio of SDS and pentanol at the interface is 1:3 as determined by the pseudophase model.

for the hexadecyltrimethylammonium bromide and hexanol system also has been found to be near a 1:3 surfactant and alcohol molar ratio, when the surfactant concentration is low (Vikholm et al., 1987).

Conclusions

The solubilization of oils and the conductivity of SDS solutions both reach their maximum at a 1:3 molar interfacial SDS to pentanol ratio. A two-region pentanol partitioning model is proposed in which alcohol partitions into the interface and acts as a cosurfactant at interfacial mole fraction up to 0.75. After interfacial mole fractions reach 0.75, however, the alcohol penetrates into the inner core, and acts as a polar oil. This model applies to the L1 region and to SDS concentrations that are below 5%. The model is inferred from indirect evidence, and needs further molecular level study for verification.

CHAPTER 4

SORPTION OF SDS AND PENTANOL ON SOILS

Introduction

Microemulsions show significant potential for application in enhancing the remediation of NAPL contaminated aquifers. Effectiveness of the microemulsion in remediation depends largely on surfactant/cosurfactant's interactions with not only the NAPL but also the aquifer media. Surfactant sorption by soil may not only reduce surfactant/cosurfactant remediation efficiency by decreasing the amount of surfactant available for solubilization of NAPL, and by reducing hydraulic conductivity of the aquifer media, but also by inhibiting biodegradation after aquifer remediation. Precipitation has been recognized as the main anionic surfactant sorption mechanism for soils (Jafvert and Heath, 1991; West and Harwell, 1992). Studies involving another anionic surfactant sorption mechanism, adsorption, have been mostly focused on positively charged sorbents such as alumina

(Blokhus, 1990; Blokhus and Sjoblom, 1990; Sjoblom et al., 1990; Ruths et al., 1991; Fu et al., 1995; Forland et al., 1996) and rutile (Bohmer and Koopal 1992; Koopal et al., 1995). It is unclear from the literature which sorption mechanism, adsorption or precipitation, will dominate an anionic surfactant/high iron oxide soil system. The effect of a cosurfactant on surfactant sorption on soils, in general, is also not well documented.

The adsorption isotherm for an anionic surfactant on a metal oxide surface can be described as Langmuir-like in the sense that maximum adsorption occurs at the CMC. Four regions on the isotherm have been identified (Somasundaran and Fuerstenau, 1966; Scamehorn et al., 1982; Harwell et al., 1985; Koopal et al., 1995). Region I adsorption obeys Henry's Law, with the adsorption of isolated molecules. The slope of the isotherm increases sharply when going from Region I into Region II, which has been attributed to the formation of surface aggregates. These aggregates are "head on" adsorbed surfactant molecules (hemimicelles), or both "head on" and "head off" adsorbed surfactant molecules (admimicelles), or something in between. It has been proposed that the change in slope between Region II and Region III may be due to

increasing competition for the remaining surface area (Levitz and Van Damme, 1986), a more complete transition from hemimicelles to admicelles (Chandar et al., 1987), or heterogeneities in the substrate surface (Harwell et al., 1985). Region IV occurs once the CMC is reached, and for many surfactants the adsorption in this region is nearly constant for all concentrations above the CMC, presumably because the micelles form a sink of nearly constant chemical potential. The primary forces involved in the formation of ionic surfactant aggregates at the liquid/solid interface are analogous to those in micelles, including Columbic interactions between the surfactant ionic head and the charged surface, and the surfactant tail-tail hydrophobic interaction.

Adsorption of cosurfactants on metal oxide surfaces only takes place if the surfactant is already present at the solid surface. Cosurfactants, which can effect the interfacial properties of a surfactant system, also have an impact on surfactant adsorption. Lee et al. (1990) investigated the adsorption of SDS and alcohol on positively charged alumina. Their results indicated that, in the presence of alcohols, there was an increase in surfactant adsorption below the CMC, with a decrease in the adsorption plateau of the surfactant.

O'Haver and Harwell(1995) also found similar results. Their study also showed that with alcohol in the system, there was a higher adsorption density of SDS in the Henry's region than without alcohol. They concluded that this resulted from the coadsorption of small surfactant monomer-alcohol aggregates of unknown size in Region I. The concentration of SDS at this point in Region I is so close to Region II in their study, it is possible that the adsorption isotherm was shifted from Region I to Region II due to HMC (hemimicelle concentration) reduction with the addition of alcohol. In Region I, alcohol should have little or no effect on sorbed SDS due to low surface coverage and, therefore, its effect on adsorption should be through interactions primarily in the solution phase.

The precipitation of ionic surfactants in solution due to the presence of divalent cations has been extensively studied (Somasundaran et al., 1984; Kallay et al., 1985, 1986; Matheson et al. 1985a; Stellner and Scamehorn, 1989a). Below the CMC, precipitation is controlled by the solubility of divalent cationic surfactants. Above the CMC, formation of the precipitate phase is effected by the interactions of cations with micelles, with the ion complexation between

micelle and divalent cations playing a significant role. Addition of nonionic surfactant to the solution causes the formation of mixed micelles, thereby increasing the hardness tolerance of the ionic surfactant (Matheson et al., 1985b; Fan et al., 1988; Stellner and Scamehorn, 1989b).

Jafvert and Heath (1991) used a similar approach to study the precipitation of ionic surfactant in soils and sediments. They adapted results obtained from pure solution studies to calculate the precipitation boundary, and found that calculated calcium concentrations agreed with their experimental values except at low SDS concentrations. Schweich and coauthors (Schweich and Sardin, 1985; Krebs et al., 1987) on the other hand, included cation exchange on a mineral surface and solubilization of trace calcite in a predictive model for the transport of anionic surfactant in a 1-D column at a surfactant concentration below the CMC.

The effect of different soil properties on ionic surfactant sorption has not been studied in detail, and the effect of a cosurfactant on ionic surfactant sorption also has not been well addressed. In this chapter, surfactant/cosurfactant (SDS/pentanol) sorption behavior (adsorption and precipitation) on different soils at

different concentrations will be investigated. A combination of aqueous solution anionic precipitation theory and carbonate dissolution will be used to predict surfactant precipitation. The effect of pentanol on SDS sorption will also be examined.

Theory

When an anionic surfactant is in equilibrium with a sand aquifer media, the ionic surfactant is present in several states or phases which include (i) monomers, (ii) micelles, (iii) precipitates, and (iv) adsorbed monomers and aggregates such as hemimicelles and admicelles. Soil properties have a strong influence on these states or phases, especially with respect to precipitation and adsorption.

When a soil has very low clay and organic carbon contents and relatively high pH, such as sandy calcareous soils, surfactant adsorption may be insignificant when compared to precipitation. It can be assumed that Ca and Mg are the dominant cationic species in these soils, as they are mainly from the dissolution of various carbonates. By comparison, exchangeable Ca and Mg from ion-exchange sites can be assumed to be insignificant. From the solubility products of $\text{Ca}(\text{DS})_2$, $\text{Mg}(\text{DS})_2$, CaCO_3 , MgCO_3 , and the concentration of Ca and Mg in

most calcareous soils, Ca ion can be assumed to control both surfactant precipitate formation and carbonate dissolution.

The following equations are from carbonate solubilization, and aqueous solution precipitation theory. Since the soil, water, and surfactant are in a closed system, a finite amount of Ca ion can be dissolved from existing carbonates. Thus, the Ca ions available to precipitate with DS are also limited. The sorption of ionic surfactant in calcareous soil media can be divided into three regions (Figure 4-1). In Region a, the Ca concentration in solution is controlled by carbonate dissolution. Because the product of DS^- and Ca^{2+} activity in solution is less than the solubility product of $Ca(DS)_2$ in this region, SDS sorption is mainly due to adsorption. The Ca concentration in the solution should be controlled by the carbonate solubilization process, which can be defined by the solubility product of calcium carbonate and the ionization constants of carbonic acid and water. The solution also can be assumed to be ideal, since the ion concentrations are very low, with

$$K_1 = [Ca^{2+}] [CO_3^{2-}] \quad (4-1)$$

where the $[]$ indicates aqueous concentrations. Further more,

$$K_2 = [H^+] [HCO_3^-] / [H_2CO_3] \quad (4-2)$$

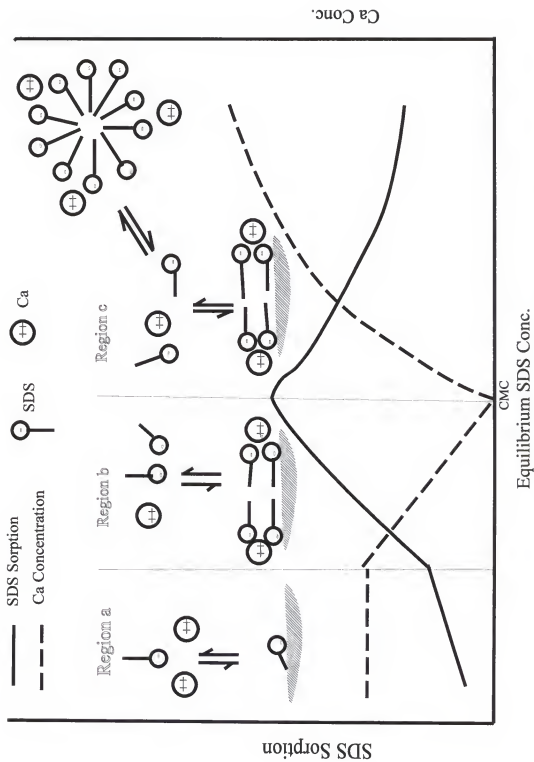


Figure 4-1. Anionic surfactant sorption by calcareous soils.

$$K_3 = [\text{H}^+] [\text{CO}_3^{2-}] / [\text{HCO}_3^-] \quad (4-3)$$

$$K_4 = [\text{H}^+] [\text{OH}^-] \quad (4-4)$$

with all K constants as listed in Table 4-1.

Electroneutrality of the solution yields:

$$[\text{H}^+] + 2[\text{Ca}^{2+}] = 2[\text{CO}_3^{2-}] + [\text{HCO}_3^-] + [\text{OH}^-] \quad (4-5)$$

In Region b, Ca concentration in solution and SDS sorption are controlled by the precipitation-dissolution of $\text{Ca}(\text{DS})_2$. As more surfactant is added to the system, the precipitation of surfactant begins to occur and can be described by the solubility product of $\text{Ca}(\text{DS})_2$:

$$K_{\text{sp}} = [\text{Ca}^{2+}] [\text{DS}^-] \gamma_{\text{Ca}} \gamma_{\text{DS}}^2 \quad (4-6)$$

where γ is the activity coefficient which can be calculated by Davis's equation:

$$\log \gamma = -0.5 Z_i \left(\frac{\sqrt{I}}{\sqrt{I} + 1} - 0.3 I \right) \quad (4-7)$$

where Z_i is the charge on species i , I the ionic strength, is calculated from the total Ca, Mg and Na concentrations in solution by assuming the anion to be originally associated with Ca and Mg as a divalent species such as CO_3^{2-} , since the pH is near 10 in a closed carbonate system.

Table 4-1 List of constants^a

constant	value	constant	value
pK1	8.42	α	-0.23
pK2	6.30	β	8×10^{-4}
pK3	10.3	$[\text{Ca}^{2+}]^b$	4.58 ppm
pK4	14.0		

^a All values are from Stumm and Morgan (1995) except for α and β , which are from Kallay et al. (1985).

^b This Ca^{2+} concentration which was calculated from equations 4-1, 4-2, 4-3, 4-4 and 4-5 was used only in Region I.

$$I = 0.5 \sum Z_i^2 C_i \approx 4 ([Ca^{2+}]_T + [Mg^{2+}]_T) + [Na^+]_T \quad (4-8)$$

where $[Ca^{2+}]_T$, $[Mg^{2+}]_T$, and $[Na^+]_T$ represent the total Ca, Mg and Na ion concentrations, respectively. Micelles may only contribute a fraction of their total charge to ionic strength. Fortunately, this model is not very sensitive to the activity coefficients and, therefore, a reasonable estimate can be made based on the total concentration of cations in solution.

In Region c, Ca concentration and SDS sorption are both controlled by $Ca(DS)_2$ precipitation-dissolution and by the micellar association of Ca. Ca ions begin to associate with the micelle when the surfactant concentration in the solution exceeds the CMC. The association constant, X_{Ca} , has been defined as the fraction of DS^- in the micelles that is neutralized by a divalent cation.

$$X_{Ca} = \frac{2 [Ca^{2+}]_m}{[DS^-]_m} \quad (4-9)$$

The relationship between CMC and Ca and Mg concentration in solution can be described by an empirical equation (Rosen, 1989):

$$CMC = [DS^-] = \beta \{ [Mg^{2+}]_T + [Ca^{2+}]_T \}^{-\alpha} \quad (4-10)$$

where α and β are empirical constants (Table 4-1).

A material balance of SDS yields:

$$[DS^-]_T = [DS^-] + [DS^-]_m \quad (4-11)$$

where $[DS^-]_T$ is the total DS concentration in solution, $[DS^-]$ the monomer concentration, and $[DS^-]_m$ the micelle concentration. Similarly, the total Ca concentration $[Ca^{2+}]_T$ in solution is given by

$$[Ca^{2+}]_T = [Ca^{2+}] + [Ca^{2+}]_m \quad (4-12)$$

where $[Ca^{2+}]_m$ is the micelle-bound Ca^{2+} concentration. The total Ca concentration ($[Ca^{2+}]_T$) can be measured by atomic absorption analysis, the aqueous Ca concentration ($[Ca^{2+}]$) can be calculated from the solubility product of $Ca(DS)_2$, and the micelle-bound Ca concentration ($[Ca^{2+}]_m$) can be calculated from the difference between $[Ca^{2+}]_T$ and $[Ca^{2+}]$.

When a soil contains a highly positively charged mineral such as iron oxide and concurrently has a low divalent cation content, surfactant precipitation can be expected to be insignificant when compared to adsorption. The adsorption of ionic surfactants and cosurfactants then can be divided into four regions as shown in Figure 4-2.

If the initial SDS and equilibrium SDS concentrations are known, then SDS sorption can be calculated using the following equation:

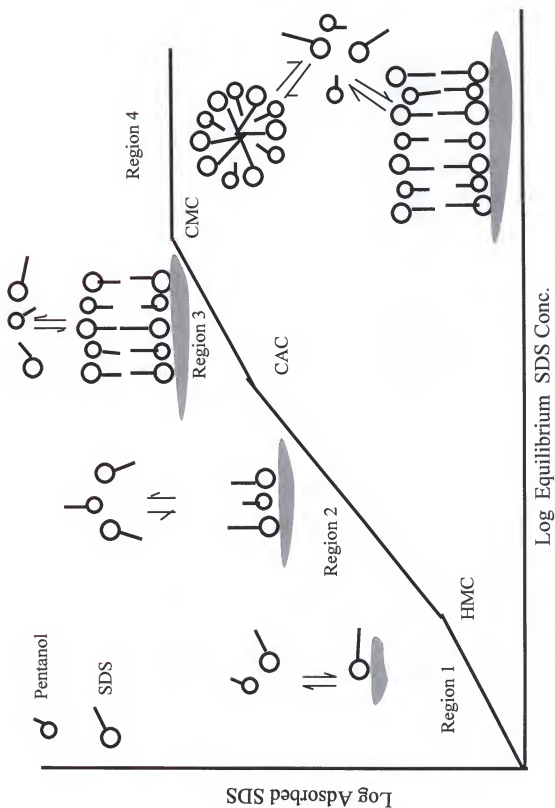


Figure 4-2. Anionic surfactant/cosurfactant adsorption isotherm.

$$S_{DS} = \frac{1000V}{M} (C_{DS}^i - C_{DS}^{eq})$$

where S_{DS} is SDS sorption (mg/g), V the volume of the aqueous phase (dL), M the mass of soil (g), C_{DS}^i the initial concentration of DS^- (mg/dL), and C_{DS}^{eq} the equilibrium concentration of DS^- (mg/dL).

Materials and Methods

Three soils were used in this study. Hill Soil 1 is an uncontaminated soil from Hill Air Force Base, Utah. Hill Soil 2 is a treated LNAPL contaminated soil from the same site. Not all NAPL in this soil was removed by 1:1 methylene chloride/acetone extraction for 24 hours followed by 4 acetone washes and ending with 4 washes with tap water from Hill Air Force Base. Dover Soil 3 is an uncontaminated soil from Dover Air Force Base, Delaware. All soils were air-dried and passed through a 2mm sieve.

Pure SDS (>99%) and pentanol (>99%) from Fisher Scientific were used as surfactant and cosurfactant, respectively.

Surfactant/cosurfactant sorption was determined at 1:7.5 and 1:2 soil:solution ratios, with all samples being rotated

for 24 hours at room temperature. Solution and soil were separated by centrifuging at 2000 RPM for 30 minutes. The total surfactant concentration in solution was determined by a two-phase titration method (Witco, 1994), with the cosurfactant concentration being determined by GC. The Ca and Mg concentrations in the solution were measured by AA.

The organic carbon content (Walkley and Black, 1934), particle-size distribution (Gee and Bauder, 1986), and citrate-dithionite extractable Fe (Olson and Ellis, 1986) in these soils were also analyzed.

Carbonates in the fine (clay and silt) and sand fractions were identified and determined using X-ray diffraction and TGA analysis. The fine and sand fractions were separated by washing the soils through a 270 mesh sieve using pH 10 water. Once separated, both fractions were air-dried and ground before X-ray diffraction or TGA analysis.

Results and Discussion

Soil Properties

Uncontaminated and treated contaminated Hill soils (Hill soils 1 and 2) had similar soil physical and chemical

properties (Table 4-2). These two soils had relatively high pH; therefore, positive surface charge should be insignificant even if any variable charge minerals was present. Calcite, which is the predominant carbonate in the Hill soils, and dolomite were also identified by X-ray diffraction. Organic carbon content of the treated contaminated soil was twice higher than in the uncontaminated soil; this may be because the acetone/methylene chloride wash could not remove some of the high molecular weight organic material from the contaminated soil. The uncontaminated Dover soil had a low pH and high citrate-dithionite extractable Fe content (Table 4-2). Iron oxide in the Dover soil existed mainly in the amorphous form because no appreciable iron oxide peaks were identified by X-ray diffraction analysis. Any positive charge should have been located at the amorphous iron oxide surface, since the ZPC of iron oxide is normally higher than this soil's pH. Therefore, a locally positively charged surface can be expected to exist in the Dover soil.

Kinetics of SDS Sorption

Plots of SDS sorption vs time are shown in Figures 4-3, 4-4, and 4-5. The SDS sorption in these soils is controlled

Table 4-2. Chemical and physical properties of the soils

	Soil 1	Soil 2	Soil 3
pH	8.5	8.4	5.6
Sand (%)	96.9	96.8	87.0
Silt (%)	2.5	3.0	9.4
Clay (%)	0.6	0.2	5.7
O.C. (%)	0.18	0.37	0.01
Carbonate in sand fraction (%)	3.9	3.8	nd ^a
Carbonate in fine fraction (%)	15.5	15.6	nd
Iron oxide in sand fraction (%)	nd	nd	nd
Iron oxide in fine fraction (%)	nd	nd	nd
Citrate-dithionite Fe (%)	0.02	0.03	0.69

a: not detectable

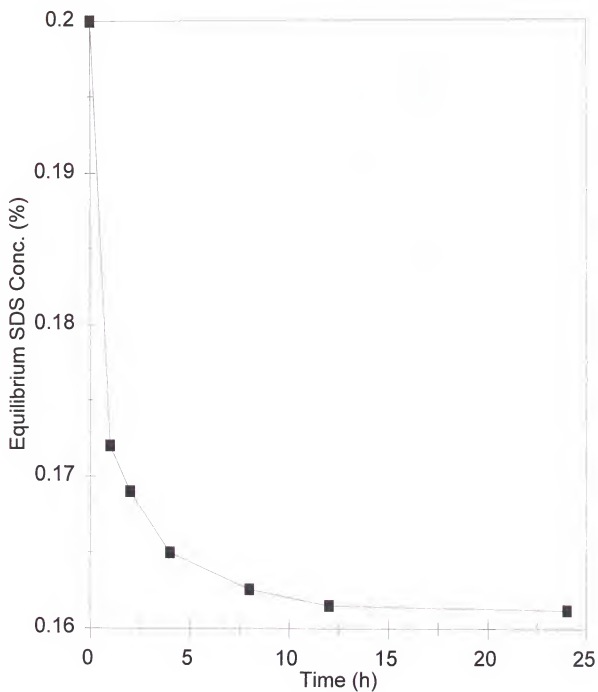


Figure 4-3. Kinetics of SDS sorption on Hill soil 1.

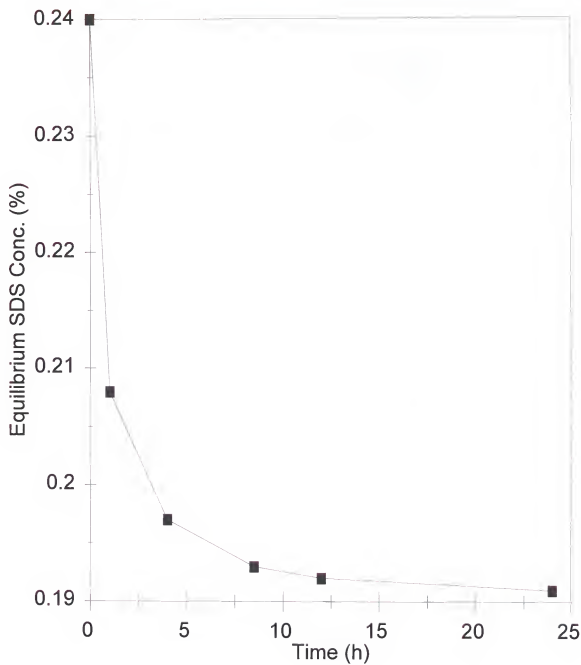


Figure 4-4. Kinetics of SDS sorption on Hill soil 2.

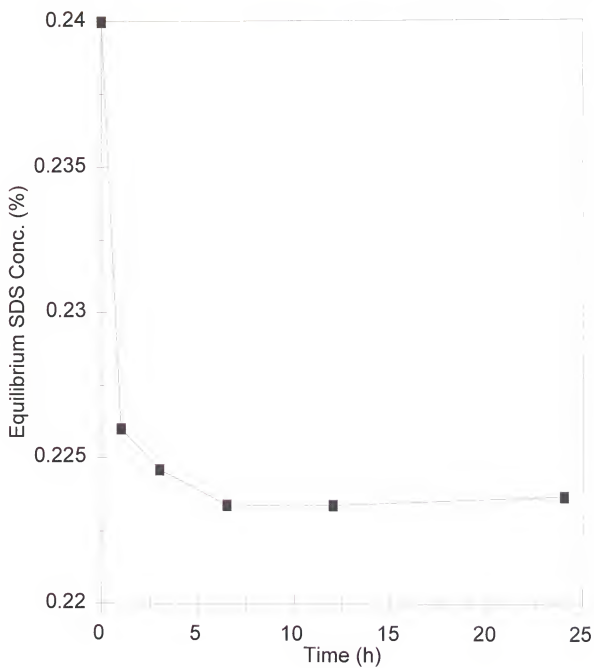


Figure 4-5. Kinetics of SDS sorption on the Dover soil.

by kinetic processes, with SDS sorption in the Dover soil tending to reach equilibrium much faster than for either of the Hill soils. The observed differences in sorption rates between the three soils may well be due to differing mechanisms governing the sorption process.

Precipitation in Hill Soils

Figures 4-6 and 4-7 show the relationship between Ca and Mg concentrations in solution and SDS sorption for the Hill soils. In the very low SDS concentration region (Region a), Ca concentrations in solution were nearly constant and lower than calculated from the $\text{Ca}(\text{DS})_2$ solubility product ($\text{pK}_{\text{sp}} = 10$) which is from a best fit of the Ca and DS concentration data in Region b using equations 4-6, 4-7 and 4-8. The Ca concentrations in the treated contaminated soil were the same as those from the calculation of calcite dissolution in water using equations 4-1, 4-2, 4-3, 4-4, 4-5 and the pK values in Table 4-1. This suggests that Ca concentration may be controlled by carbonate dissolution and that the surfactant lost is mainly due to adsorption. The significant change in the slope of Ca concentration and DS sorption at the boundary of Regions a and b may also indicate different mechanisms for

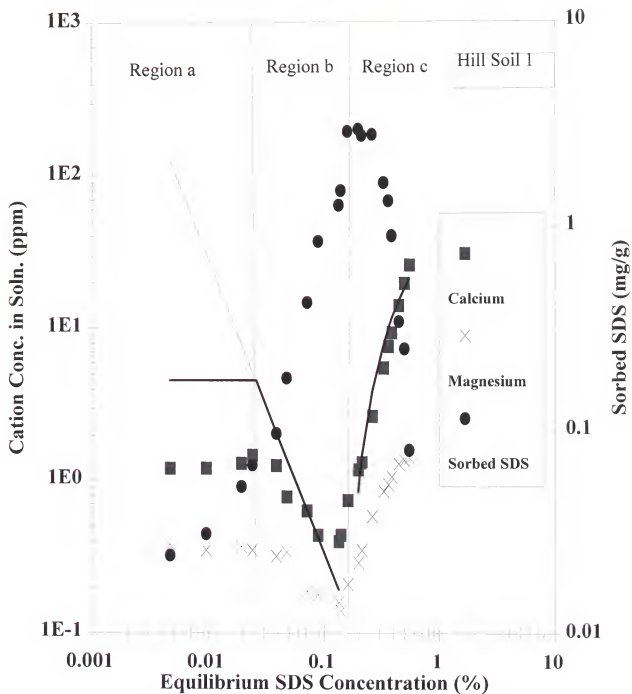


Figure 4-6. The relationship between divalent cation concentrations in solution and SDS sorption for Hill soil 1 (uncontaminated soil).

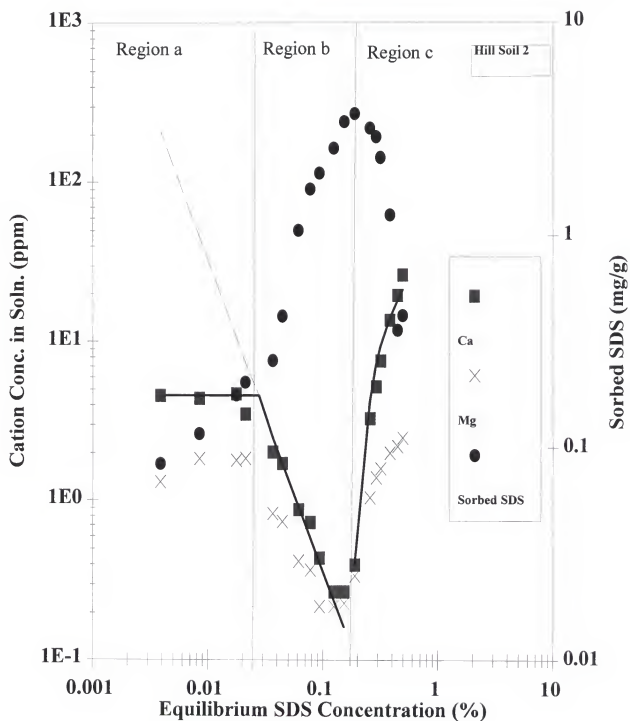


Figure 4-7. The relationship between divalent cation concentrations in solution and SDS sorption for Hill soil 2 (treated contaminated soil).

SDS sorption in these two regions. Ca concentration in the uncontaminated soil was lower than that calculated using calcite dissolution theory. The fact that more dolomite was present in the uncontaminated Hill soil may explain this difference. Mg may also precipitate with DS in Region b, since the Mg concentration also decreases as the SDS concentration increases. However, precipitation of $\text{Mg}(\text{DS})_2$ may not be as important as $\text{Ca}(\text{DS})_2$, because of the lower concentration of Mg and the higher solubility product of $\text{Mg}(\text{DS})_2$.

The solubility product of $\text{Ca}(\text{DS})_2$ ($\text{pK}_{\text{sp}} = 10$) from best fitting the data in Region b was the same for both Hill soils. The pK value in this study was higher than reported by Stellner and Scamehorn (1989) ($\text{pK}_{\text{sp}} = 9.3$) and Kallay et al. (1985) ($\text{pK}_{\text{sp}}=9.67$) using aqueous solutions without soils. Soil solids may lower the solubility by promoting $\text{Ca}(\text{DS})_2$ precipitation at the solid surface. The pK_{sp} value obtained by Ilic and coworkers (1996), who studied SDS precipitation for a Ca-montmorillonite, is similar to the one we obtained in this study.

When the SDS concentration exceeds the CMC, SDS sorption in soils decreases as the surfactant concentration increases.

This may be because Ca ions can associate with the SDS micellar surface by replacing the bound Na ions. Rathman and Scamehorn (1987) reported that about 65% of the Na ions bind with the pure DS micelle. As the SDS concentration increases, more and more Ca ions bind to the micelle surface, which results in a decrease of $\text{Ca}(\text{DS})_2$ precipitation. Equations 4-7 to 4-12 and some constants from table 1 were used to fit the Ca concentration in Region c. This yielded X_{Ca} averages of 0.08 and 0.07 for the treated contaminated soil and uncontaminated soil, respectively. Our value of X_{Ca} is a bit lower than that reported by Ilic et al. (1996) ($X_{\text{Ca}} = 0.1$). This may be due to the presence of Mg ions in our system, which may compete for binding sites on the micelle surface.

The effect of pentanol on SDS sorption by the Hill soils was studied at the Region b and c boundary. Surfactant sorption decreases as the cosurfactant (pentanol) concentration increases (Figures 4-8 and 4-9), and there is also an inverse relationship between Ca concentration in solution and sorbed SDS. As pentanol concentration increases, the CMC decreases due to the comicelleization of pentanol with SDS. From equation 4-10, we find that micellar associated Ca is dependant on the $[\text{DS}]_{\text{m}}$, which is in turn related to the

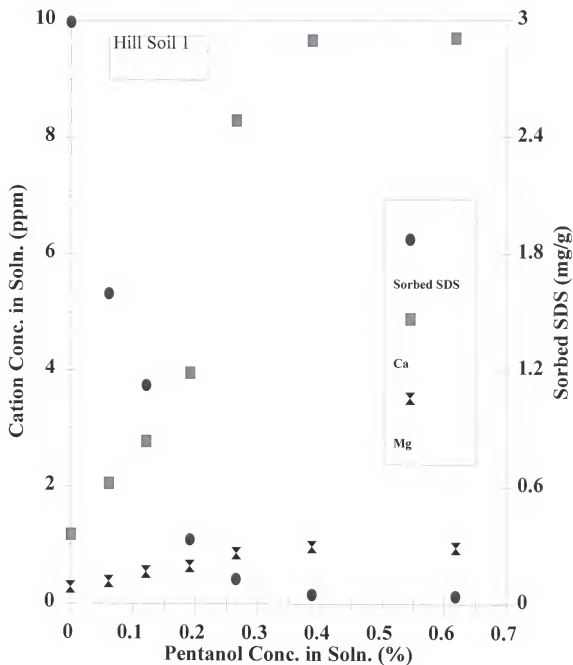


Figure 4-8. SDS sorption and divalent cation concentrations as a function of pentanol concentration in solution for Hill soil 1 (uncontaminated soil).

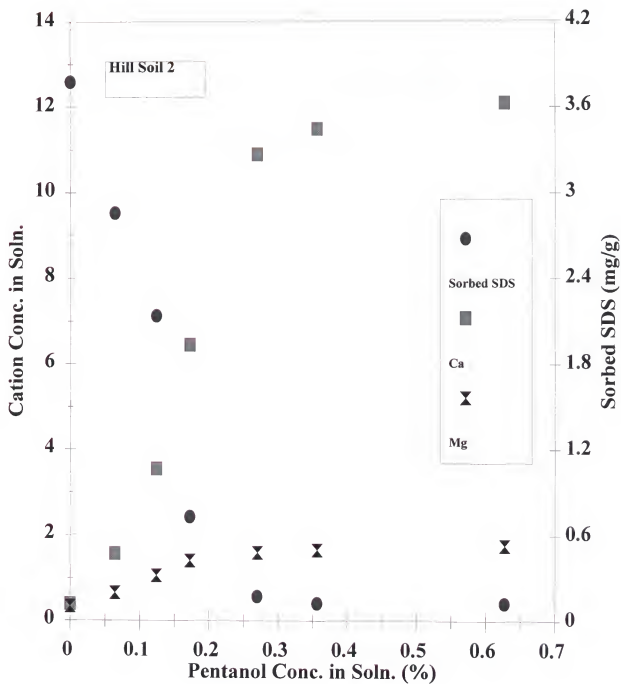


Figure 4-9. SDS sorption and divalent cation concentrations as a function of pentanol concentration in solution for Hill soil 2 (treated contaminated soil).

CMC; lower CMC means higher $[\text{DS}^-]_{\text{m}}$. Therefore, we can conclude that pentanol decreases $\text{Ca}(\text{DS})_2$ precipitation through comicellization with SDS.

Adsorption on Dover Soil

The plot of log sorbed SDS on Dover soil vs log equilibrium SDS concentration is shown in Fig 4-10. The different soil:solution ratios used had almost no effect on SDS sorption. This plot followed the typical adsorption isotherm, which can be divided into four regions.

Figure 4-11 is a plot of Ca and Mg concentration in solution and sorbed SDS vs equilibrium SDS concentration for the Dover soil. The Ca and Mg concentrations tend to increase as the equilibrium SDS concentration increases, but the slope changes abruptly near the Region II/Region III and Region III/Region IV boundaries of the adsorption isotherm. These slope changes may indicate the formation of admicelles at the iron oxide surface, and of micelles in solution. In Regions I and II, Ca and Mg concentrations in solution appear to be controlled by the exchange of Na ions from SDS with divalent cations sorbed on the soil. In Region III, Ca and Mg concentrations are controlled by ion exchange and binding with

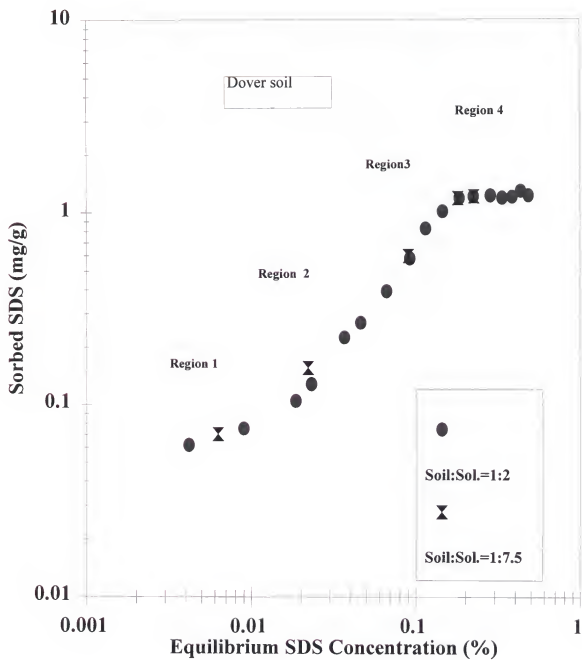


Figure 4-10. Log adsorbed SDS on Dover soil as a function of log equilibrium SDS concentration in solution.

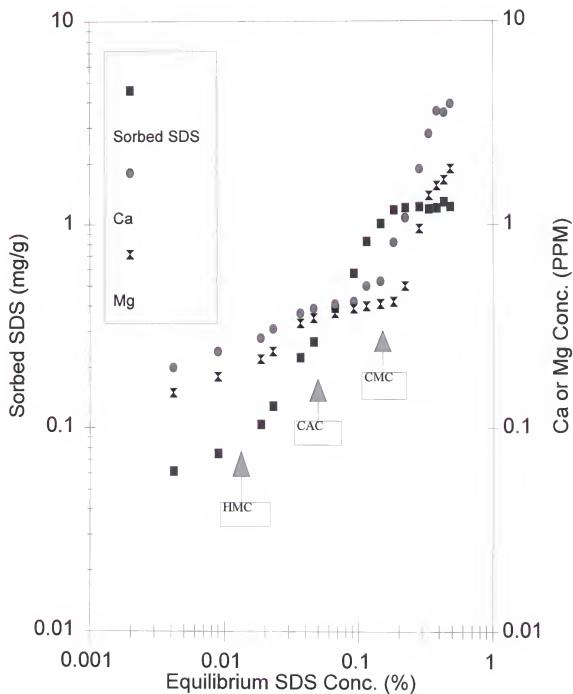


Figure 4-11. Divalent cation concentrations and adsorbed SDS as a function of log equilibrium SDS concentration in solution for the Dover soil. HMC: hemimicelle concentration. CAC: critical admicelle concentration. CMC: critical micelle concentration.

admicelles. In Region IV, Ca and Mg are also controlled by binding to micelles.

Figures 4-12, 4-13, 4-14, and 4-15 represent the effect of pentanol on SDS adsorption in four different adsorption isotherm regions. There was no appreciable adsorption of pentanol in the Henry's Law Region. SDS adsorption decreased as pentanol concentration in solution increased, which would appear to contradict the conclusions of O'Haver and Harwell (1995). However, after detailed study of their results, we found that the point they selected in the Henry's Region was located so close to Region II that it is possible that Region I shifted to Region II after the addition of alcohol, due to the decrease of HMC. An additional data point from their study, located farther away from Region II, also seems to show a decrease in SDS adsorption as a result of alcohol addition. This decrease of SDS adsorption in Region I may be due to alcohol's ability to increase the solvent power of the aqueous solution for SDS (Fu et al., 1996).

There was no measurable amount of alcohol adsorbed in Region II of the SDS adsorption isotherm. However, results show that pentanol increases SDS adsorption. This may be because small amounts of coadsorbed alcohol can enhance SDS

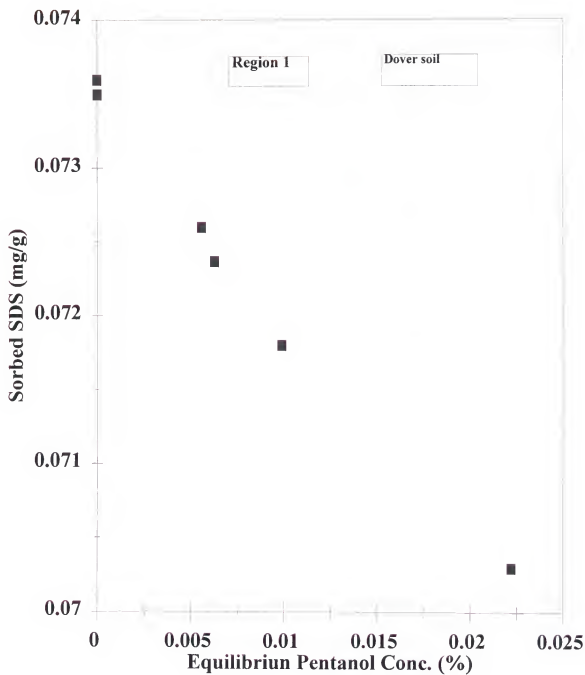


Figure 4-12. The effect of pentanol on SDS adsorption at Region I of the adsorption isotherm.

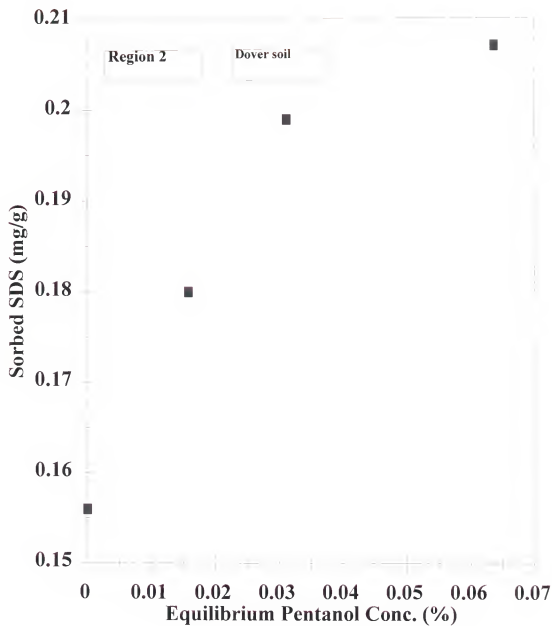


Figure 4-13. The effect of pentanol on SDS adsorption at Region II of the adsorption isotherm.

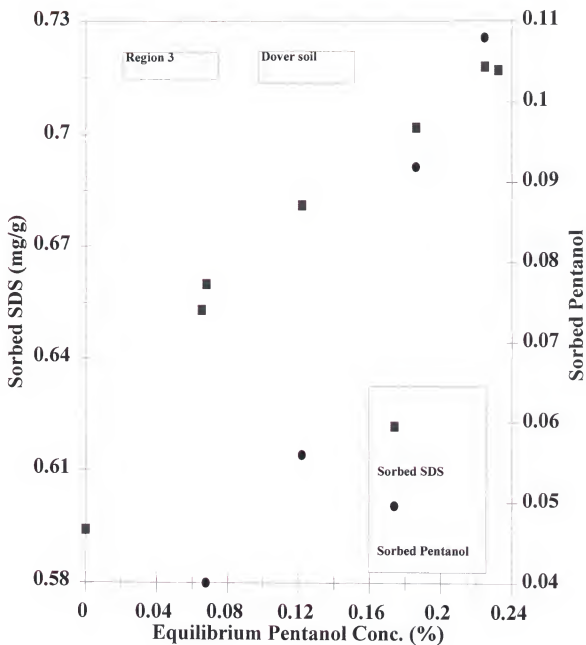


Figure 4-14. The effect of pentanol on SDS adsorption at Region III of the adsorption isotherm.

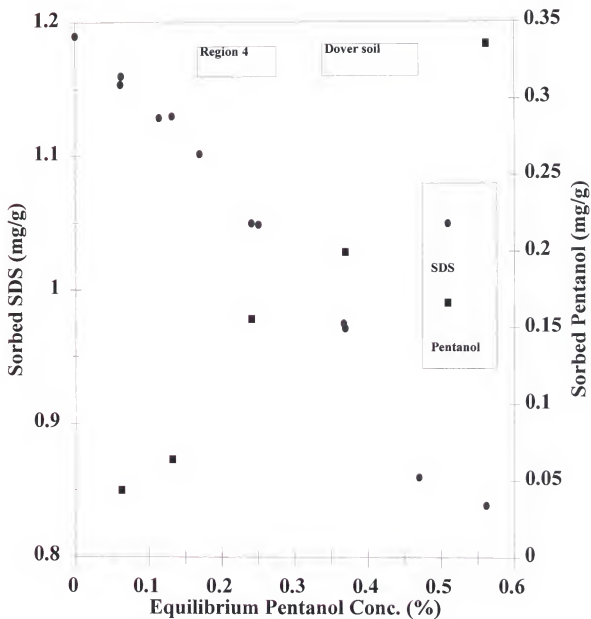


Figure 4-15. The effect of pentanol on SDS adsorption at Region IV of the adsorption isotherm.

adsorption, even though the change in the alcohol bulk concentration is at or below detection limits.

In Region III, adsorption of SDS and coadsorption of pentanol increased as the pentanol concentration in solution increased. In this study the relationship between the amount of coadsorbed pentanol and the pentanol concentration in solution was nearly linear, up to the highest pentanol:SDS molar ratio (1:2). The ability of pentanol to increase SDS adsorption decreases as pentanol concentration increases.

In Region IV, SDS adsorption decreased as pentanol concentration in solution increased. Concurrently, the coadsorbed pentanol increased as pentanol concentration in solution increased. However, the decrease in SDS adsorption was not necessarily due to the increase in pentanol coadsorption. Pentanol not only coadsorbs with SDS at the solid/liquid interface, but also comicellizes with SDS in solution.

Adsorption at the solid/liquid interface is governed by: (1) electrostatic interactions between the SDS ions and the charged surface sites; (2) hydrophobic interactions between SDS and the cosurfactant in micelles and hemimicelles or admicelles; (3) masking of the charged ionic head groups by

coadsorbed nonionic heads in the micelles and hemimicelles or admicelles; (4) changes in solvent power stemming from the dissolution of the cosurfactant; and (5) competitive adsorption of the cosurfactant with SDS. In Region I, SDS adsorption is controlled by the electrostatic interactions between SDS ions and the charged surface sites. Since the solvent power is increased when pentanol is added to the system, pentanol should decrease SDS adsorption. In Regions II and III, the hydrophobic interaction between adsorbed SDS and the cosurfactant plays an important role in SDS adsorption. Pentanol increases SDS adsorption by masking the charge of SDS ions when it coadsorbs with SDS in the hemimicelles or admicelles. In Region IV, micelle formation keeps the monomer activity nearly constant as SDS concentration increases. When pentanol comicellizes with SDS, it decreases the CMC which determines the monomer concentration in solution. The decrease of SDS adsorption after the addition of pentanol is mainly due to the comicelleization of pentanol and SDS. If the charged surface sites were nearly saturated by surfactant or the adsorption involved a Langmuir-like competition for the remaining surface area, the competition between surfactant and cosurfactant for

adsorption sites might also contribute to a decrease in SDS adsorption as pentanol concentration increased.

Conclusions

Precipitation is the main surfactant sorption mechanism for the Hill soils containing carbonate, though adsorption may dominate in the very low SDS concentration region (Region a). That more SDS was adsorbed on the treated contaminated soil than on the uncontaminated soil may be due to the somewhat higher organic carbon content of the treated contaminated soil. Adsorption is the predominant sorption mechanism for the Dover soil containing iron oxide. Soil:solution ratio had almost no effect on SDS adsorption for the soils studied.

Precipitation reaches its maximum and cation concentration reaches its minimum at SDS concentrations near the CMC. Adsorption reaches a plateau after the SDS concentration increases above the CMC. The significant changes in precipitation and adsorption behaviors near the CMC are due to the formation of micelles.

Pentanol does not sorb to soils itself, but can co-adsorb with SDS. Pentanol decreases SDS precipitation through comicellization. Pentanol can either decrease or increase SDS

adsorption through decreasing SDS activity in the aqueous phase or the sorbed phase, respectively.

Divalent cation concentration in solution is governed by one or more of the following processes: carbonate dissolution, cation exchange, precipitation of divalent cations with DS, and associations of divalent cations with micelles and admicelles, which depend on soil properties and on SDS concentration in solution.

CHAPTER 5

DYNAMIC SURFACTANT ADSORPTION AT INTERFACES

Introduction

Adsorption of surfactant in the interface is an important factor in determining surfactant properties such as emulsification. Nonequilibrium and dynamic processes play a major role in surfactant systems, especially for nonionic surfactant systems. Therefore, it is important to understand the behavior of surfactant in the interface.

The drop volume/weight method has been used to determine dynamic interfacial tensions at the air/liquid and liquid/liquid interfaces (Tornberg, 1978; Joos and Van Hunsel, 1988; Gobel and Joppien, 1997). This is the simplest method that can be used to study the dynamic processes of surfactants in the interface over a wide range of times. When nonequilibrium adsorption is assumed to be diffusion controlled, the experimental data can be used to calculate the apparent diffusion coefficient of surfactant at the interface.

It has been found that there is almost no difference between interfacial tensions from the equilibrium method and those obtained through extrapolating the dynamic data from the drop weight/volume method to infinite time using the diffusion equation (Gobel and Joppien, 1997).

Past research has focused more on dynamic surfactant adsorption at the interface below the surfactant CMC than above the CMC (Gobel and Joppien, 1997). Dynamic surfactant adsorption at surfactant concentrations above the CMC, however, is more interesting, since this is the region where emulsification occurs. Solubilization in nonionic surfactant systems has been reported by several authors (Carroll, 1981; Pennell et al., 1993; Pennell et al., 1994). Carroll (1981) proposed that the slow stage of the kinetic solubilization of nonpolar oils in nonionic surfactant solutions is due to the adsorption of micelles at the interface. Since the micelle is not itself expected to be especially surface active, there is no good reason to suppose that it will ever adsorb as an entity at the interface. More realistically it will first dissociate into monomers which, being strongly surface active, subsequently adsorb. The relaxation time that is associated with the exchange of monomers between micelles and the bulk

aqueous phase is in the microsecond range (Oh and Shah, 1993). This is a very small time scale when compared with surfactant kinetic adsorption. The diffusion controlled adsorption of surfactant in the interface, which may contribute to rate limiting processes in NAPL solubilization, needs to be evaluated.

Cosurfactant is also normally included in the microemulsion system for several good reasons, which have been noted throughout this dissertation. It has been reported that cosurfactants can modify the properties of the interface, such as reducing the interfacial tension and interfacial viscosity. The effect of cosurfactant on dynamic surfactant adsorption at the interface has not been sufficiently documented, however.

In this study the effects of cosurfactant and of concentration of surfactant on dynamic interfacial tension, and on surfactant adsorption at the air/water and oil/water interfaces, are investigated.

Theory

Diffusion-controlled adsorption kinetics, adsorption (Γ) as a function of time (t), were first treated quantitatively by Ward and Tordai (1946). In equation 5-1:

$$\Gamma = 2C_i \left(\frac{Dt}{\Pi} \right)^{\frac{1}{2}} - 2 \left(\frac{D}{\Pi} \right)^{\frac{1}{2}} \int_0^t t^{\frac{1}{2}} C_s(t-\tau) d\tau^{\frac{1}{2}} \quad (5-1)$$

where C_i is the bulk concentration of surfactant monomers, D the diffusion coefficient, C_s the subsurface concentration, and τ an auxiliary variable. This well known equation is not easily applicable to the interpretation of experimental data, because it involves two variables: Γ and C_s . A simple analytical formula was derived by Rillaerts and Joos (1982) for long adsorption times:

$$\gamma - \gamma_{\infty} = \frac{RT\Gamma^2}{C_i} \left(\frac{\Pi}{4Dt} \right)^{\frac{1}{2}} \quad (5-2)$$

where γ is the dynamic interfacial tension, γ_{∞} the equilibrium interfacial tension, R the gas constant, and T the temperature. This equation can be rearranged as a derivative of γ with respect to $t^{-1/2}$, which is the slope of the γ vs $t^{-1/2}$ plot:

$$\frac{d\gamma}{dt^{-\frac{1}{2}}} = \frac{RT\Gamma^2}{C_i} \left(\frac{\Pi}{4D} \right)^{\frac{1}{2}} \quad (5-3)$$

After integrating the convective diffusion equation and comparing to the Ward and Tordi equation, Joos and Rillaerts (1981) found that the dropping time (t_d) should be corrected by the following equation:

$$t = \frac{3}{7} t_d \quad (5-4)$$

In the case of systems containing only one surfactant, saturation adsorption (Γ) is often found in the vicinity of the CMC, with the interfacial concentration being obtained by fitting the data points to a straight line using the Gibbs adsorption equation:

$$\Gamma = -\frac{1}{2.303RT} \left(\frac{d\gamma}{d \log C_i} \right) \quad (5-5)$$

When the system contains two surface-active compounds, interfacial concentrations can also be interpreted by the Gibbs equation and saturation adsorption again occurs in the neighborhood of the CMC (Verhoeckx et al., 1987; Zhou and Dupeyrat, 1990). For commercial nonionic surfactants which have a wide distribution of EO units, the maximum adsorption (Γ) at the interface is calculated via the Gibbs equation. The Langmuir-Szskowski equation (Fainerman and Miller, 1995)

is then used to evaluate the concentration dependent adsorption (Γ_c):

$$b = \frac{\exp\left(\frac{\gamma_o - \gamma}{RT\Gamma}\right) - 1}{C_i} \quad (5-6)$$

$$\Gamma_c = \Gamma \frac{bC_i}{1 + bC_i} \quad (5-7)$$

where γ_o is the interfacial tension at which $C_i = 0$, and b is a constant.

Materials and Methods

A nonionic surfactant Brij 97 (POE(10)oleyl) was obtained from ICI Surfactants and used as received. Pure IPA (99%) and PCE (99%) were purchased from Fisher Scientific. Brij 97 is one of the best surfactants for PCE solubilization when IPA is used as a cosurfactant (see Chapter 6).

The drop weight method was used for both surface and interfacial tension measurements. The burette used for drop delivery was modified by cutting off the tip to increase its diameter. Tip diameter was measured by an ocular microscope and verified by comparing the measured values of water surface tension and PCE/water interfacial tension with published

values from the literature (Table 5-1). Drop rate was controlled by the burette's stop-cock. Twenty drops of liquid were collected inside a 20 ml vial (Figure 5-1) and weighed. The drop time (t_d) was recorded using a stop watch and ranged from 1.5 to 40 seconds/drop. The weight of a drop (W) is given by what is known as Tate's law:

$$W = 2\pi r\gamma \quad (5-11)$$

If the mass of the displaced liquid (W_d) cannot be ignored, such as in the determination of liquid-liquid interfacial tensions, the equation can be modified to the form:

$$W - W_d = 2\pi r\gamma \quad (5-12)$$

where r is the radius of the tip and γ the interfacial tension. In actual practice, a weight W' is obtained, which is less than the "ideal" value W because only the portion of the drop that has reached the point of instability actually falls. Thus, a correction factor f should be included in the equation:

$$W' - W_d = 2\pi r\gamma f \quad (5-13)$$

Harkins and Brown (1919) found that f should be a function of the dimensionless ratio $r/V^{1/3}$ (Table 5-2). The diameter of the tip was modified to yield $r/V^{1/3}$ value in the region 0.55 to 1.2, where f is varying most slowly and a linear

Table 5-1 The surface tension of water, IFT between PCE and water, and the measured and calculated diameter of burette tips.

Surface tension of water (Dyne/cm)	Outer diameter of tip for surface tensions (cm)		IFT between PCE/ water (Dyne/cm)	Inner diameter of tip for IFTs (cm)	
	Measured	Calculated		Measured	Calculated
72.5a	0.365	0.363	47.8b	0.31	0.308

a Handbook of Physics and Chemistry (1988)

b. Pennell et al. (1996)

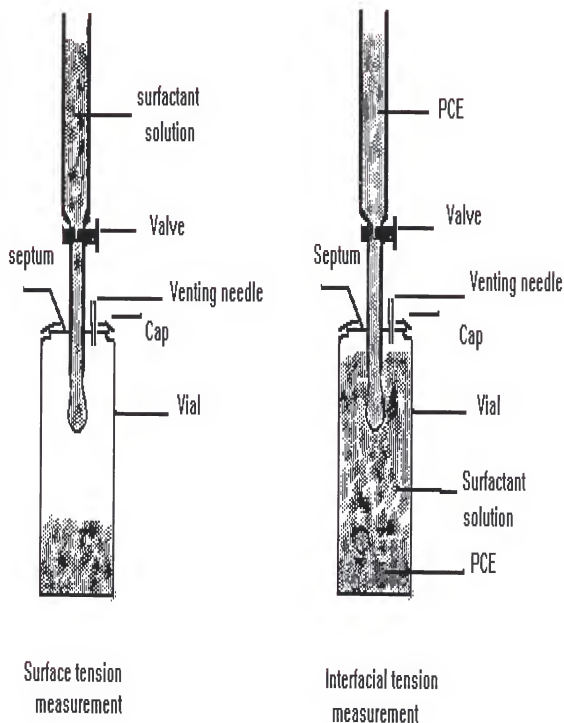


Figure 5-1. Surface and interfacial tension measurement apparatus.

Table 5-2 Correction factors for the drop weight method.

$r/V^{1/3}$	f	$r/V^{1/3}$	f	$r/V^{1/3}$	f^a
0.00	(1.00)	0.75	0.6032	1.225	0.656
0.30	0.7256	0.80	0.6000	1.25	0.652
0.35	0.7011	0.85	0.5992	1.30	0.640
0.40	0.6828	0.90	0.5998	1.35	0.623
0.45	0.6669	0.95	0.6034	1.40	0.603
0.50	0.6515	1.00	0.6098	1.45	0.583
0.55	0.6362	1.05	0.6179	1.50	0.567
0.60	0.6250	1.10	0.6280	1.55	0.551
0.65	0.6171	1.15	0.6407	1.60	0.535
0.70	0.6093	1.20	0.6535		

^a The values of f in this column are less accurate than the others.

relationship between f and $r/V^{1/3}$ within each interval can be assumed. Interfacial tension can be calculated by the following equation:

$$\gamma = \frac{\frac{W'}{\rho} \Delta \rho g}{2\pi r f} \quad (5-14)$$

where ρ is the density of the dropped liquid, $\Delta \rho$ the difference in densities of the liquids, and g the acceleration due to gravity.

Results and Discussion

Surface tensions at the water/air interface, obtained by extrapolation of dynamic surface tensions to equilibrium, are plotted against the log of Brij 97 concentration in solution (Figure 5-2). Gobel and Joppien (1997) reported that the extrapolated results did not significantly deviate from results obtained by the equilibrium method. Therefore, the CMC of Brij 97 can be determined from this plot as $1.88 \times 10^{-4} M$.

Table 5-3 shows the maximum amount of Brij 97 adsorbed at the interface. This value was calculated using the Gibbs adsorption equation and fitting some data points to a straight line (Fig 5-2, 5-3). Brij 97 adsorption at the water/air

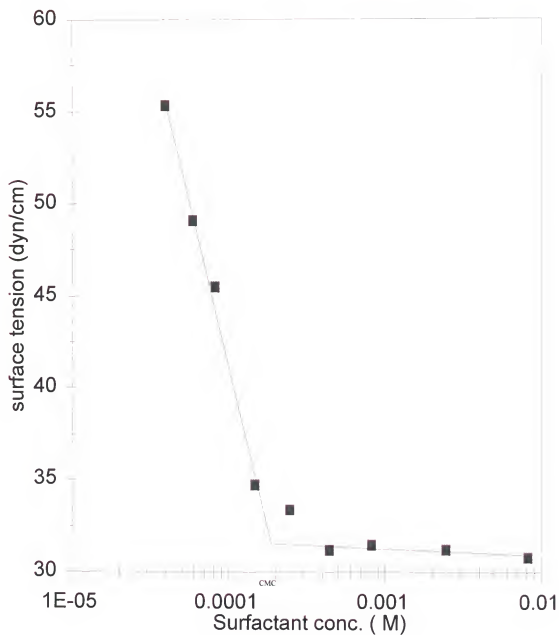


Figure 5-2. Plot of surface tension of Brij 97 solution versus log concentration. (■) extrapolated equilibrium surface tension; \ linear regression of the experimental data points.

Table 5-3 Equilibrium adsorption (Γ) of Brij 97 at the interfaces as calculated from the Gibbs equation.

Interface	Cosurfactant (IPA)	Equilibrium adsorption (Γ) (10^{-10} mol/cm ²)
Water/air	No	6.51
Water/PCE	No	2.38
Water/PCE	Yes	2.30

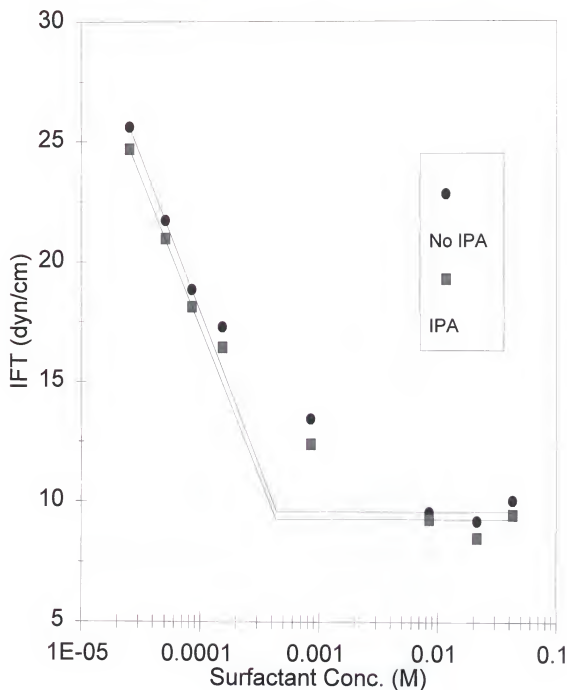


Figure 5-3. Plot of interfacial tension between Brij 97 solution and PCE versus log surfactant concentration. (■, ●) extrapolated equilibrium interfacial tension; \ linear regression of the experimental data points.

interface is much higher than at the water/PCE interface. This may be because air is more hydrophobic than PCE, and because of the wide distribution of EO units in the surfactant. A higher proportion of low EO species may adsorb at the more hydrophobic surface, with low EO unit species packing more densely in the interface than high EO unit species. IPA only slightly decreases Brij 97 adsorption at the interface, presumably because IPA is not very surface active.

Dynamic interfacial tensions at the water/air and water/PCE interfaces are plotted against $1/t^{1/2}$ in Figures 5-4 through 5-13. At low concentrations and short periods of adsorption the interfacial tension decreases very slowly, and is then followed by a rapid decrease with time. When the surfactant concentration approaches the CMC, or when IPA was added to the surfactant system, the slow adsorption of surfactant in short time periods tends to disappear. All data show a linear relationship between dynamic interfacial tensions and $1/t^{1/2}$, except for the initial short time period at low surfactant concentrations. This suggests that surfactant adsorption at the interface is controlled by diffusion even when surfactant concentrations are above the

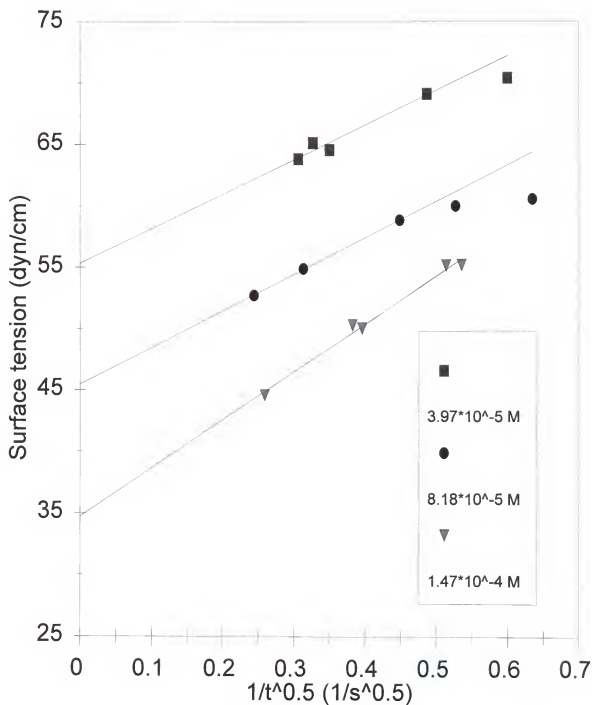


Figure 5-4. Relationship between the surface tension of Brij 97 solution and $t^{-1/2}$ at surfactant concentrations below the CMC.

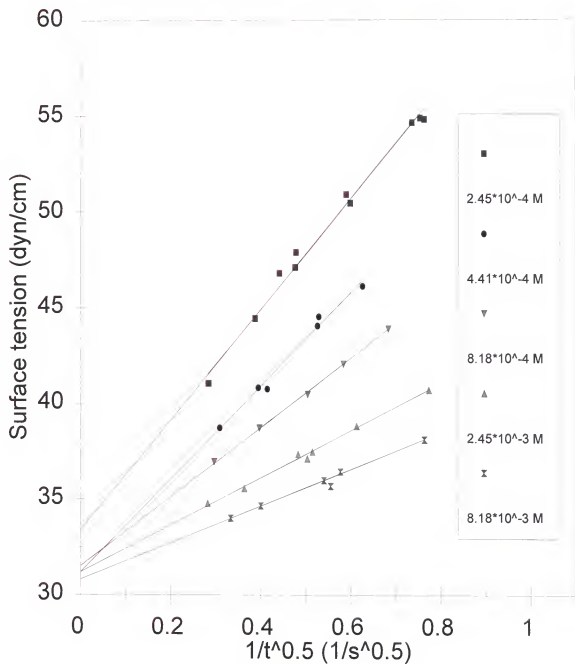


Figure 5-5. Relationship between the surface tension of Brij 97 solution and $t^{-1/2}$ at surfactant concentrations above the CMC.

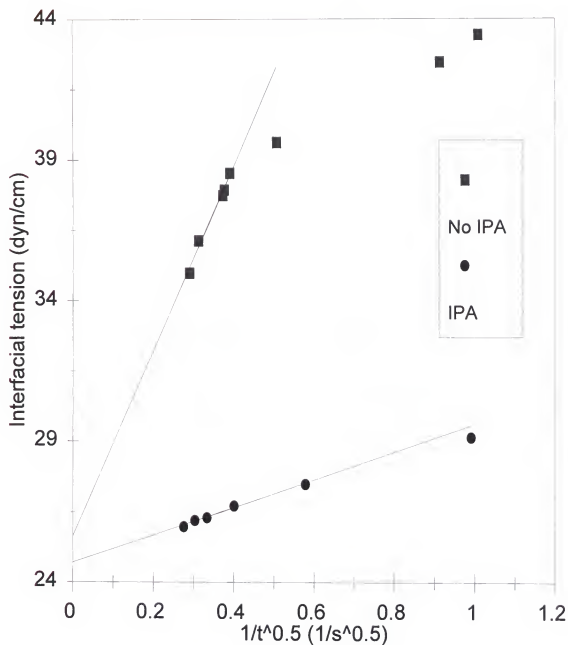


Figure 5-6. Relationship between the interfacial tension of Brij 97 solution ($C=2.45 \times 10^{-4}M$) and $t^{-1/2}$.

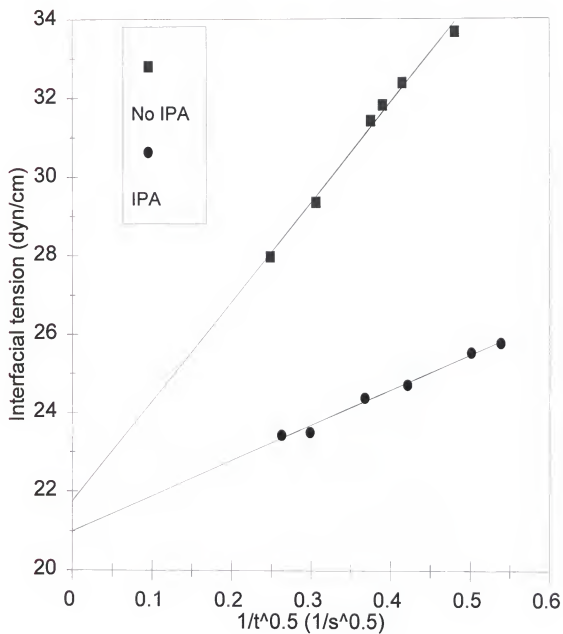


Figure 5-7. Relationship between the interfacial tension of Brij 97 solution ($C=5.08 \times 10^{-4}M$) and $t^{-1/2}$.

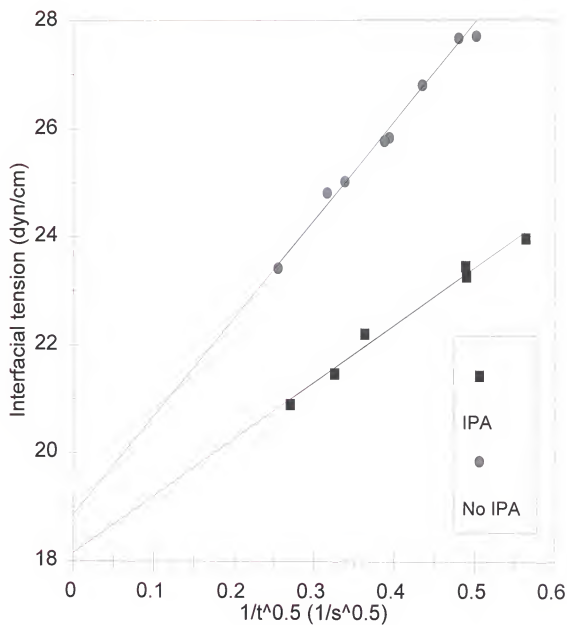


Figure 5-8. Relationship between the interfacial tension of Brij 97 solution ($C=8.47 \times 10^{-4} M$) and $t^{-1/2}$.

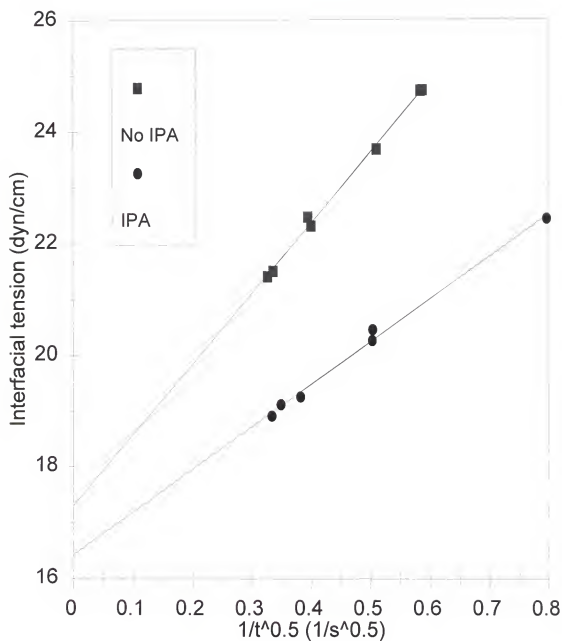


Figure 5-9. Relationship between the interfacial tension of Brij 97 solution ($C=1.53 \times 10^{-3}M$) and $t^{-1/2}$.

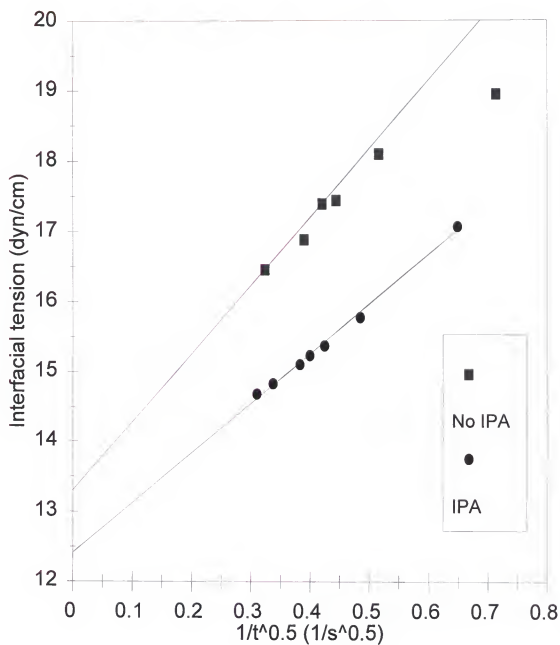


Figure 5-10. Relationship between the interfacial tension of Brij 97 solution ($C=8.47 \times 10^{-3}M$) and $t^{-1/2}$.

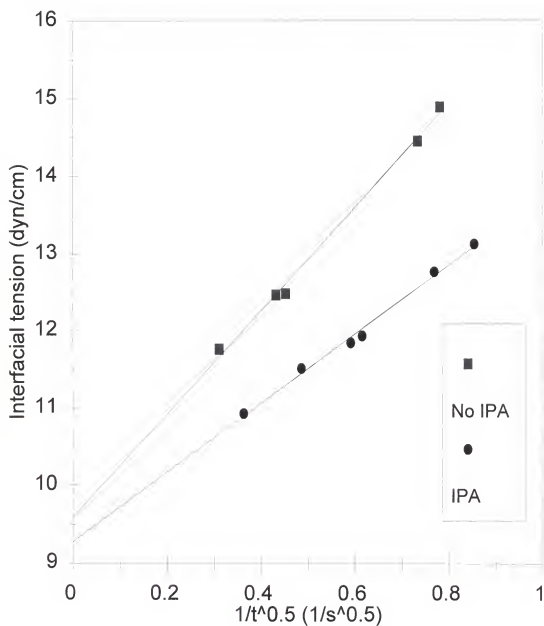


Figure 5-11. Relationship between the interfacial tension of Brij 97 solution ($C=8.47 \times 10^{-2} \text{M}$) and $t^{-1/2}$.

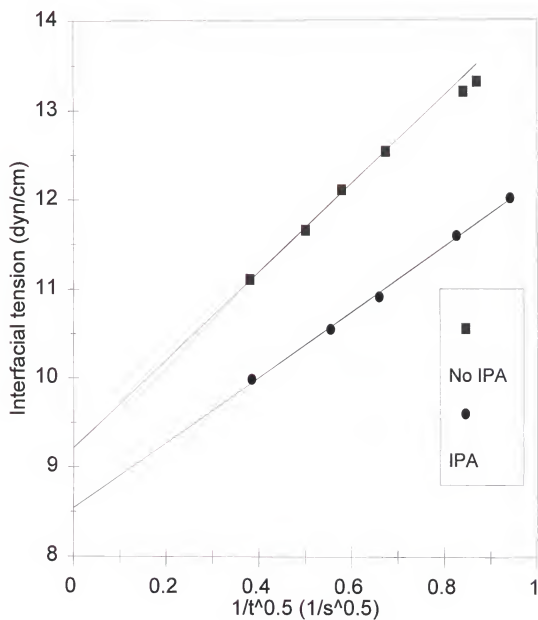


Figure 5-12. Relationship between the interfacial tension of Brij 97 solution ($C=2.12 \times 10^{-3} M$) and $t^{-1/2}$.

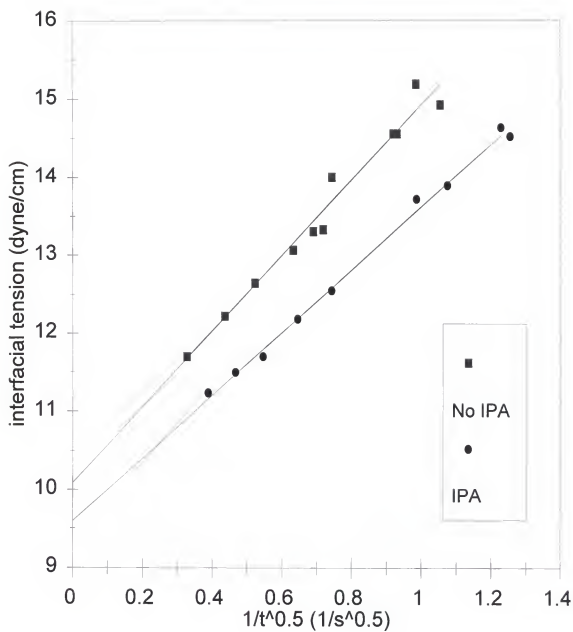


Figure 5-13. Relationship between the interfacial tension of Brij 97 solution ($C=4.24 \times 10^{-3}M$) and $t^{-1/2}$.

CMC. This allows us to calculate an apparent diffusion coefficient using equation 5-3 for the adsorption process.

IPA tends to decrease the equilibrium interfacial tension somewhat, which may relate to the low adsorbed IPA density at the interface. A relatively small amount of adsorbed IPA at the interface makes a large difference in the rate of dynamic surfactant adsorption by promoting surfactant mass transfer to the interface.

The slope of the $\gamma(t)$ vs $1/t^{1/2}$ plots for the air/water interface (Tables 5-4) increase slightly as the surfactant concentration approaches the CMC, and then decrease as the surfactant concentration increases beyond the CMC. For the water/PCE interface (Table 5-5), the slopes decrease as the surfactant concentration increases without IPA. When IPA is included in the system, the slopes are lower than without IPA, especially at low surfactant concentrations, and increase as surfactant concentration approaches the CMC.

The diffusion coefficient decreases as the surfactant concentration approaches the CMC, and then increases again after the surfactant concentration passes the CMC (Table 5-3, 5-4). Gobel and Joppien (1997) also found that the diffusion coefficient decreases as surfactant concentration increases to

Table 5-4 Apparent diffusion coefficient for Brij 97 at the water/air interface.

Brij 97 Conc. (10^{-5}M)	$d\gamma/dt^{1/2}$ ($\text{dyn/cm}\cdot\text{s}^{1/2}$)	Γ (10^{-10} mol/cm^2)	D ($10^{-6}\text{cm}^2/\text{s}$)
3.92	28.10	4.27	13.1
5.88	23.48	4.87	14.1
8.18	29.86	5.30	6.32
14.7	39.19	5.89	1.73
24.5	28.81	5.94	2.03
44.1	24.35	6.01	2.98
81.8	18.14	6.01	5.36
245	12.31	6.01	11.6
818	9.48	6.02	19.8

Table 5-5 Apparent diffusion coefficient for Brij 97 at the water/PCE interface.

Brij 97 Conc. (10^{-3}M)	IPA	$d\gamma/dt^{1/2}$ ($\text{dyn/cm}\cdot\text{s}^{1/2}$)	Γ (10^{-10} mol/cm^2)	D ($10^{-6}\text{cm}^2/\text{s}$)
2.45	N	32.91	2.33	2.17
2.45	Y	4.91	2.26	86.2
5.08	N	25.30	2.35	0.88
5.08	Y	8.89	2.28	6.33
8.47	N	18.13	2.36	0.63
8.47	Y	10.53	2.29	1.65
15.3	N	12.63	2.37	0.40
15.3	Y	7.61	2.29	0.97
84.7	N	9.74	2.37	0.44
84.7	Y	7.08	2.30	0.76
847	N	6.68	2.38	1.06
847	Y	4.47	2.30	1.89
2120	N	4.94	2.38	1.78
2120	Y	3.69	2.30	2.79
4240	N	4.83	2.38	1.86
4240	Y	3.88	2.30	2.52

the CMC. After surfactant concentration passes the CMC, increases in the diffusion coefficient may be due to demicellization, which is a source for the production of monomers and is a relatively faster process than surfactant adsorption (Oh and Shah, 1993; Joos and Van Huuesl, 1988; Geeraerts and Joos, 1994). Carroll (1981) reported that the NAPL solubilization rate is positively related to the surfactant concentration, concluding that micelle adsorption at the interface, rather than desorption, is the rate limiting process. However, because the micelle is not surface active, this study suggests that adsorption of monomers at the interface is the rate limiting process instead of micelle adsorption, with the source for monomers increasing as the surfactant concentration increases. IPA increases the diffusion coefficient of Brij 97 by a factor of 40 at low surfactant concentrations. This factor drops to 1.4 at high surfactant concentrations (Table 5-6), the lower ratio of surfactant/cosurfactant at high surfactant concentrations being responsible. The disappearance of the initial short time period adsorption stage at low surfactant concentrations, after the addition of IPA, may also result from increasing diffusion coefficient (Figure 5-6).

Table 5-6. The effect of IPA on the apparent diffusion coefficient of Brij 97 at the water/PCE interface for different surfactant concentrations.

Brij 97 Conc. (10^{-5}M)	Ratio IPA/Brij 97 (M/M)	Ratio of D^a
2.45	2.35×10^4	40
5.08	1.14×10^4	7.2
8.47	6.81×10^3	2.6
15.3	3.77×10^3	2.4
84.7	6.81×10^2	1.8
847	6.81×10^1	1.8
2120	2.72×10^1	1.6
4240	1.36×10^1	1.4

a: The ratio of apparent diffusion coefficient with IPA to without IPA.

The apparent diffusion coefficient for Brij 97 at the water/PCE interface is lower than at the water/air interface without IPA, and may be due to the following reasons. First, air is more hydrophobic than PCE and thus the surfactant monomers can be expected to adsorb faster at the more hydrophobic interface. Second, nonionic surfactants tend to partition into the oil phase, especially for low EO species (Graciaa et al., 1983b). Loss of adsorbed surfactant at the interface will lengthen the time needed for the interfacial tension to reach equilibrium, and would lead to a lower diffusion coefficient.

Conclusions

The adsorption of Brij 97 in the water/air and water/PCE interfaces appears to be controlled by surfactant diffusion. When the surfactant concentration is above the CMC, the apparent diffusion coefficient increases as the surfactant concentration increases. Micelles in solution acting as a source for surfactant monomers may be the cause of this phenomenon. Because IPA has a low surface activity, the equilibrium interfacial tensions decrease only slightly after addition of IPA to the surfactant system. IPA significantly

increases the surfactant diffusion rate at the interface by promoting surfactant mass transfer to the interface, especially at high IPA:surfactant ratios.

CHAPTER 6
SOLUBILIZATION OF PCE IN SURFACTANT/ALCOHOL SOLUTIONS

Introduction

Solubilization of contaminants by surfactant micelles and mobilization of residual trapped NAPL are the two most important aspects of surfactant-enhanced aquifer remediation. Mobilization, however, may pose a risk to the uncontaminated zone by allowing the NAPL to migrate.

It has been found that NAPL solubilization is related to the HLB and the structure of the surfactant (Mackay, 1987). Diallo et al (1994) reported that the solubilization of alkanes in dodecyl alcohol ethoxylates decreases as surfactant HLB increases above 11.9, and that the solubilization of aromatic hydrocarbons and of chlorinated alkanes go through a maximum within the same HLB range (11.9-17.6). They concluded that the solubilization of a nonpolar oil is determined by the surfactant micellar core value, which is a number correlated with the carbon number of the surfactant hydrophobic chain and

the aggregation number of the surfactant. The solubilization of a polar oil is the result of two opposing effects: (1) a decrease in solubilization capacity with increasing HLB, and (2) an increase of solubilization capacity by electron donor acceptor (EDA) complexation between the surfactant and polar oil. Other researchers have found that nonpolar oil solubilization also goes through a maximum as surfactant HLB increases when a much wider range of HLB is used and a medium chain alcohol, pentanol, is included in the system as a cosurfactant (Ballet and Candau, 1981; Rhue et al., 1997).

Location of the solubilizate depends not only on the polarity of the oil in question but also on the concentration of solubilizate (Mukerjee, 1978). At very low concentrations, benzene was found to be solubilized at the micelle/water interface, while alkyl substituted benzene and the chlorinated alkanes penetrate more deeply into the micellar core (Mackay, 1987). The oil solubilizing effect of EDA itself may be greater on low concentrations of high polarity oil than on low polarity oil. When a polar oil is solubilized in the EO shell of the micelle, interaction with the EO groups causes dehydration and thus depression of the cloud point (Mackay, 1987). Less than 0.5g benzene solubilized in 100 g of 2%

Triton-100 (POE(9.5) octylphenol) solution can decrease the cloud point from 65 °C to below room temperature (MacLay, 1956), resulting in an apparent solubilization limit which is in fact the cloud point. The depression of the cloud point to below room temperature may be an important reason for extremely low polar oil solubilization at lower surfactant HLB. Pentanol, which can increase the hydrophobicity of a hydrophilic surfactant, should increase the oil solubilization of that surfactant. However, when the cloud point of a relatively hydrophobic (low HLB) surfactant is near room temperature, addition of pentanol may well decrease apparent polar oil solubilization due to the further depression of the cloud point (Mackay, 1987).

When salt or cosurfactant is not included in the microemulsion system, Solubilization of hydrocarbons and chlorocarbons is typically less than 40,000 mg/l in batch and 20,000 mg/l in column effluents (Pennell et al., 1993; Fountain et al., 1996). Martel et al (1993) used high surfactant concentrations and alcohol cosurfactants to increase NAPL solubilization. Unfortunately, their research included no column studies, interfacial tension (IFT) measurements, or viscosity measurements. Although one pore

volume of surfactant may well solubilize all of the residual NAPL in an aquifer, which can be estimated from batch study data, the possibility of mobilization of the NAPL cannot be excluded. Mobilization normally occurs before surfactant concentration in the effluent reaches the injected concentration, and this surfactant solution front can mobilize the highest amounts of NAPL (Pennell et al. 1994).

The amount of oil that a surfactant solution solubilizes is related to the reduction of the IFT, given by the Chun-Huh (Chun, 1979) equation.

$$\gamma = \frac{C}{S^2}$$

where γ is the interfacial tension (dynes/cm), S is the solubilization ratio (ml/ml), and C is a constant equal to about 0.3 for all hydrocarbons, chlorocarbons and mixtures (Pope and Wade 1995). This constant was verified using several anionic and nonionic surfactant systems in the middle-phase microemulsion region. The Chun-Huh equation may also be useful to estimate the IFT in the Type I microemulsion region. This equation shows that as the solubilization ratio (the volume of organic liquid solubilized in the microemulsion

divided by the volume of surfactant) increases, the interfacial tension decreases. If this equation holds for all surfactant systems, it may be impossible to simultaneously have both high solubilization and high IFT, as any change made to the surfactant to increase its IFT in an effort to avoid mobilization will simultaneously decrease its effectiveness in solubilizing the NAPL. Based on calculation by Pope and Wade (1996), this means IFTs on the order of 1 dyne/cm or higher and solubilization ratios on the order of 0.6 or lower will typically translate into solubilities on the order of 30,000 mg/L or lower for DNAPL and 15,000 mg/L or lower for LNAPL in 3% surfactant solutions.

Nonionic surfactants are often used in NAPL solubilization studies because they can, without the addition of salt or cosurfactant, solubilize reasonable amounts of NAPL (10,000 to 40,000 mg/L in batch) and produce relatively high IFTs (1 to 5 dyne/cm) (Pennell et al., 1993; Fountain et al., 1996). Nonequilibrium solubilization and macroemulsion formation have both been found in nonionic systems. Okuda et al (1996) reported that macroemulsion solubilizations of 1% and 10% TX 100 contributed 20% and 35%, respectively, of the total PCE recovered from glass bead columns. Macroemulsions

may not be suitable for aquifer remediation as they are fundamentally unstable, have high viscosity, and have relatively large droplets which may cause pore clogging problems. Kinetic adsorption of nonionic surfactants at the interface may cause nonequilibrium solubilization and decrease their remediation efficiency.

Ethoxylated alcohols are the most common nonionic surfactants used for NAPL remediation, as they are relatively high NAPL solubilizers and are also biodegradable. Generally, the tendency of ethoxylated alcohols is to form persistent emulsions with NAPL, leading to the exclusion of some surfactants that may have very high NAPL solubilization. Only these surfactants that show both reasonably high solubilization ratios and rapid microemulsification with low viscosity would be good study candidates.

The objectives of this study were to 1) determine the effect of cosurfactants, especially the branched short-chain alcohols, on the phase behavior and NAPL solubilization of a surfactant/cosurfactant system, 2) compare the solubilization and mobilization of PCE by nonionic and ionic surfactants, and 3) find an effective surfactant/cosurfactant system which has

relatively high solubilization and high IFT for possible field testing.

Materials and Methods

Surfactant and Cosurfactant

Forty two water soluble commercial surfactants that were collected during a DOD\AATDF\EPA project (Rhue et al., 1997) were used in this study. Pure pentanol and isopropanol which were obtained from Fisher Scientific were used as cosurfactants.

PCE Solubilization Screening Study

Forty two surfactant systems were screened for PCE solubilization. Two ml of 3% surfactant solution was transferred to a 5 ml vial, along with five drops of PCE spiked with approximately 50 mg/L Sudan red dye. The vial was shaken several times during a one day period, and allowed to settle for two days. The pink color intensity and the amount of free unsolubilized PCE were visually inspected to estimate the relative solubilization efficiency of each system.

After visual estimation of PCE solubilization, 12 nonionic surfactants, representing the most efficient of 42 surfactants, were selected for batch equilibrium solubilization studies. Because some surfactants with high PCE solubilization formed macroemulsions, IPA was added to reduce macroemulsion stability. Two ml of 3% surfactant solution, with or without 3% IPA, were added to 0.5 ml of PCE in a 5 ml vial. The sample was then shaken several times during a one day period, and allowed to settle for one week at room temperature. The clear aqueous phase was separated and injected into a GC for PCE and IPA analysis.

PCE solubilization in SDS/pentanol/IPA was determined by the titration method described in Chapter 3.

Partitioning Tracers in Batch Experiments

The water/PCE partition coefficients (K_p) for several alcohols used as partitioning tracers was measured at 1:4, 1:6, 1:8 water:oil ratios, with all samples being duplicated. The initial concentrations of methanol, 2,2-dimethyl-3-pentanol, hexanol and 6-methyl-2-heptanol were nearly 1000, 200, 200, and 200 mg/l, respectively. After rotating for eight hours and standing overnight, the samples were

centrifuged at 2000 RPM for 15 min. The aqueous phase then was injected into a GC to determine the alcohol concentrations.

Partitioning alcohol tracer concentrations in the NAPL phase (C_n) were calculated from the difference between the initial concentration (C_o) and the equilibrium concentration in the aqueous phase (C_e). The partition coefficient (K_p) is defined as:

$$K_p = C_n / C_e \quad (6-1)$$

Column Studies

Dry glass beads were packed in a 25mm ID x 50mm long glass column obtained from Kontes Glass Co. The columns were fitted with Teflon o-rings and Teflon end pieces, with Teflon or stainless steel tubing, fittings and valves being used in the delivery and column systems. Packed columns were saturated with DI water by pumping upward through the columns at a flow rate of 0.5 ml/min using a Shimadzu HPLC pump. PCE or dodecane was slowly injected into the column, opposite to the water flow direction, until PCE or dodecane breakthrough. Free PCE or dodecane was flushed from the column with water at a flow rate as high as 2 ml/min until no free PCE or dodecane was

observed in the effluent. Residual PCE or dodecane saturation was determined using column weight differences and partitioning tracers. Residual PCE or dodecane saturation (S_n) can be calculated using the following equation:

$$W_{pd} = \rho_{NAPL} V_{NAPL} - \rho_{water} V_{NAPL} \quad (6-2)$$

$$S_n = V_{NAPL} / PV \quad (6-3)$$

where ρ_{NAPL} is the density of pure PCE (1.623g/ml) or dodecane (0.7487 g/ml), ρ_{water} is the density of water (0.998 g/ml), W_{pd} is the weight difference between the water saturated column, with or without PCE or dodecane, and PV is the pore volume determined before oil introduction. A two ml pulse of partitioning tracer was pumped into the columns before contaminating with PCE and dodecane, after contamination, and after the surfactant flush to determine the PCE and dodecane residual saturation and the hydrodynamic dispersion characteristics of the columns. Residual saturation of PCE after the surfactant/cosurfactant flush was also determined by methanol extraction. Glass beads with residual PCE from each column were washed into a 65 ml vial with 35 ml of methanol and extracted for one day. The methanol extraction solution then was analyzed for PCE by GC.

The dodecane-contaminated column was flushed with a 4.5% SDS/5% pentanol/2% IPA/50mM CaCl_2 solution using an upward flow direction. The PCE contaminated column was flushed with two different surfactant/cosurfactant solutions (1a) 3% Brij 97/3% IPA with upward flow; and (1b) 3% Brij 97/3% IPA with downward flow; and (2) 3.5% SDS/3.5% pentanol/3.5% IPA with downward flow. All surfactant/cosurfactant solutions were pumped into the columns at a flow rate of 0.5 ml/min, and flow interruption was applied to the PCE column using flushing solution (1a). After flushing the columns with surfactant/cosurfactant for nearly 10 pore volumes, the pumping solution was switched to water for another 10 pore volumes. Column effluent was collected at 2 min intervals and PCE, dodecane, pentanol, IPA and SDS in the column effluent were determined by GC. Free dodecane that mobilized in the column effluent was dissolved into methanol, and free PCE was dissolved into additional surfactant/cosurfactant solution before GC analysis.

Results and Discussion

PCE Solubilization Screen

The PCE solubilization by commercial water-soluble surfactants was estimated visually (Table 6-1), by coloring the PCE with relatively high molecular weight Sudan dye. The pink color of the Sudan dye was used as an indicator to estimate PCE solubilization in the surfactant solution. It had been found that NAPL can be selectively solubilized in some cosolvents, but that this selective solubilization is less significant in surfactant solutions. Even if there was selective solubilization, it should not affect our estimation of highest solubilization, since we used no or almost no free PCE in the vial as the criterion for choosing the highest solubilizers. If all 5 drops of PCE were solubilized, the solubilization would be more than 25000 mg/ml, which may be the lowest solubilization required to efficiently remove PCE from an aquifer. Twelve surfactants, which were all nonionic, out of the 42 surfactants screened had high PCE solubilization, and an HLB in the range of 10.8 to 13.2. Only one surfactant, Detaine PB, which is an amphoteric not included among the 12, had low PCE solubilization but was

Table 6-1. Phase behavior and visually estimated PCE solubilization in alcohol-free surfactant solutions. All surfactant solutions were 3% concentrations.

Trade Name	Solubilization	Phase Behavior
<u>anionic</u>		
SDS	+++	Clear
Rhodapon BOS	+	separation slow
Witcolate S-1285C	+++	Clear
Witcolate SE-5	+++	Clear
Standpol ES-40	+++	Clear
Witconate AOS	++	Clear
Aerosol AY 65	++	Separation slow
Aerosol MA80-1	++	Clear
Emkapon Jel BS	++	Clear
<u>Nonionics</u>		
POE(10) laural	+++	Clear
Brij 35	+++	Clear
Brij 97	++++	transparent
Genepol 26-L-45	++++	transparent
Trycol 5953	++++	transparent
Hetoxol TD-9	++++	transparent
Macol LA 790	++++	transparent
Ritoleth 10	++++	transparent
Novell II 1216-CO-7	++++	Micro/Maroemulsion
Novell 1216-CO-9	++++	Clear
Novell II 1216-CO-10.5	+++	Clear
Syn Fac TDA 92	++++	Micro/Maroemulsion
Arapol 0712	++++	transparent
Ameroxol OE-10	++++	transparent
Myrj 52	+++	Clear
Nopalcol 2-L	++	Clear
Igepal CO-630	++++	Micro/Maroemulsion
Igepal CO-730	+++	Clear

Table 6-1 (cont'd)

Trade Name	solubilization	Phase Behavior
<u>Nonionics (cont'd)</u>		
Antarox LA-EP 15	+	Clear
Antarox LA-EP 45	+	Separation slow
Antarox LF 224	+	Clear
Rexonic P-5	+	Separation slow
Pluronic L43	+	Clear
Pluronic L44	++	Clear
Aldospense ML-23	++	Clear
Tween 20	+	Clear
Tween 40	+++	Clear
Tween 80	+++	Clear
DeSulf GOS-P-70	?	Clear
Alcodet SK	++++	type II
<u>Amphoterics</u>		
Detaine PB	+++	Clear

a: Pink color intensity increases as the number of plus signs increases. +, ++, +++, ++++ represent very low, low, medium and high PCE solubilization. ?: because of the background color of the surfactant, solubilization could not be estimated.

within this HLB range (Figure 6-1). Our study indicates that PCE solubilization decreases when the surfactant HLB is beyond the 10.8 to 13.2 range. PCE solubilization also decreases faster in the lower end of the HLB range than in the higher end. Diallo et al. (1994) found similar tendencies among the dodecyl alcohol ethoxylate surfactants. This solubilization-HLB relationship may result from the following factors: (1) the micellar core becoming more hydrophilic along with increasing cloud point as the HLB increases; (2) electron donor-acceptor complexation between EO units and PCE; and (3) decrease in the cloud point as PCE is solubilized in the micelle. PCE solubilization should be higher when the cloud point of the surfactant is lower. However, a cloud point at or near room temperature may be pushed even lower upon addition of a very small amount of PCE, resulting in very low apparent PCE solubilization.

PCE solubilization by the 12 nonionic surfactants, with and without IPA, is shown in Table 6-2. There is no relationship between surfactant HLB and PCE solubilization in these systems, because hydrocarbon chain length of the surfactant is more important than its HLB over the HLB range 12.4 to 13.2. PCE solubilization appears to increase as

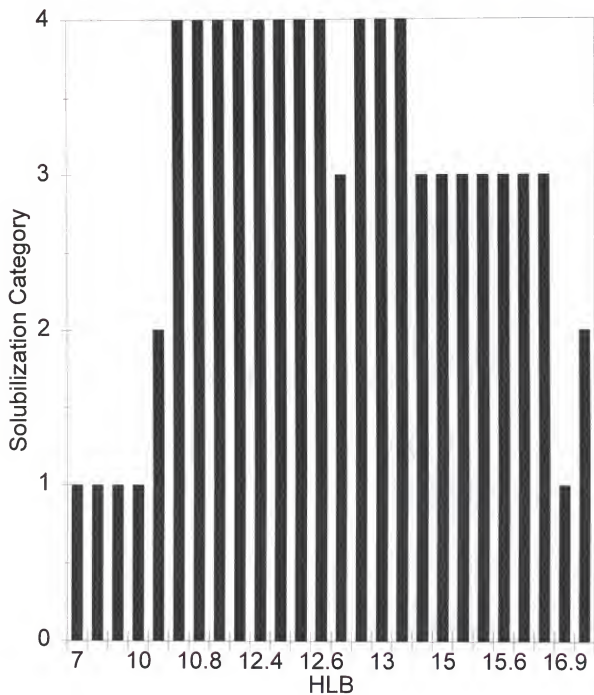


Figure 6-1. Relationship between the surfactant HLB and PCE solubilization.

Table 6-2. PCE solubilization and partition coefficient for IPA between water and PCE in 12 nonionic surfactant solutions.

Surfactant Name	HLB	PCE solubilization (mg/l)	K _{IPA}
Trycol 5953	12.4	26100	-
Trycol 5953/IPA		27500	0.0013
Novell II 1216-CO-9	N/A	32100	-
Novell II 1216-CO-9 /IPA		30200	0.0013
Syn Fac TDA 92	12.5	16000	-
Syn Fac TDA 92/IPA		14400	0.0027
Hetoxol TD-9	13.2	11400	-
Hetoxol TD-9/IPA		10800	0.0024
Arapol 0712	12.6	Macro ^a	-
Arapol 0712/IPA		41300	0.0019
Ritoleth 10	12.4	Macro	-
Ritoleth 10/IPA		75600	0.0050
Brij 97	12.4	Macro	-
Brij 97/IPA		71800	0.0027
Igepal CO-630	13	Macro	-
Igepal CO-630/IPA		43300	0.0021
Genapol 26-L-45	11.6	Macro	-
Genapol 26-L-45/IPA		Macro	-
Novell II 1216-CO-7	N/A	Macro	-
Novell II 1216-CO-7/IPA		Macro	-
Macol LA 790	10.8	Macro	-
Macol LA 790/IPA		Macro	-
Ameroxol OE-10	12	Macro	-
Ameroxol OE-10/IPA		Macro	-

a: PCE solubilization has not been analyzed due to the existence of macroemulsion.

hydrocarbon chain length increases, and to decrease as the number of EO units increase. Some nonic surfactants have a high PCE solubilization potential, but the formation of macroemulsions makes them unacceptable for remediation purposes unless IPA is added. IPA has almost no effect on PCE solubilization, since it has very little effect on surfactant cloud point, and a very low concentration in the micellar interface due to its low surface activity (Chapter 2). It does decrease macroemulsion stability in some surfactants capable of solubilizing more than 41000 mg PCE/L. This function of IPA may be due to its ability to decrease the interfacial viscosity, and increase the rate of phase equilibration. However, when the HLB of a surfactant is below 12, when the addition of 3% IPA can not increase the rate of phase equilibration sufficiently to make the surfactant useful for PCE contaminated aquifer remediation. Since macroemulsions have droplets larger than $1\ \mu$ they not only have the potential to plug soil pores, but are also highly viscous. Other researchers report PCE solubilizations of less than 41000 mg/L, presumably because they did not include a branched short chain alcohol in their systems (Fountain et al. 1991).

PCE solubilization in an SDS/pentanol system, with and without IPA, is shown in Figure 6-2. Maximum PCE solubilization occurs near the 1:3 molar ratio of SDS and pentanol at the micelle interface (Chapter 2,3) with IPA showing almost no effect on PCE solubilization.

Partitioning Tracers in Batch

The partition coefficient (K_p) of the alcohol tracers tend to increase as the ratio of oil/water decreases (Table 6-3). This may be because the alcohols tend to self-associate and/or co-associate in the oil phase, causing the partition coefficient to be related to the concentration of alcohol in the oil phase. If we assume the partitioning coefficient is a constant which can be measured from a single oil/water ratio (such as 1:4) batch study, then the NAPL residual saturation after surfactant flushing will be overestimated due to the higher water/oil ratio in the column or field, especially when using linear chain alcohols which tend to strongly self-associate in the oil phase.

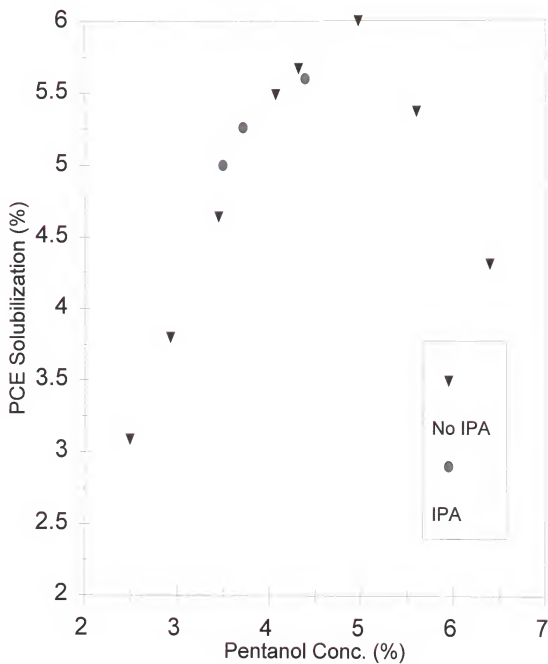


Figure 6-2. PCE solubilization in 3.5 %SDS with and without IPA as a function of the pentanol concentration in solutions.

Basic Properties of Brij 97 Solution

The basic properties of Brij 97 are shown in Table 6-4. The Brij 97/IPA solution has a relatively high IFT with PCE, and the viscosity of the Brij 97/IPA/PCE microemulsion is quite low. These properties may meet the necessary requirements for surfactant-enhanced aquifer remediation.

Column Studies

The hydrologic properties of the column are shown in Table 6-5. The initial PCE residual saturation estimated by the weight difference method and partitioning tracer method are almost the same as the estimate obtained by the mass balance method. The mass balance method is the sum of the PCE masses from the column effluents and the PCE residual in the column extracted with methanol after surfactant flushing.

Table 6-6 shows the PCE residual saturation, the PCE recovery after surfactant solution flushes, and the exponentially extrapolated estimates of surfactant solution pore volumes needed for full PCE recovery. PCE residual saturations and recoveries estimated from branched chain

Table 6-3. The partition coefficients of alcohol tracers between PCE and water.

Alcohol Tracer	Oil:Water Ratio	Partition Coefficient
2,2-dimethyl-3-pentanol	1:4	23.9
	1:6	25.9
	1:8	26.1
n-hexanol	1:4	6.7
	1:6	7.1
	1:8	7.3
6-methyl-2-heptanol	1:4	72.1
	1:6	75.2
	1:8	76.1

Table 6-4. Some basic properties of Brij 97 solutions.

CMC of Brij 97: 1.88×10^{-4} M
IFT at 3% Brij 97/PCE: 9.2 dyne/cm
IFT at 3%Brij+3%IPA/PCE: 8.90 dyne/cm
Viscosity of 3% Brij 97/3% IPA: 1.22cp
Viscosity of 3% Brij 97/ 3% IPA/3.8% PCE: 1.35cp

Table 6-5. Experimental conditions and physical properties of each PCE contaminated column.

parameter	column 1	column 2	column 3
surfactant solution	3% Brij 97/3%IPA	3%Brij 97/3%IPA	4.5%SDS/4.5%IPA 3.5%IPA
Flow mode	down	up	down
S_n^i (%) ^a	0.207	0.132	0.226
S_n^i (%) ^b	0.201	0.128	0.219
S_n^i (%) ^c	0.197	0.126	0.222
ρ_b (g/ml)	1.91	1.91	1.91
θ_s	43	43	42
L(cm)	5	5	5
P_e^i ^d	65	71	71
P_e^a ^e	57	58	34
v(cm/hr)	8.9	8.9	9.1

a: initial PCE saturation estimated from the weight difference method

b: initial PCE saturation estimated from hexanol partitioning using the K_p from 1:4 oil to water ratio

c: initial PCE saturation estimated from the sum of PCE mass in column effluents and final PCE residual mass extracted by methanol

d: Peclet number of the columns before PCE contamination

e: Peclet number of the columns after PCE contamination

Table 6-6. Recovery of PCE from columns and estimation of the surfactant solution pore volumes required for full recovery of PCE.

parameter	column 1	column 2	column 3
surfactant solution	3% Brij 97/3%IPA	3%Brij 97/3%IPA	4.5%SDS/4.5%IPA 3.5%IPA
Flow mode	down	up	down
S_n^f (%) ^a	0.024	0.009	0.005
S_n^f (%) ^b	0.015	0.005	0.004
S_n^f (%) ^c	-	0.004	0.002
S_n^f (%) ^d	0.017	0.004	0.003
Recovery (%) ^e	88.0	93.0	97.7
Recovery (%) ^f	92.5	96.2	98.2
Recovery (%) ^g	-	96.9	99.1
Recovery (%) ^h	91.5	96.9	98.6
PVs surfactant flushed	11	11	9.5
Estimated PVs for full recovery ⁱ	16	13	11

a: final PCE saturation estimated from hexnaol partitioning using K_p from 1:8 oil to water ratio

b: final PCE saturation estimated from 2,2-dimethyl pentanol partitioning using K_p from 1:8 oil to water ratio

c: final PCE saturation estimated from 6-methyl-2-heptanol partitioning using K_p from 1:8 oil to water ratio

d: final PCE saturation estimated from methanol extraction.

e: PCE recovery saturation estimated from hexanol partitioning

f: PCE recovery saturation estimated from 2,2-dimethyl pentanol partitioning

g: PCE recovery saturation estimated from 6-methy-2-heptanol partitioning

h: PCE recovery saturation estimated from methanol extraction

i: estimated pore volumes of surfactant solution required to recover all PCE in the column

alcohol partitioning are in good agreement with the results obtained from the methanol extractions.

When estimating residual oil saturation, the non-linear partitioning of linear alcohols between water and oil (Figure 2-2) must be taken into account. Assuming a constant partition coefficient can lead to overestimation of residual oil saturation, particularly at low oil contents and when the partition coefficient has been estimated at high oil:water ratios.

Eleven pore volumes of 3% Brij 97/3% IPA solubilized nearly 92% and 97% of the total PCE in columns 1 and 2, respectively. Nine and one-half pore volumes of 3.5% SDS/3.5% pentanol/3% IPA removed 98% of the total PCE in column 3. PCE solubilization in the BTC tail showed a nearly exponential decrease as more pore volumes of surfactant solution was pumped through (Figure 6-3). The use of exponential extrapolation to estimate the pore volumes of surfactant solution required to completely recover PCE from columns 1, 2, and 3 resulted in values of 16, 13, and 11, respectively.

PCE solubilization and mobilization breakthrough curves are shown in Figures 6-4, 6-5, 6-6, 6-7. No free PCE was found in the column effluent when Brij 97/IPA was used as the

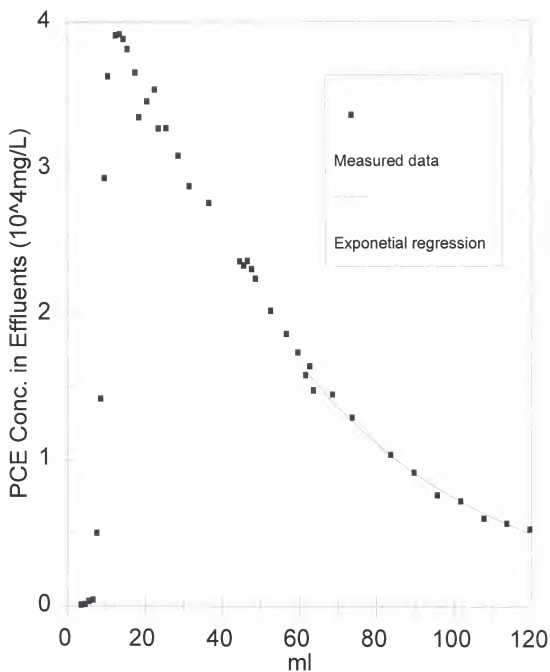


Figure 6-3. The exponential decrease of PCE solubilization in the BTC tail.

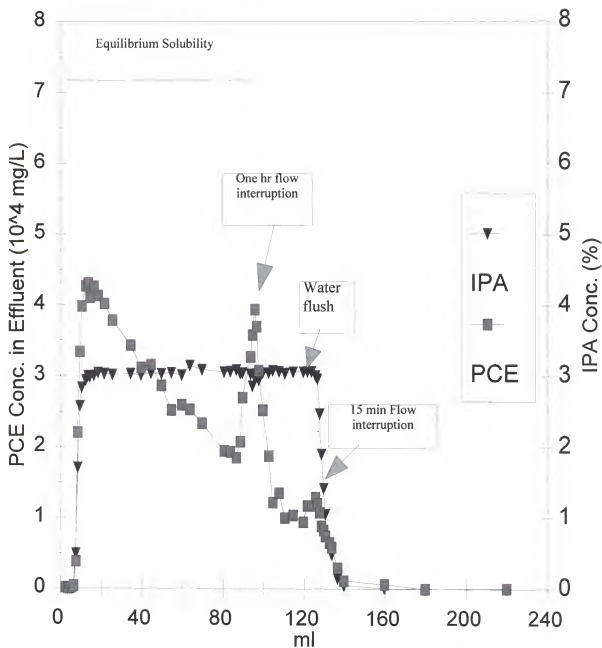


Figure 6-4. PCE and IPA concentrations in effluent from a glass column flushed with 3% Brij 97/3% IPA with upward flow mode.

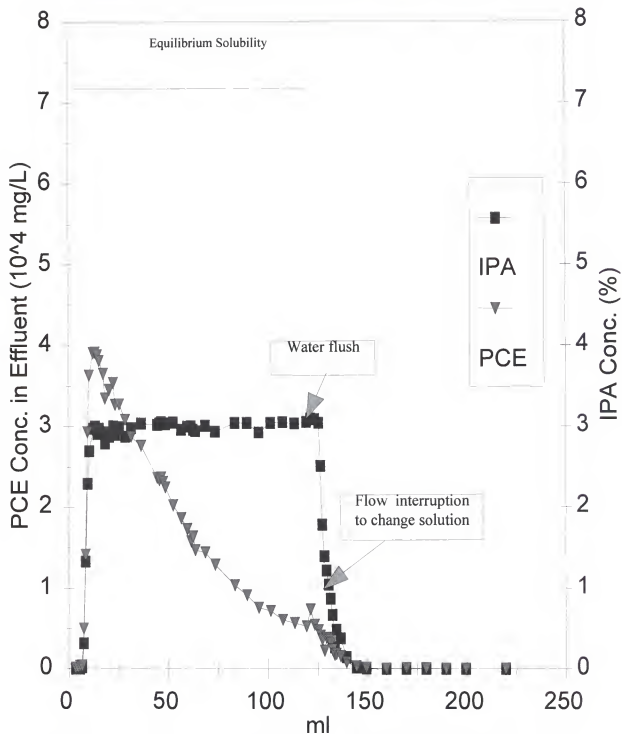


Figure 6-5. PCE and IPA concentrations in effluent from a glass column flushed with 3% Brij 97/3% IPA with downward flow mode.

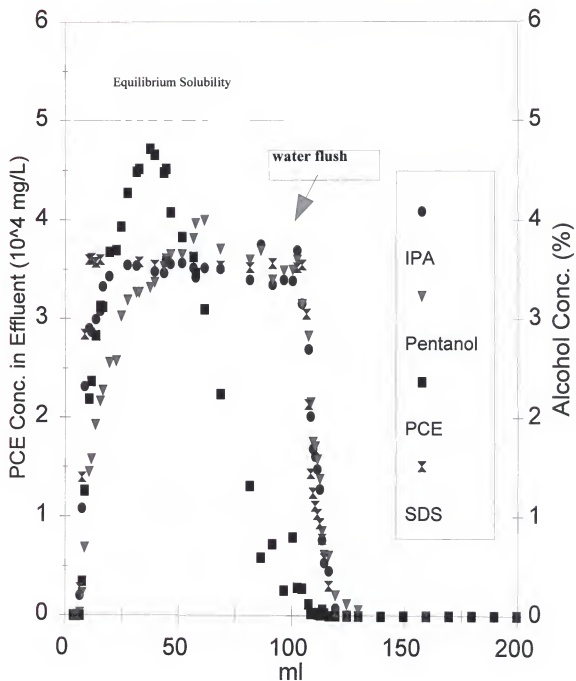


Figure 6-6. Pentanol, IPA and solubilized PCE concentrations in effluent from a glass column flushed with 3.5% SDS/3.5%/pentanol/3.5% IPA with downward flow mode.

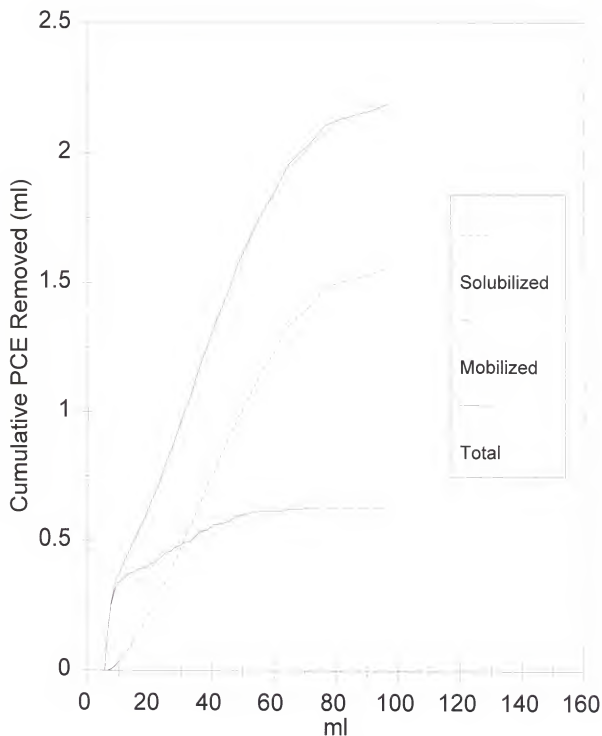


Figure 6-7. Solubilized, mobilized PCE volumes from a glass bead column flushed with 3.5% SDS/3.5% pentanol/3.5% IPA solution.

microemulsion processor, and there was almost no difference between the BTCs of the upward and downward flow modes of the Brij 97/IPA solution flushes. Upward flow mode would be less likely to cause mobilization of DNAPL since the capillary and buoyancy forces would be in opposing directions (Longino and Kueper, 1995). Similar BTCs between the two flow modes suggest that PCE did not mobilize within the columns, which was visually verified by the gradual uniform disappearance of the pink dye color observed during surfactant flushing. The column effluent was clear or transparent, and stable, which suggests that the removal of PCE from the column was due to the microemulsion solubilization process. The interfacial tension of Brij 97/IPA/PCE (9.6 dyne/cm) is much higher than the critical value of (1.7-4.3 dyne/cm) for mobilization of PCE reported by Pennell and coworkers(1996). This interfacial tension should be very good for solubilization-only remediation even when groundwater hardness is high, which tends to decrease interfacial tension. If we want a higher solubilizing system, it is possible to add salt to increase solubilization without decreasing the IFT to the critical value. However, the phase behavior and viscosity of the salt enhanced microemulsion should be further investigated. The

SDS/Pentanol/IPA system, on the other hand, solubilizes a similar amount of PCE in its column effluents as the Brij 97/IPA system but it also mobilizes PCE. This mobilization accounts for 30% of total PCE recovered from the column. The interfacial tension of PCE in this system cannot be determined by the drop weight method, as very low IFT causes PCE to automatically fall from the delivery tube. The IFTs between the SDS/pentanol/IPA solution and PCE, and between the Brij 97/IPA solution and PCE can be estimated using the Chun-Huh equation and the maximum PCE solubilized in the column effluents for the calculation. The IFTs for the SDS/pentanol/IPA system and the Brij 97/IPA system are 0.55 and 0.37 dyne/cm, respectively. The Chun-Huh equation has been successfully used to estimate the IFTs of ionic and nonionic surfactant middle phase microemulsions, and ionic surfactant Type I microemulsions (Pope and Wade, 1995). The results from our study shows that this equation underestimates the IFT of the nonionic surfactant Type I microemulsion. Relatively high solubilization and IFT can exist simultaneously in the nonionic surfactant Type I microemulsion.

PCE in the column effluent reaches its maximum concentration after flushing with nearly one pore volume of surfactant solution. This maximum PCE concentration in the column effluent is almost the same as PCE solubilization in the batch study for the SDS/pentanol/IPA solution, while maximum PCE concentration in the column effluent is only about 55% of PCE solubilization in the batch study for the Brij 97/IPA solution. PCE solubilization in the ionic surfactant solution may be an equilibrium process, while that in the nonionic surfactant solution is a nonequilibrium process. Pennell and coworkers (1993) found that the PCE concentration in their column effluent was less than that in the batch study for a POE (20) sorbitan monooleate solution. The NAPL solubilization in the SDS system could require less energy than in Brij 97 system because of lower interfacial tension in the SDS system. In addition, the lower interfacial tension also could cause the oil/water interfacial area to increase. Therefore, the lower IFT system may reach equilibrium more easily than the higher IFT system. Kinetic controlled adsorption of nonionic surfactant in the interface (see Chapter 5) may also contribute to nonequilibrium solubilization. The decrease in PCE solubilization as more

PCE is removed from the column may be due to a decrease in the interfacial area and/or a dilution effect. Flow interruption dramatically increases the PCE solubilization, allowing reduction of the surfactant solution pore volumes required to achieve a near full recovery of PCE. There is a very small amount of IPA partitioning into the PCE phase when 3% Brij 97, 3% IPA and PCE are the surfactant, cosurfactant and oil in the Type I microemulsion system (Table 6-2). However, a significant amount of pentanol may partition into the oil phase, depending on the polarity of the oil. Pentanol has been successfully applied as a cosurfactant for the remediation of alkane hydrocarbon dominated jet fuel contaminated aquifers in Lab and field studies (Rhue et al. 1997; Jawitz et al., 1997). When dodecane, which has a carbon number similar to the effective alkane carbon number (ACN) of jet fuel is used as the oil phase the effect of pentanol partitioning on remediation efficiency is insignificant, and can be found in Figures 6-8, 6-9 and 6-10. Seven and one-half pore volumes of 4.5% SDS/5% Pentanol/ 50mM CaCl_2 /2% IPA removed 99.9% of the dodecane in a glassbead column without significantly retarding the pentanol breakthrough. When more polar PCE is used as the oil, pentanol partitioning can be expected to increase

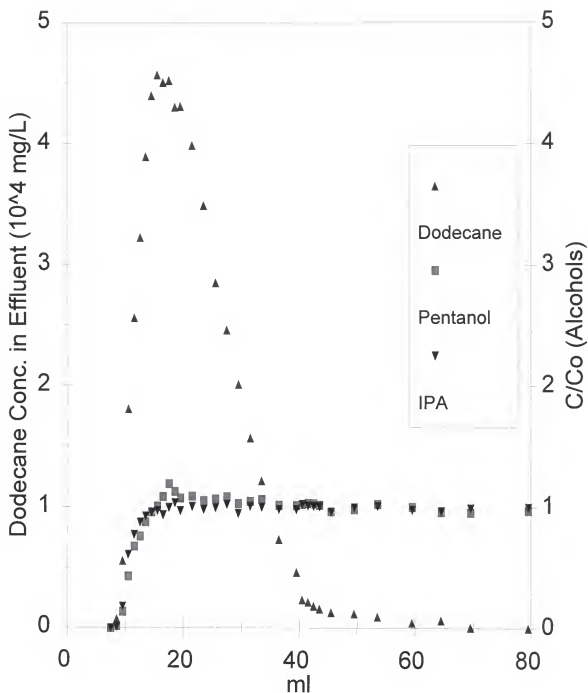


Figure 6-8. Pentanol, IPA and solubilized dodecane concentrations in effluent from a glass bead column flushed with 4.5% SDS/5% pentanol/2% IPA/50 mM CaCl_2 solution.

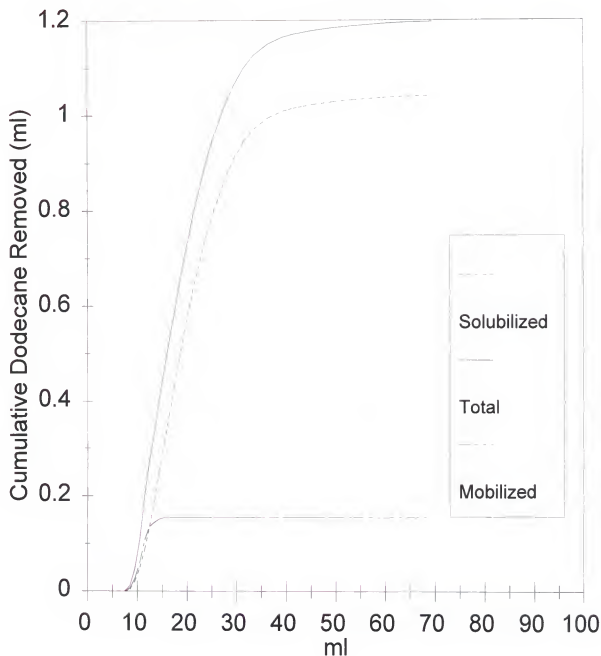


Figure 6-9. Solubilized and mobilized dodecane volumes from a glass bead column flushed with 4.5% SDS/5% pentanol/2% IPA/50 mM CaCl_2 solution.

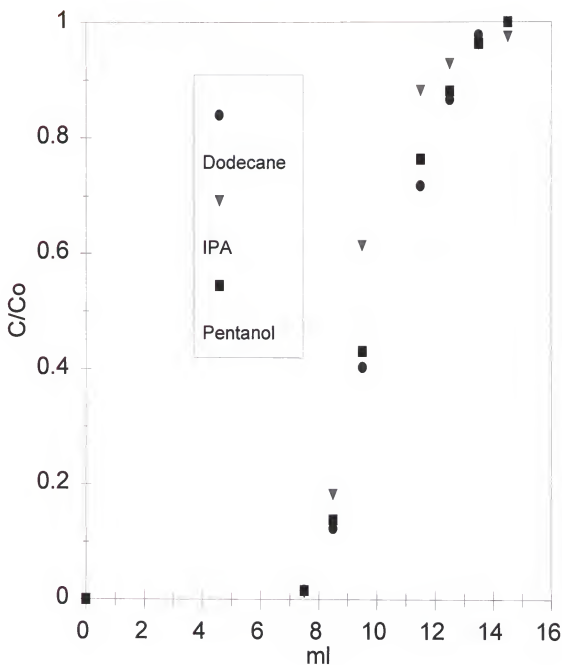


Figure 6-10. Normalized pentanol, IPA and solubilized dodecane concentrations in effluent of front BTC from a glass bead column flushed with 4.5% SDS/5% pentanol/2% IPA/50 mM CaCl_2 solution.

significantly since the partitioning coefficient between the pentanol monomers in the oil and pentanol in the water is higher for PCE ($K_w=1.4$) than that for dodecane ($K_w=0.49$). A detailed description of the equation used to calculate K_w is in Chapter 2. Pentanol retardation is quite high when the surfactant/cosurfactant is pumped through a PCE contaminated column (Figure 6-11).

Conclusions

Nonionic surfactants have higher PCE solubilization than anionic surfactants, without the addition of salts or cosurfactants. PCE solubilization appears to peak at an HLB between 10.8 and 13.2. Nonionic surfactants have PCE solubilizations as high as 71000 mg/L in batch equilibrium but reached a value of only 40000 mg/L in the 1-D columns used in this study. Nonequilibrium solubilization might be occurring in the nonionic surfactant system as evidenced by lower PCE concentrations in the column effluent as opposed to the batch study, and increased PCE solubilization during flow interruption. The nonionic surfactant/IPA has a much higher IFT between PCE and the aqueous phase than the anionic surfactant/cosurfactant. The anionic system, while

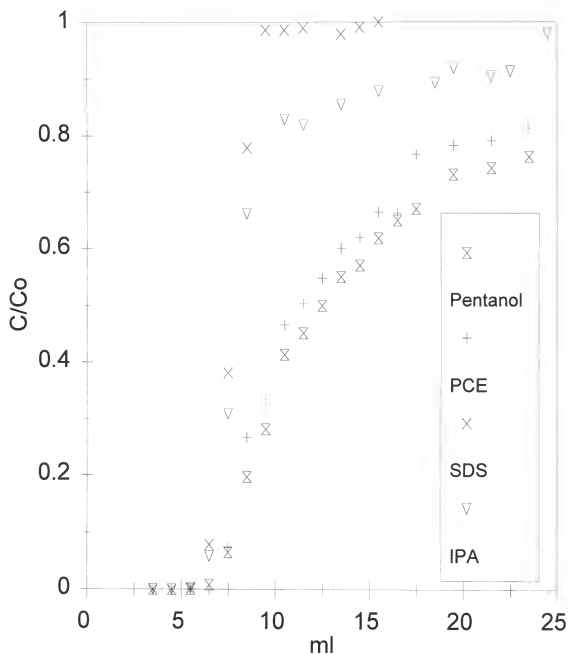


Figure 6-11. Normalized IPA, pentanol, SDS and solubilized PCE concentrations in effluent of front BTC from a glass bead column flushed with 3.5% SDS/3.5% pentanol/3.5% IPA solution.

solubilizing a similar amount of PCE as the nonionic system, also mobilizes PCE in the column.

All of the nonionic surfactants screened that had high PCE solubilizations (>41000 mg/L) formed macroemulsions which did not break into low viscosity equilibrium microemulsions within one week unless IPA was included in the systems. IPA increases the microemulsion phase separation speed and helps to produce good phase behavior. IPA may also increase the PCE solubilization rate by promoting surfactant mass transfer to the interface. The chromatographic separation of surfactant and alcohol is minute since there is no significant amount of alcohol partitioning into the PCE phase.

The nonionic surfactant/IPA flow modes (down and up) generated similar PCE solubilization breakthrough curves. Eleven pore volumes of 3% Brij 97/3% IPA solution removed 92% and 97% of the initial PCE saturations of 20% and 13%, respectively, in glassbead columns. Linear chain partitioning alcohols tend to overestimate the residual PCE saturation after surfactant/IPA flushing. Branch chain partitioning alcohols, however, are in good agreement with methanol extraction and mass balance methods. Exponential extrapolation estimated the pore volumes of Brij 97/IPA required to remove

nearly all the PCE from contaminated glassbead columns as 16 and 13 pore volumes, respectively, for the two columns studied. Using flow interruption should reduce the required pore volumes to less than ten for both systems.

Relatively high PCE solubilization and IFT can be achieved by using a nonionic surfactant/IPA system. We believe the nonionic surfactant/IPA system shows the greatest potential for successful field testing because it is a high PCE solubilizer and not a PCE mobilizer.

CHAPTER 7

SUMMARY AND CONCLUSIONS

The study of alcohol partitioning behavior and the role of alcohol in NAPL solubilization is necessary for the formulation of optimum microemulsions. The alcohol partitioning behavior between aqueous and oil phases, and between aqueous and interfacial phases was investigated using the pseudophase model coupled with the alcohol self-association model. Pentanol tends to self-associate in the oil phase. The pentanol partition coefficient between the total pentanol in the aqueous phase and the oil depends on the polarity of the oil. More pentanol partitions into PCE than into dodecane because the pentanol monomers prefer to partition into polar oils rather than nonpolar oils. Branched short-chain alcohols appear to co-associate with pentanol in the oil phase instead of self-associate.

Dodecane solubilization increased linearly with the pentanol mole fraction in the interface. The pentanol in the microemulsion system acts as a cosurfactant and not a

cosolvent. When the interface is pentanol saturated, addition of pentanol will decrease oil solubilization. We propose a two region pentanol partitioning model in which alcohol located in the interface acts like a cosurfactant, and then when the interface is pentanol saturated it penetrates into the inner core of the micelle and acts like a polar oil. Under no condition, did pentanol behave as a cosolvent in the presence of SDS.

Knowledge of the effect of alcohol, soil properties, and surfactant concentration on surfactant sorption is essential for designing a microemulsion system with a low surfactant loss. The two main surfactant loss mechanisms are the precipitation of ionic surfactant with divalent cations, and the adsorption of surfactant on soil surfaces. Precipitation is the main surfactant loss mechanism on calcareous soils, while adsorption is the predominant sorption mechanism on high iron oxide soils. Precipitation reaches a maximum at SDS concentrations near the CMC and decreases at SDS concentrations above the CMC. On the other hand, adsorption plateaus as the SDS concentration approaches the CMC. The significant changes in sorption behavior near the CMC are due to the formation of micelles. Pentanol decreases SDS

precipitation and adsorption through micellization, which decreases the CMC. A lower CMC means that less SDS monomers are available for precipitation and adsorption, and more micelles are available for complexation of divalent cations.

Divalent cation concentration in the soil solution is governed by one or more of the following processes: carbonate dissolution, cation exchange, precipitation of cations with dodecyl sulfate (DS), and the association of divalent cations with micelles and admicelles, which is dependant on the soil properties and the SDS concentration.

The selection of a good surfactant and alcohol system for NAPL solubilization depends on the properties of the NAPL and surfactant. The results from the NAPL solubilization study suggest that pentanol is a good cosurfactant for nonpolar LNAPL, such as dodecane, solubilization. Pentanol increases the LNAPL solubilization by water soluble surfactants by increasing the hydrophobicity of the interfaces. However, pentanol may not be a very good cosurfactant for a polar DNAPL such as PCE. Polar organics, like pentanol and PCE, tend to decrease the cloud point of nonionic surfactants. Adding pentanol to the system may cause over depression of the cloud point. Moreover, pentanol appears to have a high partition

coefficient between the aqueous phase and the polar oil (PCE). IPA, which can increase the rate of microemulsion phase separation and promote surfactant mass transfer to the interface, is a good interfacial modifier for PCE solubilization in nonionic surfactant systems.

Nonionic surfactants had higher PCE solubilization than anionic surfactants under the conditions employed in this study (no pentanol and no salt). PCE solubilization appears to peak at an HLB between 10.8 and 13.2. Nonionic surfactants had PCE solubilizations as high as 71000 mg/l in batch equilibrium but reached only 40000 mg/l in the 1-D columns. Nonequilibrium solubilization have occurred in the nonionic surfactant system as evidenced by the PCE concentration in the column effluent being lower than in the batch study, and PCE solubilization increasing after flow interruption.

All nonionic surfactants with high PCE solubilization (>41000 mg/L) formed macroemulsions which did not break into low viscosity equilibrium microemulsions within one week, unless IPA was included in the systems.

Eleven pore volumes of 3% Brij 97/3% IPA solution removed 92% and 97% of the PCE in glassbead columns at initial PCE saturations of 20% and 13.2%, respectively. Linear chain

partitioning alcohols tended to overestimate residual PCE saturation after surfactant/alcohol flushing, when a single constant value for the partition coefficient was used. Use of branched chain alcohols as partitioning tracers resulted in estimation of residual saturations that agreed well with the methanol extraction and mass balance methods. Exponential extrapolation estimated the pore volumes necessary to remove nearly all the PCE from the two Brij 97 columns at 16 (for downward flow and 20% initial PCE residual saturation) and 13 (for upward flow and 13% initial PCE residual saturation) pore volumes respectively. Use of flow interruption should reduce the required number of pore volumes to less than ten.

The Chun-Huh equation underestimated the IFT of nonionic surfactant/PCE Type I microemulsions. Relatively high PCE solubilization and high IFT can be simultaneously achieved by using nonionic surfactant/IPA systems. The Brij 97/IPA system, which had relatively high PCE solubilization and did not mobilize PCE in glass bead column experiments, has the greatest potential for use in the field of all the surfactant/alcohol systems evaluated.

ABBREVIATIONS

AATDF	Advanced Technology Demonstration Facility
BTC	Breakthrough curve
CAC	Critical admicelle concentration
C_e	Equilibrium partitioning alcohol concentration in the aqueous phase (g/dL)
C_{DS}^{eq}	Equilibrium concentration of DS (g/dL)
C_i	Concentration of ion species i (M)
C_{DS}^i	Initial concentration of DS (g/dL)
CMC	Critical micelle concentration
C_N	Partitioning alcohol concentration in the NAPL phase (g/dL)
C_1^o	Alcohol monomer concentration in the oil phase (g/dL)
C_A^o	Total alcohol concentration in the oil phase (g/dL)
C_P^o	Total pentanol concentration in the oil phase (g/dL)
C_A^w	Percent of alcohol concentration in water (g/dL)
D	Diffusion coefficient (cm ² /s)

DNAPL	Dense nonaqueous phase liquid
DOD	Department of Defense
DS	Dodecyl sulfate
EDA	Electron donor acceptor
EPA	Environmental Protection Agency
f	Correction factor related to the interfacial tension calculation
HLB	Hydrophile-lipophile balance
HMC	Hemimicelle micelle concentration
I	Ionic strength
IPA	Isopropanol
IFT	Interfacial tension (dyne/cm)
K	Equilibrium constant of alcohol self-association in the oil phase
K'	Partition coefficient of alcohol between alcohol in the aqueous phase and alcohol monomers in the oil phase
K_{IPA}	Partition coefficient of IPA between the PCE and microemulsion phases
K_p	Partition coefficient for alcohol between the NAPL and aqueous phases
K_1	Solubility product of calcite

K_2	Acidity constant for carbonate acidity
K_3	Acidity constant for bicarbonate acidity
K_4	Equilibrium constant for ionization of water
K_{sp}	Solubility product of $\text{Ca}(\text{DS})_2$
cK_A	Ratio of total alcohol concentration in the oil phase to alcohol concentration in the aqueous phase
$^cK_{IPA}$	Ratio of total IPA concentration in the oil phase to IPA concentration in the aqueous phase
cK_P	Ratio of total pentanol concentration in the oil phase to alcohol concentration in the aqueous phase (g/dL)
xK_A	Mole fraction-based partition coefficient of alcohol between the aqueous phase and the micelle interface
$^xK_{IPA}$	Mole fraction-based partition coefficient of IPA between the aqueous phase and the micelle interface
xK_P	Mole fraction-based partition coefficient of pentanol between the aqueous phase and the micelle interface
L	Length of the column (cm)

LNAPL	Light nonaqueous phase liquid
L1	Normal micelle
L2	Reverse micelle
M	Mass of soils (g)
NAPL	Nonaqueous phase liquid
o/w	Oil-in-water microemulsion
P_e	Peclet number
PCE	Tetrachloroethylene
PV	Pore volume
S	Solubilization parameter (volume of oil or water solubilized per unit volume of neat surfactant, ml/ml)
SDS	Sodium dodecyl sulfate
S_n^f	Residual NAPL saturation after surfactant solution flushing
S_n^i	Initial residual NAPL saturation (%)
r	Radius of modified burette tip (cm)
S_{DS}	SDS sorption on soils (mg/g)
t	Time (s)
ν_k	Kinematic viscosity (cp cm ³ /g)
v	Linear velocity (cm/hr)
V	Volume of aqueous phase (dL)

V_{NAPL}	Volume of residual NAPL in the water saturated column (ml)
W	Weight of an ideal drop of liquid (g)
W'	Weight of an actual drop of liquid (g)
W_d	Weight of the displaced liquid (g)
W_{pd}	Weight difference between the water saturated column with or without NAPL (g)
w/o	Water in oil microemulsion
X_{Ca}	Binding constant of Ca ion with micelles
Z_i	Charge on ion species i
$[\text{Ca}^{2+}]$	Aqueous phase Ca ion concentration (M)
$[\text{Ca}^{2+}]_m$	Micelle bound Ca ion concentration (M)
$[\text{Ca}^{2+}]_T$	Total Ca ion in solution (M)
$[\text{CO}_3^{2-}]$	Aqueous phase carbonate ion concentration (M)
$[\text{DS}^-]$	Monomer DS ion concentration
$[\text{DS}^-]_m$	Micelle DS ion concentration (M)
$[\text{DS}^-]_T$	Total DS ion concentration in solution (M)
$[\text{H}^+]$	Aqueous phase hydrogen ion concentration (M)
$[\text{HCO}_3^-]$	Aqueous phase bicarbonate ion concentration (M)
$[\text{H}_2\text{CO}_3]$	Aqueous phase carbonic acid concentration (M)
$[\text{Mg}^{2+}]_T$	Total Mg ion concentration in solution (M)
$[\text{Na}^+]_T$	Total Na ion concentration in solution (M)

$[\text{OH}^-]$	Aqueous phase hydrogen oxide ion concentration (M)
α	Empirical constant for CMC calculation
β	Empirical constant for CMC calculation
Γ	Maximum surfactant adsorption at the interface (mol/cm ²)
Γ_c	Concentration dependent surfactant adsorption at the interface (mol/cm ²)
γ	Interfacial tension (dyne/cm)
γ_{Ca}	Activity coefficient of Ca ion
γ_{DS}	Activity coefficient of DS ion
η	Dynamic viscosity (cp)
θ_s	Saturated volumetric water content
ρ	Density (g/cm ³)
ρ_b	Bulk density of glass beads (g/cm ³)
ϕ_A°	Total alcohol volume fraction in the oil phase
ϕ_1°	Volume fraction of alcohol monomers in the oil phase

LIST OF REFERENCES

- Abdul A.S. and T.L. Gibson. 1991. Laboratory Studies of Surfactant-Enhanced Washing of Polychlorinated Biphenyl from Sandy Material. Environ. Sci. Technol. 25, 665-671.
- Abe M., D. Schechter, R.S. Schechter. W.H. Wade, U. Weerasooriya and S. Yiv. 1986. Microemulsion Formation with Branched Tail Polyoxy Ethylene Sulfonate Surfactants. J. Colloid Interface Sci. 114, 342-356.
- Abuin E.B. and E.A. Lissi. 1983. Partitioning of n-Hexanol and n-Heptanol in Micellar Solutions of Sodiumdodecyl Sulfate. J. Colloid and Interface Sci. 95, 198-203.
- Adeel Z. and R.G. Luthy. 1995. Sorption and Transport Kinetics of a Nonionic Surfactant through an Aquifer Sediment. Environ. Sci. Technol. 29, 1032-1042.
- Aoudia M., M.A.J. Rodgers and W.H. Wade. 1991. Light Scattering and Fluorescence Studies of o/w Microemulsion: The Sodium 4-Dodecylbenzenesulfonate-Butanol-Water-NaCl-Octane System. J. Colloid Interface Sci. 144, 353-362.
- Attwood D., V. Mosquera, J. Rodriguez, M. Garcia and M.J. Suarez. 1995. Effect of Alcohols on the Micellar Properties in Aqueous Solution of Alkyltrimethylammonium Bromides. Colloid Polymer Sci. 272, 584-591.
- Ballet F. and F. Candau. 1981. Water-Oil Solubilization by Long Chain Poyoxyethylene Nonionic Surfactants. Colloid Polymer Sci. 259, 548-552.

- Barakat Y., J.L.N. Fortney, R.S. Schechter, W.H. Wade and S.Yiv. 1983. Criteria for Structuring Surfactants to Maximize Solubilization of Oil and Water: II. Alkylbenzene Sodium Sulfonates. J. Colloid Interface Sci. 92, 561-574.
- Biais J., B. Clin and P. Lalanne. 1988. Phase Diagrams and Pseudophase Assumption. In: Microemulsions: Structure and Dynamics. S. E. Friberg and P. Bothorel, eds. CRC Press, Boca Raton, FL.
- Blokhuis A.M. 1990. Effect of Different Butanols on the Adsorption of Sodium Dodecylsulfate on Alumina. Colloid Polymer Sci. 268, 679-682.
- Blokhuis A.M. and J. Sjöblom. 1991. Surfactant and Cosurfactants in Lamellar Liquid Crystals and Adsorbed on Solid Surfaces: II. Influence of Electrolyte on the Model System Sodium Dodecyl Sulphate/Benzyl Alcohol and α -Alumina. J. Colloid Interface Sci. 141, 395-399.
- Bohmer M. and L.K. Koopal. 1992. Adsorption of Ionic Surfactants on Variable-Charge Surfaces. 1. Charge Effects and Structure of the Adsorbed Layer. Langmuir 8, 2649-2659.
- Bourrel M. and R.S. Schechter. 1988. Microemulsions and Related Systems. Marcel Dekker, Inc. New York.
- Bowcott J.E. and J.H. Schulman. 1955. Emulsions: Control of Droplet Size and Phase continuity in Transparent Oil-Water Dispersions Stabilized with Soap and Alcohol. Z. Elektrochem. 59, 283-288.
- Brownawell B.J., H. Chen, W. Qhang and J.C. Westall. 1991. Adsorption of Surfactants. In: Organic Substances and Sediments in Water: Processes and Analytical. Vol 2, Robert A. Baker, ed. Lewis Publishers, Ann Arbor.
- Carroll B.J. 1981. The Kinetics of Solubilization of Nonpolar Oils by Nonionic Surfactant Solutions. J. Colloid Interface Sci. 79, 126-135.

- Chander P., P. Somasuundaran and N.J. Turro. 1987. Fluorescence Probe Studies on the Structure of the Adsorbed Layer of Dodecyl Sulfate at the Alumina-Water Interface. *J. Colloid Interface Sci.* 117, 31-46.
- Ching Y. and C.J. Jafvert. 1997. Sorption of Linear Alcohol Ethoxylate Surfactant Homologues to Soils. *J. Contaminant Hydrology* 28, 311-325.
- Choi Y.T., M.S. El-Asser, E.D. Sudol and J.W. Vanderhoff. 1985. Polymerization of Styrene Miniemulsions. *J. Polymer Sci. Polymer Chem. Edn.* 23, 2973-2987.
- Chun H. 1979. Interfacial Tensions and Solubilization Ability of a Microemulsion Phase That Coexists with Oil and Brine. *J. Colloid Interface Sci.* 71, 408-426.
- Clausse M., A. Zradba and L. Nicolas-Morgantini. 1987. Water/Sodium Dodecyl sulfate/1-Pentanol/N-Dodecane Microemulsions. Realm-of-Existence and Transport Properties. In: Microemulsion systems. H.L. Rosano and M. Clausse, eds. Marcel Dekker, Inc. New York.
- De Gennes P.G. and C. Taupin. 1982. Microemulsions and the Flexibility of Oil/Water Interfaces. *J. Phys. Chem.* 86, 2294-2304.
- Desnoyers J.E., F. Quirion, D. Hetu and G. Perron. 1983. Tar Sand Extractions with Microemulsions: I. The Dissolution of Light Hydrocarbons by Microemulsions Using 2-Butoxyethanol and Diethylamine as Cosurfactants. *Canadian J. Chem. Eng.* 61, 672-679.
- Diallo M.S., L.M. Abriola and W.J. Weber, Jr. 1994. Solubilization of Nonaqueous Phase Liquid Hydrocarbons in Micellar Solutions of Dodecyl Alcohol Ethoxylates. *Environ. Sci. Technol.* 28, 1829-1837.
- Edwards D.A., Z. Liu and R.G. Luthy. 1994. Surfactant Solubilization of Organic Compounds in Soil/Aqueous Systems. *J. Environ. Eng.* 120, 4-21.

- Edwards D.A., R.G. Luthy and Z. Liu. 1991. Solubilization of Polycyclic Aromatic Hydrocarbons in Micellar Nonionic Surfactant Solutions. *Environ. Sci. Technol.* 25,127-133.
- Environmental Protection Agency (EPA). 1992. Dense Nonaqueous Phase Liquid -- A Workshop Summary. EPA, EPA/600/R-92/030.
- Fainerman V.B. and Miller R. 1995. Dynamic Surface Tensions of Surfactant Mixtures at Water-Air Interface. *Colloids Interfaces* 97, 65-82.
- Fan X., P. Stenius, N. Kallay and E. Matijevic. 1988. Precipitation of Surfactant Salts: II. The Effect of Nonionic Surfactants on Precipitation of Calcium Dodecyl Sulfate. *J. Colloid Interface Sci.* 121, 571-578.
- Forland G.M., T. Rahman, H. Hoiland and K.J. Borve. 1996. Adsorption of Sodium Dodecyl Sulfate and Butanol onto Acidic and Basic Alumina. *J. Colloid Interface Sci.* 182, 384-355.
- Forland G.M., J. Samseth, H., Hoiland and K. Mortensen. 1993. The Effect of Medium Chain Length Alcohols on the Micellar Properties of Sodium Dodecyl Sulfate in Sodium Chloride Solutions. *J. Colloid Interface Sci.* 164, 163-167.
- Fountain J.C. 1997. The Role of Field Trials in Development and Feasibility Assessment of Surfactant-Enhanced Aquifer Remediation. *Water Environment Research.* 69, 188-195.
- Fountain J.C., R.C. Starr, T Middleton, M. Beikirch, C. Taylor and D. Hodge. 1996. A Controlled Field Test of Surfactant-Enhanced Aquifer Remediation. *Ground Water.* 34, 910-916.
- Fu E., P. Somasundaran and C. Maltesh. 1996. Hydrocarbon and Alcohol Effects on Sulfonate Adsorption on Alumina. *Colloids Surfaces* 112, 55-62.

- Gao Z., J.C.T. Kwak, R.L. Labonte, D.G. Marangoni and R.E. Wasylishen. 1990. Solubilization Equilibria of Alcohols and Polymers in Micellar Solutions: NMR Paramagnetic Relaxation Studies. *Colloid Surfaces* 45, 269-281.
- Gao Z., R.E. Wasylishen and J.C.T. Kwak. 1989. An NMR Paramagnetic Relaxation Method to Determine Distribution Coefficients of Solubilizates in Micellar Systems. *J. Phys. Chem.* 93, 2190-2192.
- Gee G.W. and J.W. Bauder. 1986. Particle-Size Analysis. In: Methods of Soil Analysis. Part 1. Physical and Mineralogical Methods. 2nd Edition. A. Klute ed. American Society of Agronomy. Soil Science Society of America. Madison, WI.
- Geeraerts G. and P. Joos. 1994. Dynamic Surfactant tensions of Micellar Triton X-100 Solutions. *Colloids and Surfaces*. 90, 149-154.
- Gobel J.G. and G.R. Joppien. 1997. Dynamic Interfacial Tensions of Aqueous Triton X-1000 Solutions in Contact with Air, Cyclohexane, n-Heptane, and n-Hexadecane. *J. Colloid Interface Sci.* 191, 30-37.
- Graciaa A., J. L.N. Fortney, C. Lalanne-Cassou, R.S. Schechter, W.H. Wade, U. Weerasooriya and S. Yiv. 1983a. The Phase Behavior of Simple Salt-Tolerant Sulfonates. *Soc. Pet. Eng. J.* 23, 913-918.
- Graciaa A., J. L.N. Fortney, R.S. Schechter, W.H. Wade and S. Yiv. 1982. Criteria for Structuring Surfactants to Maximize Solubilization of Oil and Water: Part 1- Commercial Nonionics. *Soc. Pet. Eng. J.* 22, 743-749.
- Graciaa A., J. Lachaise, C. Cucuphat, M. Bourrel and J.L. Salager. 1993. Improving Solubilization in Microemulsions with Additives. 2. Long Chain Alcohols as Lipophilic Linkers. *Langmuir* 9, 3371-3374.
- Graciaa A., J. Lachaise, J.G. Sayous, P. Grenier, S. Yiv, R.S. Schechter and W.H. Wade. 1983b. The Partitioning of

- Complex Surfactant Mixtures between Oil/Water/Microemulsion Phases at High Surfactant Concentrations. *J. Colloid Interface Sci.* 93, 474-486.
- Guerinand G. and A.M. Bellocq. 1988. Effect of Salt on the Phase Behavior of the Ternary System Water-Pentanol-Sodium Dodecyl Sulfate. *J. Phys. Chem.* 92, 2550-2557.
- Harkins W.D. and F.E. Brown. 1919. The Determination of Surface Tension (Free Surface energy), and the Weight of Falling Drops: The Surface Tension of Water and Benzene by the Capillary Height Method. *J. Am. Chem. Soc.* 41, 499-524.
- Harwell J.H., J. Hoskins, R.S. Schechter and W.H. Wade. 1985. Pseudophase Separation Model for Surfactant Adsorption: Isomerically Pure Surfactants. *Langmuir* 1, 251-262.
- Hayase K. and S. Hayano. 1978. Effect of Alcohols on the Critical Micelle Concentration Decrease in the Aqueous Sodium Dodecyl Sulfate Solution. *J. Colloid and Interface Sci.* 63, 446-451.
- Hoiland H., E. Ljosland and S. Backlund. 1984. Solubilization of Alcohols and Alkanes in Aqueous Solutions of Sodium Dodecyl Sulfate. *J. Colloid and Interface Sci.* 101, 467-471.
- Ilic M., J. Gonzalez, A. Pohlmeier, H.D. Narres and M.J. Schwuger. 1996. Interaction of Sodium Dodecylsulfate (SDS) with Homoionic Montmorillonites: Adsorption Isotherms and Metal-Ion Release. *Colloid Polymer Sci.* 274, 966-973.
- Jafvert C.T. and J.K. Heath. 1991. Sediment-and Saturated-Soil-Associated Reaction Involving an Anionic Surfactant (Dodecylsulfate). 1. Precipitation and Micelle Formation. *Environ. Sci. Technol.* 25, 1031-1038.

- Jafvert C.T., P. Van Hoof and J.K. Heath. 1994.
Solubilization of Nonpolar Compounds by Nonionic
Surfactant Micelles. *Water Res.* 28, 1009-1017.
- Jawitz J.W., M.D. Annable, P.S.C. Rao and R.D. Rhue. 1997.
Field Implementation of a Winsor Type I
Surfactant/Alcohol Mixture for In-Situ Solubilization
of a Complex LNAPL as a Single-Phase Microemulsion.
Submitted for publication in *Environmental Science &
Technology*.
- John A.C. and A.K. Rakshit. 1995. Effects of Mixed Alcohols
as Cosurfactants on Single Phase Microemulsion
Properties. *Colloids Surfaces.* 95,201-210.
- Joos P. and E. Rillaerts. 1981. Theory on the Determination
of the Dynamic Surface Tension with the Drop Volume and
Maximum Bubble Pressure Methods. *J. Colloid Interface
Sci.* 79, 96-100.
- Joos P. and J. Van Hunsel. 1988. Adsorption Kinetics of
Micellar Brij 58 Solutions. *Colloids Surfaces* 33, 99-
108.
- Kahlweit M., R. Strey and G. Busse. 1991. Effect of
Alcohols on the Phase Behavior of Microemulsion. *J.
Phys. Chem.* 95, 5344-5352.
- Kallay N., X. Fan and E. Matijevic. 1986. Precipitation of
Surfactant Salts: The Effect of Counterion Exchange on
Micelles. *Acta Chem. Scand. A.* 40, 257-260.
- Kallay N., M. Pastuovic and E. Matijevic. 1985. Solubility
and Enthalpy of Precipitation of Magnesium, Calcium,
Strontium, and Barium Dodecyl Sulfates. *J. Colloid
Interface Sci.* 106, 452-458.
- Koopal L.K., E.M. Lee and M.R. Bohmer. 1995. Adsorption of
Cationic and Anionic Surfactants on Charged Metal Oxide
Surfaces. *J. Colloid Interface Sci.* 170, 85-97.

- Krebs R., M. Sardin and D. Schweich. 1987. Mineral Dissolution, Precipitation, and Ion Exchange in Surfactant Flooding. *AIChE J.* 33, 1371-1378.
- Lalanne P, B. Clin and J. Biais. 1984. Application of the Theoretical Models to the Estimate of Microemulsion Properties. *Chem. Eng. Comm.* 27, 193-208.
- Lee C., M.A. Yeskie, J.H. Harwell and E.A. O'Rear. 1990. Two-Site Adsolubilization Model of Incorporation of Alcohols into Adsorbed Surfactant Aggregates. *Langmuir* 6, 1758-1762.
- Leung R. and D.O. Shah. 1986. Dynamic Properties of Micellar Solutions. I. Effects of Short-Chain Alcohols and Polymers on Micellar Stability. *J. Colloid and Interface Sci.* 113, 484-498.
- Levitz P. and H. Van Damme. 1986. Fluorescence Decay Study of the Adsorption of Nonionic Surfactants at the Solid-Liquid Interface. 2. Influence of Polar Chain Length. *J. Phys. Chem.* 90, 1302-1310.
- Longino B.L. and B.H. Kueper. 1995. The use of Upward Gradients to Arrest Downward Dense, Nonaqueous Phase Liquid (DNAPL) Migration in The Presence of Solubilizing Surfactants. *Can. Geotech. J.* 32, 296-308.
- Mackay R. 1987. Solubilization. In: Nonionic Surfactants: Physical Chemistry. Surfactant Science Series Volume 23. M.J. Schick, ed. Marcel Dekker, Inc. New York.
- MacLay W.N. 1965. Factors Affecting the Solubility of Nonionic Emulsifiers. *J. Colloid Sci.* 11, 272-285.
- Manable M., M. Koda and K. Shirahama. 1980. The Effect of 1-Alcohols on Ionization of Sodium Dodecyl Sulfate Micelles. *J. Colloid and Interface Sci.* 77, 189-194.
- Martel R. and P.J. Gelinas. 1996. Surfactant Solutions Developed for NAPL Recovery in Contaminated Aquifers. *Ground Water* 34, 143-154.

- Martel R., P.J. Gelinas, J. E. Desnoyers and A. Masson. 1993. Phase Diagrams to Optimize Surfactant Solutions for Oil and DNAPL Recovery in Aquifers. Ground Water. 31, 789-800.
- Matheson K.L., M.F. Cox and D.L. Smith. 1985a. Interactions Between Linear Alkylbenzene Sulfonates and Water Hardness Ions. I. Effect of Calcium Ion on Surfactant Solubility and Implications for Detergency Performance. JAOCS. 62, 1391-1396.
- Matheson K.L., M.F. Cox and D.L. Smith. 1985b. Interactions Between Linear Alkylbenzene Sulfonates and Water Hardness Ions. II. Reducing Hardness Sensitivity by the Addition of Micelle Promotion Agents. JAOCS. 62, 1396-1399.
- Mitchell D.J. and B.W. Ninham 1981. J. Chem. Soc. Faraday Trans. 2. 77, 601
- Mukerjee P. 1979. Solubilization in Aqueous Micellar Systems. In: Solution Chemistry of Surfactants. Volume 1. K.L. Mittal, ed. Plenum Press. New York.
- Muto Y., K. Yoda, N. Yoshida, K. Esumi, K. Meguro, W. Binana-Limbele and R. Zana. 1989. The Effect of Alcohols on Properties of Aqueous Solutions of Hydrocarbon and Fluorocarbon Surfactants. J. Colloid Interface Sci. 130, 165- 175.
- National Research Council (NRC). 1994. Alternatives for Groundwater Cleanup. Washington, D.C., National Academy Press.
- National Research Council (NRC). 1997. Innovations in Groundwater and Soil Cleanup. Washington, D.C., National Academy Press.
- Nguyen C. M., J.F. Scaimehorn and S.D. Christian. 1988. Solubilization of n-hexanol in Mixed Micelles. Colloids Surfaces 30, 335-344.

- Noik C., M. Baviere and D. Defives. 1987. Anionic Surfactant Precipitation in Hard Water. *J. Colloid Interface Sci.* 115, 36-45.
- Oh S.G. and D.O. Shah. 1993. The Effect of Micellar Lifetime on the Rate of Solubilization and Detergency in Sodium Dodecyl Sulfate Solutions. *JAOCs*. 70, 673-678.
- O'Haver J.H. and J.H. Harwell. 1995. Adsolubilization: Some Expected and Unexpected Results. In: Surfactant Adsorption and Surface Solubilization. ACS Symposium Series 615. American Chemical Society. Washington, D.C.
- Okuda I., J.F. McBride, S.N. Glyzer and C.T. Miller. 1996. Physicochemical Transport Processes Affecting the Removal of Residual DNAPL by Nonionic Surfactant Solutions. *Environ. Sci. Technol.* 30, 1852-1860.
- Olson R.V. and R. Ellis Jr. 1986. Iron. In: Methods of Soil Analysis. Part 2. Chemical and Microbiological Properties. 2nd Edition. A.L. Page, R.H. Miller and D.R. Keeney, eds. American Society of Agronomy. Soil Science Society of America. Madison, WI.
- Palmer C., D.A. Sabatini and J.H. Harwell. 1992. Sorption of Hydrophobic Organic Compounds and Nonionic Surfactants with Subsurface Materials. In: Transport and Remediation of Subsurface Contaminants. D.A. Sabatini and R.C. Knox, eds. ACS, Washington, D.C. pp. 169-181.
- Pennell K.D., L.M. Abriola and W.J. Weber Jr. 1993. Surfactant-Enhanced Solubilization of Residual Dodecane in Soil Columns. 1. Experimental Investigation. *Environ. Sci. Technol.* 27, 2332-2340.
- Pennell K.D., M. Jin, L.M. Abriola and G.A. Pope. 1994. Surfactant Enhanced Remediation of Soil Columns Contaminated by Residual Tetrachloroethylene. *J. Contaminant Hydrology* 16, 35-53.
- Pennell K.D., G.A. Pope and L. M. Abriola. 1996. Influence of Viscous and Buoyancy Forces on the Mobilization of

Residual Tetrachlorethylene during Surfactant Flushing.
Environ. Sci. Technol. 30, 1328-1335.

- Pithapurwala Y.K. and D.O. Shah. 1984. Interfacial Composition of Microemulsions: Modified Schulman-Bowcott Model. Chem. Eng. Commun. 29, 101-112.
- Pope G.A. and W.H. Wade. 1996. Lessons from Enhanced Oil Recovery Research for Surfactant-Enhanced Aquifer Remediation. In: Surfactant-Enhanced Subsurface Remediation. ACS Symposium Series 594. D.A. Sabatini, R.C. Knox and J.H. Harwell, eds. American Chemistry Society, Washington, D.C.
- Prigogine, I. and R. Defay. 1965. Chemical Thermodynamics Translated by D.H. Everett. Longmans, London.
- Rathman J.F and J.F. Scamehorn. 1987. Counterion Binding on Mixed Micelles: Effect of Surfactant Structure. Langmuir 3, 372-377.
- Rhue R.D., M.D. Annable, and P.S.C. Rao. 1997. Lab and Field Evaluation of Single-Phase Microemulsion (SPME) for Enhanced In-Situ Remediation of Contaminated Aquifers. Phase I: Laboratory Studies for Selection of SPME Precursors. AATDF Report. University of Florida, Gainesville, FL.
- Rillaerts E. and P. Joos. 1982. Rate of Demicellization from the Dynamic Surface Tensions of Micellar Solutions. J. Phys. Chem. 86, 3471-3478.
- Rosen M.J. 1989. Surfactants and Interfacial Phenomona, 2nd ed. John Wiley and Sons. New York.
- Ruths M., J. Sjoblom and A.M. Blokhuis. 1991. Surfactants and Cosurfactants in Lamellar Liquid Crystals and Adsorbed on Solid Surfaces: III. The Model System Sodium Decanoate/Benzyl Alcohol and α -Alumina. J. Colloid Interface Sci. 145, 108-112.
- Scamehorn J.F., R.S. Schechter and W.H. Wade. 1982. Adsorption of Surfactant on Mineral Oxide Surfaces from

Aqueous Solutions. I: Isomerically Pure Anionic Surfactants. J. Colloid Interface Sci. 85, 463-478.

Schweich D. and M. Sardin. 1985. Transient Ion Exchange and Solubilization of Limestone in an Oil Field Sandstone: Experimental and Theoretical Wavefront Analysis. AIChE J. 31, 1882-1890.

Shah D. 1971. Significance of the 1:3 Molecular Ratio in Mixed Surfactant Systems. J Colloid Interface Sci. 37, 744-752.

Shih L.B. and R.W. Williams. 1986. Raman Spectroscopic Determination of Solubilization Equilibria in Surfactant Solutions. J. Phys. Chem. 90, 1615-1620.

Shinoda K. 1978. Principles of Solution and Solubility. Marcel Dekker, New York.

Sjoblom J., A.M. Blokhuis, W.M. Sun and S.E. Friberg. 1990. Surfactants and Cosurfactants in Lamellar Liquid Crystals and Adsorbed on Solid Surfaces: I. The Model System Sodium Dodecyl Sulfate/Butanol or Sodium Dodecyl Sulfate/Benzyl Alcohol and α -Alumina. J. Colloid Interface Sci. 140, 481-491.

Somasundaran P., M. Celik, A. Goyal and E. Manev. 1984. The Role of Surfactant Precipitation and Redissolution in the Adsorption of Sulfonate on Minerals. Soc. Pet. Eng. J. 24, 233-239.

Somasundaran P. and D.W. Fuerstenau. 1966. Mechanisms of Alkyl Sulfonate Adsorption at the Alumina-Water Interface. J. Phys. Chem. 70, 90-96.

Stellner K.L. and J.F. Scamehorn. 1989a. Hardness Tolerance of Anionic Surfactant Solutions. 1. Anionic Surfactant with Added Monovalent Electrolyte. Langmuir 5, 70-77.

Stellner K.L. and J.F. Scamehorn. 1989b. Hardness Tolerance of Anionic Surfactant Solutions. 2. Effect of Added Nonionic Surfactant. Langmuir 5, 77-84.

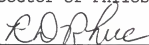
- Stilbs P. 1982. Fourier Transform Pulsed-Gradient Spin Echo (FT-PGSE) Self-Diffusion Measurements of Solubilization Equilibria in SDS Solutions. *J. Colloid Interface Sci.* 87, 385-394.
- Strey S. and M. Jonstromer. 1992. Role of Medium-chain Alcohols in Interfacial Films of Nonionic Microemulsions. *J. Phys. Chem.* 96, 4537-4542.
- Stumm W. and J.J. Morgan. 1995. Aquatic Chemistry: Chemical Equilibria and Rates in Natural Waters. 3rd Edition. John Wiley & Sons, Inc. New York.
- Tornberg E. 1978. The Application of the Drop Volume Technique to Measurements of the Adsorption of Proteins at Interfaces. *J. Colloid Interface Sci.* 64, 391-402.
- Treiner C., A. A. Khodja and M. Formon. 1987. Micellar Solubilization of 1-Pentanol in Binary Surfactant Solutions: A Regular Solution Approach. *Langmuir* 3, 729-735.
- Treiner C., A.A. Khodja, M. Fromon and Chevalet. 1989. Effect of Sodium Salicylate and other Electrolytes on the Partition of 1-Pentanol between Sodium Dodecylsulfate Micelles and Water: A Gas-Chromatographic Study. *J. Solution Chem.* 18, 217.
- Van Hunsel J., G. Bleys and P. Joos. 1986. Adsorption Kinetics at the Oil/Water Interface. *J. Colloid Interface Sci.* 114, 432-441.
- Van Hunsel J and P. Joos. 1989. Study of the Dynamic Interfacial Tension at the Oil/Water Interface. *Colloid Polymer Sci.* 267, 1026-1035.
- Verhoeckx G.J., P.L. De Bruyn and J.T.J. Overbeek. 1987. On Understanding Microemulsions I. Interfacial Tensions and Adsorptions of SDS and Pentanol at the cyclohexanol/Water Interface. *J. Colloid Interface Sci.* 119, 409-421.

- Vikholm I., G. Douheret, S. Backlund and H. Hoiland. 1987. Shape Transitions in the Aqueous Phase of the System Hexadecyltrimethylammonium Bromide-Hexanol-Water. *J. Colloid and Interface Sci.* 116, 582.
- Voca B.R., J.P. Canselier, C. Noik and M. Baviere. 1988. Three-phase Behavior of Brine/Alkane/Alcohol/Alpha-Olefinsulfonate Mixtures. *Progress in Colloid and Polymer Science* 76, 144-152.
- Walkley A. and I.A. Black. 1934. An Examination of the Degtjareff Method for Proposed Modification of the Chromic Acid Titration Method. *Soil Sci.* 37, 29-38.
- Wang C.C., N.S. Yu, C.Y. Chen and J.F. Kuo. 1996. Kinetic Study of the Miniemulsion Polymerization of Styrene. *Polymer* 137, 2509-2516.
- Ward A.F.H. and L. Tordai. 1946. Time-Dependence of Boundary Tensions of Solutions I. The Role of Diffusion in Time-Effects. *J. Chem. Phys.* 14, 453-461.
- West C.C. and J.H. Harwell. 1992. Surfactants and Subsurface Remediation. *Environ. Sci. Technol.* 26, 2324-2330.
- Witco. 1994. Determination of Anionic Actives by Two-Phase Titration with Bromocresol Green. Code KL 631.20.
- Yalkowsky S.H. 1987. Solubility of Organic Solutes in Mixed Aqueous Solvents. Project Completion Report, CR# 812581-01. U.S. Environmental Protection Agency, Ada, OK.
- Zhou J.S. and M.J. Dupeyrat. 1990. Alcohol Effect on Interfacial Tension in Oil-Water-Sodium Dodecyl Sulphate Systems. *J. Colloid Interface Sci.* 134, 320-335.

BIOGRAPHICAL SKETCH

Meifang Zhou was born on June 2, 1965, in Zhejiang, China. In 1985, he received a B.S. degree in soil and agrochemistry from Zhejiang Agricultural University in Hangzhou, China. Immediately following graduation, he began work as a research associate in the Institute of Soil and Fertilizers, Zhejiang Academy of Agricultural Sciences, Hangzhou, China. In January 1993, he started his MS program of study in the Soil and Water Science Department of the University of Florida. After receiving his MS degree in December, 1994, he continued on with his Ph.D. degree program in the same department.

I certify that I have read this study and that in my opinion it conforms to acceptable standards of scholarly presentation and is fully adequate, in scope and quality, as a dissertation for the degree of Doctor of Philosophy.



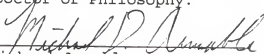
R. Dean Rhue, Chair
Professor of Soil and Water
Science

I certify that I have read this study and that in my opinion it conforms to acceptable standards of scholarly presentation and is fully adequate, in scope and quality, as a dissertation for the degree of Doctor of Philosophy.



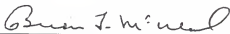
P. Suresh C. Rao
Graduate Research Professor
of Soil and Water Science

I certify that I have read this study and that in my opinion it conforms to acceptable standards of scholarly presentation and is fully adequate, in scope and quality, as a dissertation for the degree of Doctor of Philosophy.



Michael Annable
Assistant Professor of
Environmental Engineering
Sciences

I certify that I have read this study and that in my opinion it conforms to acceptable standards of scholarly presentation and is fully adequate, in scope and quality, as a dissertation for the degree of Doctor of Philosophy.



Brian McNeal
Professor of Soil and Water
Science


I certify that I have read this study and that in my opinion it conforms to acceptable standards of scholarly presentation and is fully adequate, in scope and quality, as a dissertation for the degree of Doctor of Philosophy.



Paul Chadik
Assistant Professor of
Environmental Engineering
Sciences

This dissertation was submitted to the Graduate Faculty of the College of Agriculture and to the Graduate School and was accepted as partial fulfillment of the requirements for the degree of Doctor of Philosophy.

May, 1998



Dean, College of
Agriculture

Dean, Graduate School